

Portable Wind Turbine Blade Leading Edge Erosion Test
Final Design Review
November 24, 2020

by
Joe Blakewell, jblakewe@calpoly.edu
Tim Holt, tiholt@calpoly.edu
Kevin Vartan, kmvartan@calpoly.edu

for
Turbine Technology Partners, LLC (TTP)

Mechanical Engineering Department
California Polytechnic State University San Luis Obispo
2020

Executive Summary

Turbine Technology Partners, LLC (TTP) is a company located in Santa Barbara, California that provides expert independent engineering (IE) consulting services to the wind energy industry - supporting its goal of generating cost effective and reliable carbon-free renewal energy for the world. TTP customers include some of the largest wind turbine original equipment manufacturers (OEMs), wind turbine power plant developers, and wind turbine owner/operators.

One of the biggest problems challenging the wind energy industry currently is the power loss that results from the leading edge (LE) erosion of wind turbine blades. The purpose of our senior design project is to create an erosion test chamber that will simulate erosion conditions and compare the relative effectiveness of different erosion-resistant solutions, such as coatings or tapes. This document highlights our team's goals for the project, which are a result of sponsor and user interviews, technical background research, product research, and project objectives research. Our key findings from research and interviews are that testing units for LE protection solutions should follow the guidelines set forth in the recommended practices 0171 from Det Norske Veritas Germanischer Lloyd (DNVGL), an international accredited energy registrar. We have gone through a rigorous design process to come up with the design that we have chosen as our final design. The included Gantt chart shows our project's timeline of completion.

This document, the Final Design Review (FDR), is designed to describe the process by which ideation and down-selection occurred and to explain and defend the chosen concept.

Statement of Disclaimer

Since this project is a result of a class assignment, it has been graded and accepted as fulfillment of the course requirements. Acceptance does not imply technical accuracy or reliability. Any use of information in this report is done at the risk of the user. These risks may include catastrophic failure of the device or infringement of patent or copyright laws. California Polytechnic State University at San Luis Obispo and its staff cannot be held liable for any use or misuse of the project.

Table of Contents

1. Introduction	7
2. Background	7
2.1 Turbine Blade Makeup	7
2.2 LE Erosion Main Causes	8
2.3 Current Solutions	9
2.4 Current Testing Machines on the Market	10
2.5 DNVGL Recommended Practices	10
3. Objectives	11
3.1 Problem Definition	11
3.2 Boundary Diagram	11
4. Concept Design	14
4.1 Design Selection Process	14
4.2 Design Based on Analysis and Hazard Prevention	18
5. Final Design	20
5.1 Structural Support Design	21
5.2 Fluid Path Design	25
5.3 Reservoir Design	30
5.4 Rotating Blade System	30
5.5 Safety and Maintenance	33
5.6 Cost Overview	34
6. Manufacturing	34
6.1 Procurement	34
6.2 Manufacturing	34
6.3 Assembly	36
6.4 Outsourcing	37
7. Design Verification Chapter	37
7.1 Dropper Configuration Verification	37
7.2 Finite Element Analysis	39
8. Project Management	52
8.1 Completed Analysis	53
8.2 Purchases	53
8.3 Effectiveness of Planning	54
9. Conclusions and Recommendations	54
References	55
Appendix A: Relevant Patents	A-1
Appendix B: Quality Function Deployment	B-1
Appendix C: Ideas from Ideation	C-1
Appendix D: Pugh Matrices	D-1
Appendix E: Morphological Matrix	E-1
Appendix F: Weighted Decision Matrix	F-1
Appendix G: Design Hazard Checklist	G-1
Appendix H: Preliminary Calculations	H-1
Appendix I: Gantt Chart	I-1
Appendix J: Concept Model Build Day Images	J-1
Appendix K: DVP&R	K-1

Appendix L: Indented Bill of Materials	L-1
Appendix M: Design Verification Plan	M-1
Appendix N: Water Drop Spacing Calculations	N-1
Appendix O: Links to each part	O-1
Appendix P: Failure Modes and Effects Analysis	P-1
Appendix Q: Centrifugal Force Excel Calculation	Q-1
Appendix R: Bolt Stress Excel Calculations	R-1
Appendix S: EES File For One Dropper Configuration	S-1
Appendix T: Screenshot of Excel File ‘ME 430 Experiment Data’	T-1
Appendix U: MatLab Script for fluid Pathway through FDS	U-1
Appendix V: Technical Drawing Package	V-1

List of Tables

Table 1. DNVGL Requirements	11
Table 2. Engineering Specifications and Requirements for Water Delivery System	12
Table 3. Engineering Specifications and Requirements for Rotating Blade System	13
Table 4. Summary of results from Crude Structural FEA	25
Table 5. Summarized Bill of Materials	34
Table 6. Statistical results for each nozzle size	39
Table 7. Blade and Bolt Parameters.....	40
Table 8. Bolt Forces	40
Table 9. Resulting Max Von Mises bolt stresses and F.O.S.	46
Table 10. Material Properties for Bolts and Sheath	48
Table 11. Max Von Mises Stress and F.O.S. for Sheath and Bolts	50
Table 12. Disk Max Von Mises Stress and Yielding F.O.S.	52
Table 13. Key Deliverables.....	53

List of Figures

Figure 1. Section view of a standard wind turbine blade.....	9
Figure 2. Sandia Labs data for severe LE erosion and energy production losses	10
Figure 3. R&D Test Systems turnkey solution to the LE testing problem	11
Figure 4. Leading Edge Erosion Tester Boundary Diagram	13
Figure 5. Straight leg supports, peristaltic pump driven system.....	17
Figure 6. Arch supports, pressure driven dropper system	18
Figure 7. Cylinder support, rotating paddle to block satellite drops system	18
Figure 8. Telescoping leg supports, peristaltic pump driven system	19
Figure 9. Wheeled leg supports, pressure driven dropper system	19
Figure 10. Solidworks model of initial CAD concept.....	20
Figure 11. Concept model prototype.....	21
Figure 12. Peristaltic Pump CAD.....	21
Figure 13. CAD assembly drawing.....	22
Figure 14. Support Structure design.....	23
Figure 15. Leg design for structural support	24
Figure 16. Crude leg deflection FEA with conservative 50 lbf load per leg	24
Figure 17. Crude leg stress FEA with conservative 50 lbf load per leg	25
Figure 18. Support ring dimensions.....	26
Figure 19. Crude ring deflection FEA with conservative 200 lbf load.....	26
Figure 20. Crude ring stress FEA with conservative 200 lbf load	27
Figure 21. Peristaltic pump and inside view.....	27
Figure 22. In-line tubing filter	28
Figure 23. Barbed reducer tubing fitting.....	28
Figure 24. Barbed Y-connector	28
Figure 25. 1:12 flow splitter	28
Figure 26. Dropper configuration	29
Figure 27. ¼” tubing to ½” NPT male adapter	29
Figure 28. Dropper assembly PVC.....	29
Figure 29. Thread-to-luer lock adapter	30
Figure 30. 32 Ga nozzle	30
Figure 31. PVC rail.....	31
Figure 32. Nozzles for creating the 2mm drop	31
Figure 33. Reservoir.....	32
Figure 34. Rotating blade system	33
Figure 35. DU 96-W-180 6061 aluminum airfoil blade	33
Figure 36. Central mounting disk.....	34
Figure 37. Blade sheath	34
Figure 38. Verification prototype for nozzle sizing test.....	37
Figure 39. Custom dropper configuration.....	38
Figure 40. Experimental setup for drop collection with our verification prototype	39
Figure 41. Average drop size results	40
Figure 42. Blade FBD	42
Figure 43. System Loading.....	43
Figure 44. Blade/Bolt Assembly.....	43
Figure 45. Model 1 Centrifugal Body Force Loading.....	43

Figure 46. Model 2 Centrifugal Rotational Body Force Loading	44
Figure 47. Bolt boundary conditions	44
Figure 48. Meshed Model 1 Assembly	44
Figure 49. Node Checked for Model 1 Mesh Convergence Study	45
Figure 50. Model 1 Mesh Convergence Plot	45
Figure 51. Meshed Model 2 Assembly	46
Figure 52. Node Checked for Model 2 Mesh Convergence Study	46
Figure 53. Model 2 Mesh Convergence Plot	46
Figure 54. Bolt Deflection Contour Plot	47
Figure 55. Model 1 Bolt Von Mises Stress Contour Plot	47
Figure 56. Model 2 Bolt Von Mises Stress Contour Plot	48
Figure 57. Model 1 Blade Von Mises Stress Contour Plot	49
Figure 58. Model 2 Blade Von Mises Stress Contour Plot	49
Figure 59. Sheath and Sheath Bolt Assembly	50
Figure 60. Body Centrifugal Force Load on Sheath	51
Figure 61. Boundary Condition on Bolts	51
Figure 62. Contour Plot of Von Mises Stress on Sheath Bolts	51
Figure 63. Contour Plot of Von Mises Stress on Sheath	52
Figure 64. Disk and Bolt Assembly	52
Figure 65. Centrifugal Body Force Loading on Bolts	53
Figure 66. Boundary Conditions on Disk	53
Figure 67. Disk Von Mises Stress Contour Plot	54

1. Introduction

Our team is made up of three fourth-year students studying mechanical engineering at Cal Poly San Luis Obispo. We have partnered with Turbine Technology Partners (TTP) to design the water delivery system and rotating blade system for a turbine blade coating testing unit. TTP is a consulting company based in Santa Barbara, CA with specialized experience in the wind power industry. Recently, they have been working to develop blade coatings that provide leading-edge protection from erosion during turbine operation. The testing unit is needed to verify the degree of leading-edge protection that the TTP blade coating solutions provide relative to their industry competition. We agreed to work with TTP from January 2020 to December 2020 to develop the water delivery system and designs for the rotation system for this testing unit. This document goes over the background research, objectives, and design process and timeline for this project. Due to the changing nature of things surrounding the COVID-19 pandemic, we agreed with TTP that it was best to design the rotating blade system in place of building the water delivery system designed in quarters 1 and 2.

2. Background

As wind turbine blades continue to get larger to keep up with demand for electricity, the blade tips are reaching linear speeds of around 90-150 m/s, which is approximately 200-350 mph. This high velocity leads to rapid erosion of the leading edge of composite blades, especially when there is any surrounding precipitation. TTP has been developing protective leading-edge coatings to solve this problem, but the product development presents a new challenge; product verification. TTP needs a testing device to help them verify the effectiveness of their protective coatings because reflecting on field data is too costly and time consuming. Our testing unit will allow TTP to directly compare their new products with competitors and industry standards. Our final product will meet the specifications outlined by TTP and the industry standards in DNVGL.

2.1 Turbine Blade Makeup

The blades on a wind turbine are fundamentally composed of two shells forming an airfoil shape from thermosetting polymer matrix, e.g. epoxy or polyester, with reinforcing fibers [1]. These two shells are bonded using adhesive and create the leading and trailing edges [2]. This airfoil-shaped blade is stiffened by spars or webs from balsa wood, foam, or combinations of both. The underlying layer of polymer and reinforcing fibers is hereon referred to as substrate [3]. A generalized picture of an airfoil can be seen below in Figure 1. Breakthrough refers to when the erosion damage has penetrated the protective coating and breached the substrate.

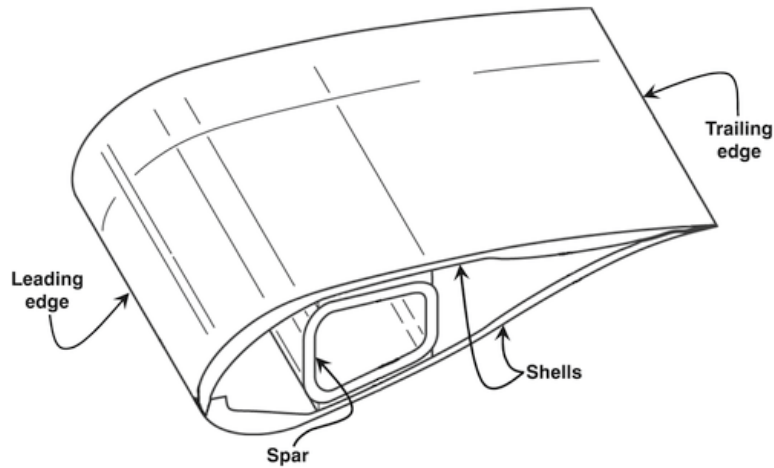


Figure 1. Section view of a standard wind turbine blade [3]

All parts of the blade are subject to loading and failure, but the most common failure is the one that we are being tasked with assisting; the erosion of the leading edge.

2.2 LE Erosion Main Causes

When the LE of an airfoil or wing is damaged, the performance of the blade is impacted far more than when the trailing edge of the blade is damaged [4]. This is because the damaged LE trips the boundary layer over the blade from laminar flow to turbulent flow, which makes the blade less aerodynamically efficient [5].

Due to most wind farms being at or near sea level, rain is a far more common occurrence than hail or snow [6]. This means that rain causes more damage than hail or snow to the LE of a wind turbine blade [7]. The leading edge erosion problem is currently plaguing the wind energy industry and has many companies competing to become the leading solution provider [8]. LE erosion can be a huge problem for energy companies as the efficiency of the turbine decreases significantly when the LE has eroded [9]. This causes massive losses in energy generation over entire wind farms and therefore a large loss in profit for the energy companies. Sandia Laboratory's wind tunnel research at Texas A&M and found that the Annual Energy Production (AEP) can be reduced up to 5% with significant LE erosion [10], as can be seen below in Figure 2.

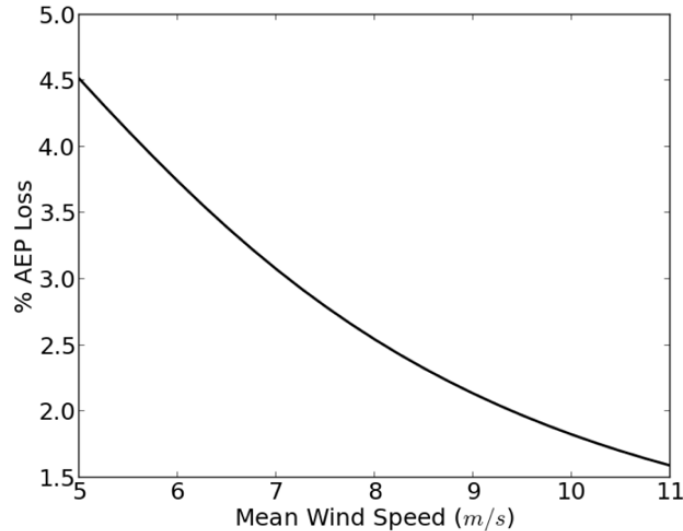


Figure 2. Sandia Labs data for severe LE erosion and energy production losses[10]

It is difficult to replicate the conditions experienced by these turbines out in their true environment, but several testing devices do exist to test out these blades and protective coatings. They follow the DNVGL – RP0171 standard guidelines [11] which set safe and verified operating procedures for LE erosion testing as put forth by ASTM G73-10 [12]. Since this is a developing field with relatively little data to draw conclusions from, much of the design and testing parameters are left up to the engineers who design the testing equipment and procedures [13].

The exposure of the composite substrate to water could also pose significant threats to the performance of the blade [14]. Primarily, the removal of any surface coating will mean that the substrate itself will be exposed to further erosion [15].

2.3 Current Solutions

The technologies employed vary widely; however, the two most common approaches to creating an effective surface coating are:

- (1) In-mold application. A surface coating layer is added to the surface of the blade as part of the molding process [16]. For manufacturing reasons, the coatings created through this approach typically consist of a layer of material similar to that of the matrix material used in the substrate (e.g. epoxy/polyester).
- (2) Post-mold application. Surface coatings can be applied to the blade after the molding process through painting or spraying. This approach allows more flexibility with regards to material choice (in the absence of molding considerations), with some manufacturers choosing to apply more ductile/elastic material components such as polyurethanes. The industry is also currently using protective tape as a solution to the LE problem. These technologies usually consist of a highly elastic and durable polyurethane material, designed to (in some cases sacrificially) absorb the impact energy from airborne particulates [17]. The tape is often very difficult to apply correctly which leads to air pockets and a reduced time that the tape protects the blade.

Manufacturers of tapes highlight the proposed benefits of applying elastomeric materials to the leading edge (i.e. leading edge tapes), but also state that tapes must be replaced frequently as they become worn [18].

2.4 Current Testing Machines on the Market

Despite this being a relatively small field, there are a few devices that perform similar tests to the device we are going to design. During our patent search we found the ‘Wind Tunnel for Erosion Testing’ which exposes samples to high winds and droplet impacts. This patent is listed in Appendix A. The wind tunnel example is unique in that it is the only device that replicates airflow over a blade tip by pushing air over the blade instead of accelerating the blade itself. The remaining patents found in our search are also listed in Appendix A. They outline devices that perform smaller functions within a testing unit. The University of Barcelona has a machine that has a single arm with a single jet of water to perform repetitive impact testing. R&D Test Systems offers a turnkey solution which includes the rain system, a rotor with test specimen holders, drainage, ventilation and control system delivered in a housing of 20-foot containers. This machine can be seen below in Figure 3.



Figure 3. R&D Test Systems turnkey solution to the LE testing problem.

This is clearly expensive and huge, neither of which is a helpful to TTP in their quest for a portable, cheap testing solution. Another test unit was built in Bristol and is used by the University of Bristol for Ph.D. students collecting data for their dissertations. It was funded by an EU Demowind-funded Offshore Demonstration Blade project, led by a company called Catapult. The total cost of building this test system exceeded £200k.

2.5 DNVGL Requirements

We have mentioned a recommended practice from DNVGL several times, so below, in Table 1, is a table of elements they require as part of a sufficient testing device. There are many other elements mentioned in the document, but in order to keep this table brief we have included elements that have clear goals that are measurable. Other requirements often have the nominal condition as ‘to be calculated,’ or ‘to be monitored,’ or ‘to be specified.’

Table 1. DNVGL Test rig parameters

Test Parameter	Unit	Nominal Condition
Rotating carrier arm	[-]	Aerofoil shaped with and integrated specimen
Number of specimen carrier arms	[-]	Max. 3
Radial position for the center of the specimen	[m]	Min. 1.0
Vertical distance from origin of droplet (needle) to center of specimen in rotor plane, x	[m]	Min. 0.2
Angle of incidence, α	[°]	90
Distance of test specimen to side wall, b	[m]	To be documented
Gauge zone length of specimen, l_{gz}	[m]	Min. 0.2
Mean droplet size, diameter, d	[mm]	2.0
Rain intensity, I	[m/s]	To be measured from rig design, optimal 9.0e-6

Many of these requirements we have made our own, and specified some of the more ambiguous options.

3. Objectives

We began this project with our customer, TTP, in mind. As a wind turbine LE protective coating developer, TTP needs a way to test their protective coatings at reduced cost because analyzing field data after full-scale coating installation is a very expensive testing method. TTP wants a testing unit that can produce relevant and consistent evidence comparing LE protection options. Finally, the unit needs to have verifications for design process, validity, and safety.

3.1 Problem Definition

Leading edge protective coating developers need a way to test their protective coatings with a machine that is cheaper and smaller than commercially available products currently on the market.

3.2 Boundary Diagram

The boundary diagram in Figure 4 conveys the specific goals we aimed to achieve for our final design. Main components of our final design include a motor, three DU 96-W-180 airfoil-shaped arms, sample attachment zones, water droppers, and a transparent covering. The resulting material and component selection will be primarily driven by our \$1,000 budget, blade tip speed requirement of 100 m/s, and single operator goals.

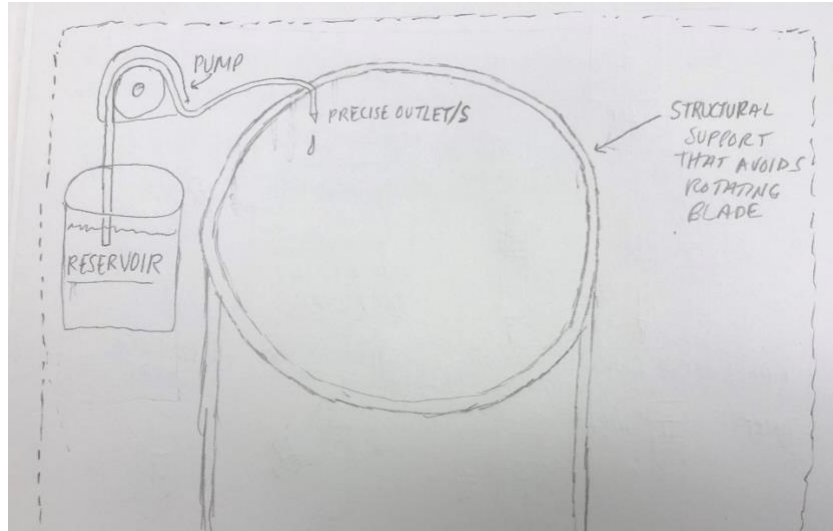


Figure 4. Leading Edge Erosion Tester Boundary Diagram. Similar to machine used at University of Dayton Research Institute [19]

The specifications listed in Table 2 and Table 3 come from our Quality Function Deployment (QFD) analysis, which is shown in Appendix B. One of the sections in the QFD considers customers, which lists TTP as well as other people who interact with the product, such as manufacturers and testers. While forming the QFD, we considered these customer’s wants and needs and listed the relative engineering specifications, along with the target values of those specifications. We then used the symbols to show how the wants and specifications overlap and considered the importance of specifications to tester function. In addition, the QFD includes a list of current products and their ability to meet the requirements of the wants and needs. Our resulting specifications show what requirements guided our product design.

Table 2. Engineering Specifications and Requirements for Water Distribution System

Spec #	Specification description	Requirement or targets	Tolerance	Risk*	Compliance (T,I,A,S)**
1	Weight	100 kg	max	M	A
2	Outer Radius of Support Ring	1.10 m	±0.01	L	A
3	Rain Intensity in Exposure Zone	9.0E-6 m/s	min	M	A
4	Droplet Size	2 mm	±1.0	M	A, T
5	Number of Operators	1 person	max	L	A

*Risk: L = Low
M = Medium
H = High

**Compliance: A = Analysis
T = Test
I = Inspection
S = Similarity

Table 3. Engineering Specifications and Requirements for Rotating Blade System

Spec #	Specification description	Requirement or targets	Tolerance	Risk*	Compliance (T,I,A,S)**
1	Total Weight	680 kg	max	H	A
2	Test Arm Length	1.10 m	min	H	A
3	Blade Tip Speed	100 m/s	min	H	A
4	Airfoil Shape	DU 96-W-180 Airfoil Shape	-	H	A
5	Lifespan	100 test runs	min	H	A
6	Size of Gauge Zone	20 cm	min	H	A

*Risk: L = Low
M = Medium
H = High

**Compliance: A = Analysis
T = Test
I = Inspection
S = Similarity

The ‘Requirement or Targets’ column lists what we aimed to meet, and the tolerance refers to whether that number is a maximum value, or minimum value that we attempted to achieve. The risk column refers to how confident we were that we could complete the requirement. High risk means that there was some doubt as to whether we could meet this target. Low risk means we were confident that the requirement would be met. The compliance column shows how we aimed to prove that we have met these requirements, whether by inspection (I), Analysis (A), Testing (T), or Similarity (S). The final product that we created involves a detailed test plan for how to run this machine.

The total weight of the machine is listed as a requirement because we are aiming to make the machine as portable as possible, but size constraints from DNVGL recommended practices mean that we had only a medium level of confidence that we could hit this goal. We planned to meet this requirement by designing our structure for easy disassembly and reassembly for easy transportation and setup. The test arm length refers to the distance from the center of rotation of the machine to the center of the samples that are mounted on the blade. In DNVGL they require a minimum distance of 1 m to the center of the test specimen and given a required gauge zone of 20 cm minimum, we anticipated a minimum length of 1.10 m for the blade arm. The gauge zone and blade length are critical for success so we were very confident that these requirements would be met. The blade tip speed refers to the linear speed of the center of the test specimen. According to our research, several companies suggest different testing speeds. We took that data into consideration and decided that a variable speed motor that can accelerate the specimen to a minimum speed of 100 m/s was our design goal.

The rain specifications are also a key to the success of this machine as the water droplets will be what erodes the sample. DNVGL suggests an average rainfall intensity of 9.0E-6 m/s for accurate testing. To translate that into volumetric flow rate, we have determined the area over which the rain will be simulated. DNVGL also suggests a droplet size of 2 mm in diameter [20], which we will replicate using interchangeable off-the-shelf nozzles. Our ability to meet the drop

size and frequency specifications was validated using a simple scale and the assumption that the falling drops are spherical. We report drop variability statistics such as mean diameter and standard deviation. In order to replicate conditions that wind turbines experience, DNVGL suggests having climate control so that the temperature of the unit stays between 20 – 25 °C, and humidity ranges from 20 – 90 % relative humidity. We plan to meet this requirement by recommending our system be used in rooms or environments that match the specification description. The shape of the blade is specified as ‘Aerofoil shaped’ by DNVGL, and after speaking to TTP, we have decided that a DU 96-W-180 airfoil shape will best represent wind turbines from today’s market. The highest risk specification is the reliability and longevity of our machine. We want the unit to work safely and effectively for 100 test runs. This is a high-risk specification because different tests may run for different amounts of time, so overall run-time is difficult to predict. Data from other testing units suggest that a single test could take anywhere from 10 – 85 consecutive hours to complete. If we were to assume the longest operating case, then our machine would be running for 8500 hours to complete 100 test runs. This is almost a year of total operating time. Since the final product will be going through many operation cycles in its lifetime, we focused on cyclic loading and fatigue in our designs. We also performed finite element analysis to complement the cyclic loading calculations.

4. Concept Design

While working on our concept design we took inspiration from leaders in the field of design like the Stanford Design School and IDEO. With their methods of creating innovative solutions we aspired to come up with solutions to our own problems. One of the ways both design maestros come up with their ideas is by brainstorming solutions for completing specific functions and promoting play. In an attempt to replicate this, we played games and got into the creative spirit with all ideas for solutions to function performance encouraged, no matter how impractical or outright ludicrous. These ideas might spawn additional, more realistic ideas. The functions we began brainstorming ideas for were creating droplets, measuring erosion rate, and supplying fluid. We chose to specifically pursue brainstorming solutions to these functions because they are the most important to the success of our system. Pictures of the models we constructed based on the brainstormed ideas are shown in Appendix K. These constructed models were among the most hopeful from our brainstorming sessions. By building them we were able to better assess their potential to meet our design specifications. After these brainstorming sessions we went to the toy chest and attempted to build our best ideas so that we could see if they were feasible. Once we had our ideas and determined which ones could work, we went forward with a more in-depth process to select the best possible design.

4.1 Design Selection Process

In order to help us eliminate some ideas and develop more effective ones, we utilized Pugh matrices. The Pugh Matrices allowed us to evaluate which combinations of our different function ideas would create better overall systems. Our Pugh matrices for supporting water delivery system and creating water droplets are shown in Appendix D. In the Pugh matrix for supporting the water delivery system, we used a straight leg support system as the datum and compared arched legs, cylinder base, telescoping legs, wheeled legs, and hydraulic shocks. The criteria we used for comparisons were stability, portability, safety, ability to integrate, and height change.

After analyzing our ideas against the datum using these criteria, it was evident that the hydraulic shocks were the best alternative for supporting the water delivery system. The next function we analyzed using a Pugh matrix was creating water droplets. We used an eyedropper as the datum and compared it to a peristaltic pump, filter, pressure driven dropper tube, and syringes driven by a lead screw, rack and pinion, or belt. The criteria we used was weight, cost, length of continuous operation time, safety, ease of achieving specified rainfall intensity, 2 mm raindrops, and constant flow rate. The peristaltic pump paired with blunt tipped hypodermic needles with specified diameters was the clear winner because it outperformed the water dropper in more criteria than any other idea. Although we created a Pugh matrix for dampening vibrations, we will not use a vibration dampening component in the water delivery system because TTP suggested that the dampening mechanism be a part of the rotating blade system.

We used the results of the Pugh matrices for each function to create the morphological matrix, which is shown in Appendix E. Our morphological matrix took the best 5 concepts for each of our functions and combined the most compatible functions to create 5 different concepts systems. It is important to note that after speaking TTP, we decided that all concept systems would use nozzles for the create water droplet function. Next, we took the resulting 5 systems from our morphological matrix and compared them using a weighted-decision matrix that can be seen in Appendix F. One of the systems we compared in the matrix was straight legs with a peristaltic pump, as seen below in Figure 5. A peristaltic pump, or roller pump, works by using internal rollers to compress flexible tubing and push the fluid to its destination.

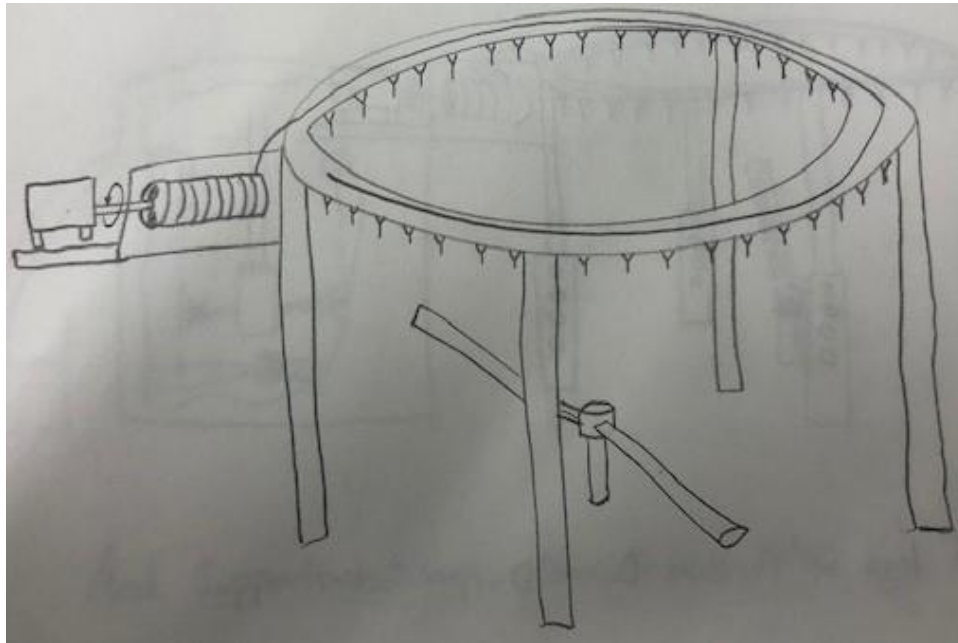


Figure 5. Straight leg supports, peristaltic pump driven system

The second system that we analyzed was a system with arches for supports, using a pressure-driven dropper to create drops, as seen in Figure 6.

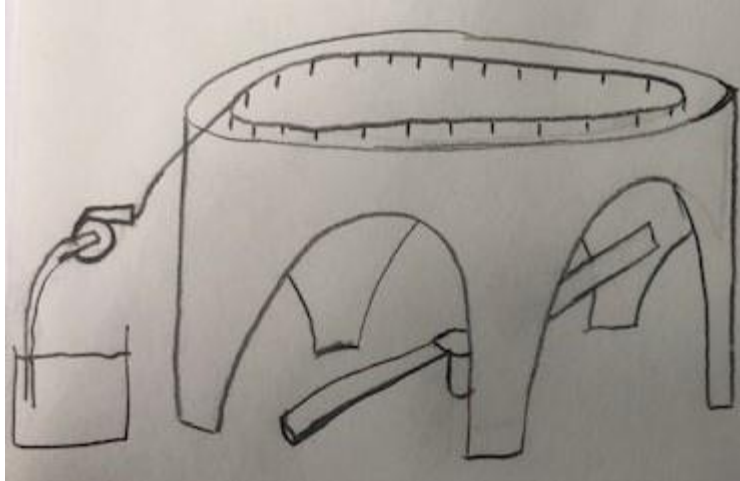


Figure 6. Arch supports, pressure driven dropper system.

The third system in the decision matrix had a cylinder for supports with a rotating paddle to block satellite drops, as seen in Figure 7.

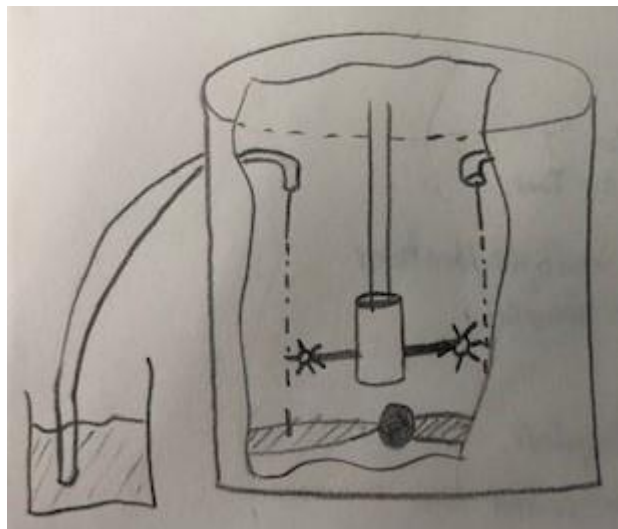


Figure 7. Cylinder support, rotating paddle to block satellite drops system.

Our fourth design utilized telescoping legs with a peristaltic pump, shown in Figure 8.

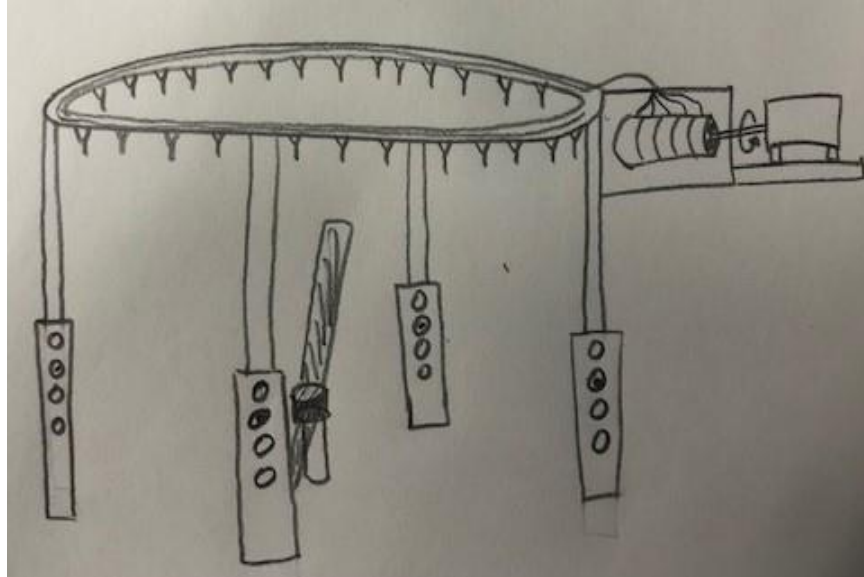


Figure 8. Telescoping leg supports, peristaltic pump driven system

The fifth and final system had wheeled legs and used a pressure driven dropper, as can be seen in Figure 9.

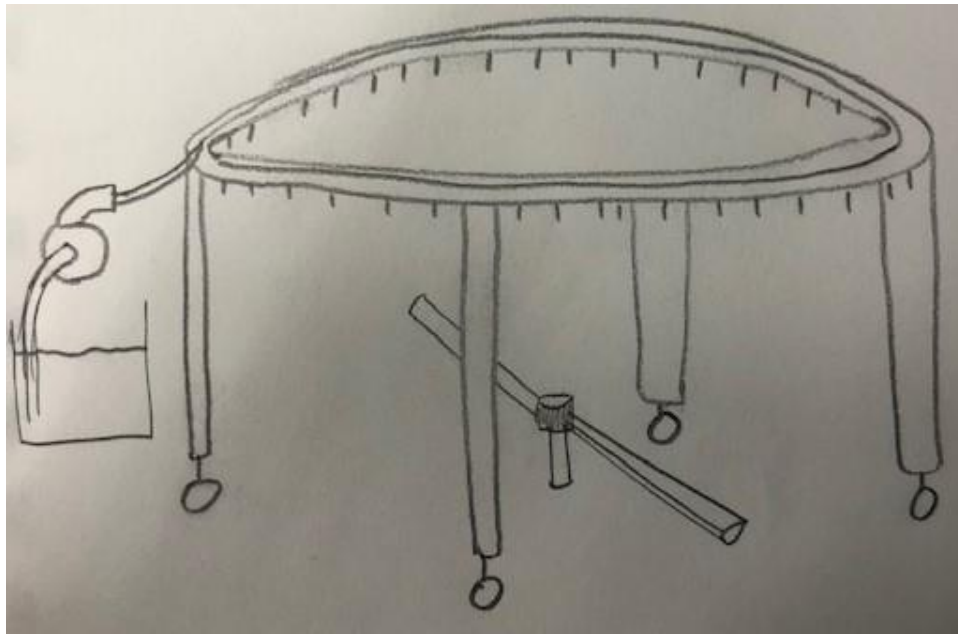


Figure 9. Wheeled leg supports, pressure driven dropper system

After applying a weight of importance to each criterion, we found that the simple straight legs with a peristaltic pump scored the best, which is why we are going forward with this design.

Our design for the water delivery system utilizes peristaltic pumps to deliver necessary volumetric flowrates to droppers of specific nozzle size. Our peristaltic pumps provide consistent flowrates for long periods of time, and the nozzles can deliver precise water droplet sizes to

specific locations. When paired, this equipment provides reliable and repeatable droplet delivery. We arrived at this design after using ideating methods such as brainstorming and brainwriting to create as many solution ideas as possible. Then we experimented with many ideas to find the most accurate and consistent droplet formation methods. According to our design criteria, the 3D printed peristaltic pumps performed far better than our other ideas for water delivery. A complete list of our ideas is in Appendix C.

4.2 Design Based on Analysis and Hazard Prevention

In order to deliver the rain intensity described in Table 1, we have decided that there will be three droppers at each angle location with a radial distance of 1 cm between them. The droppers will be supplied water by peristaltic pumps. These decisions were driven by our decision matrix shown in Appendix E, and sponsor input. The DNVGL guidelines require that the blade be dry before the next set of drops hits the blade, so based on analysis shown in Appendix H, we have concluded that the angular locations of the droppers should be separated by 7.5° . The circular frame will be an aluminum ring with a diameter of two meters. This ring will be held up by steel pipe legs. The ring and legs will be attached so that they are secure, but also able to be disassembled and fit in the bed of a truck. Figure 10 shows the initial CAD model of our concept. A full CAD drawing is available in Appendix J.

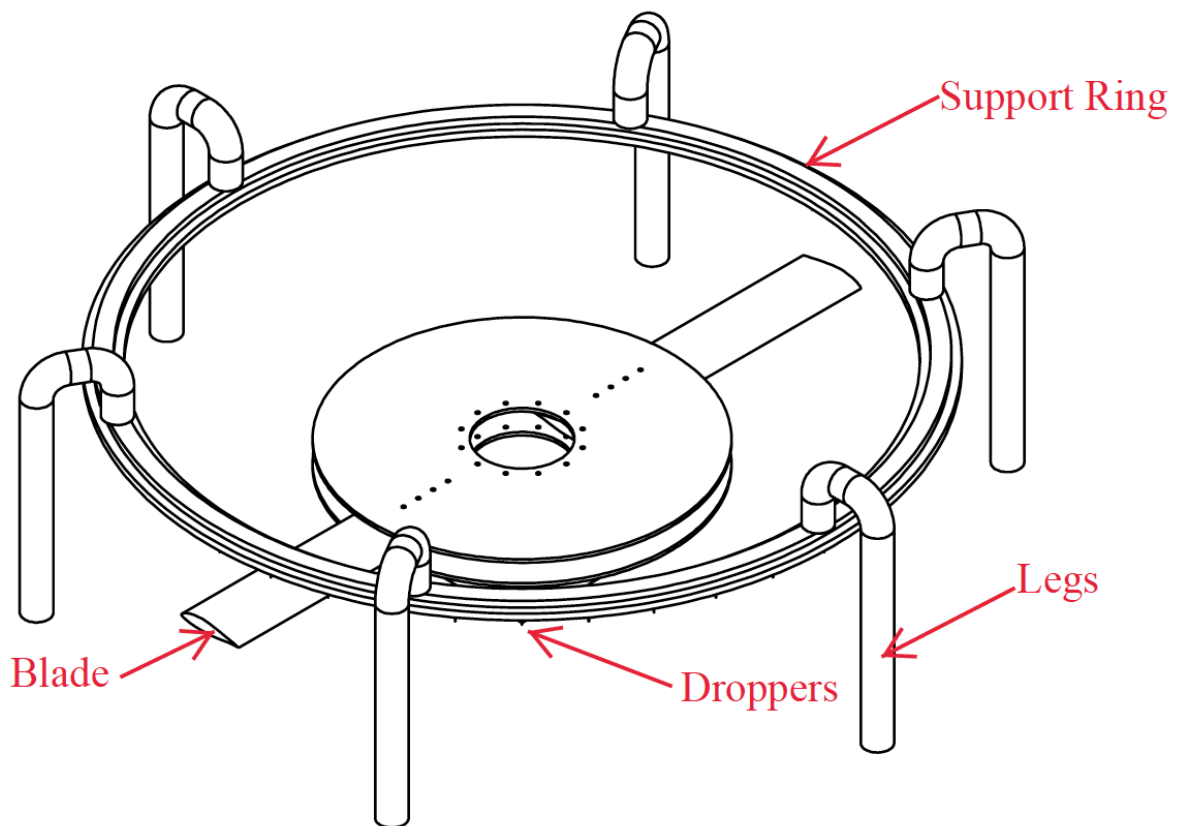


Figure 10. Solidworks model of initial CAD concept

We arrived at this conclusion after coming up with a wide range of ideas for water droplet creation and delivery. These ideas ranged from making prosthetic udders to a rack and pinion

driven dropper. We created a concept model prototype help explain our concept model designs visually. This model showcases the concepts we chose for the structural and water droplet delivery systems. An image of this concept model is shown in Figure 11.

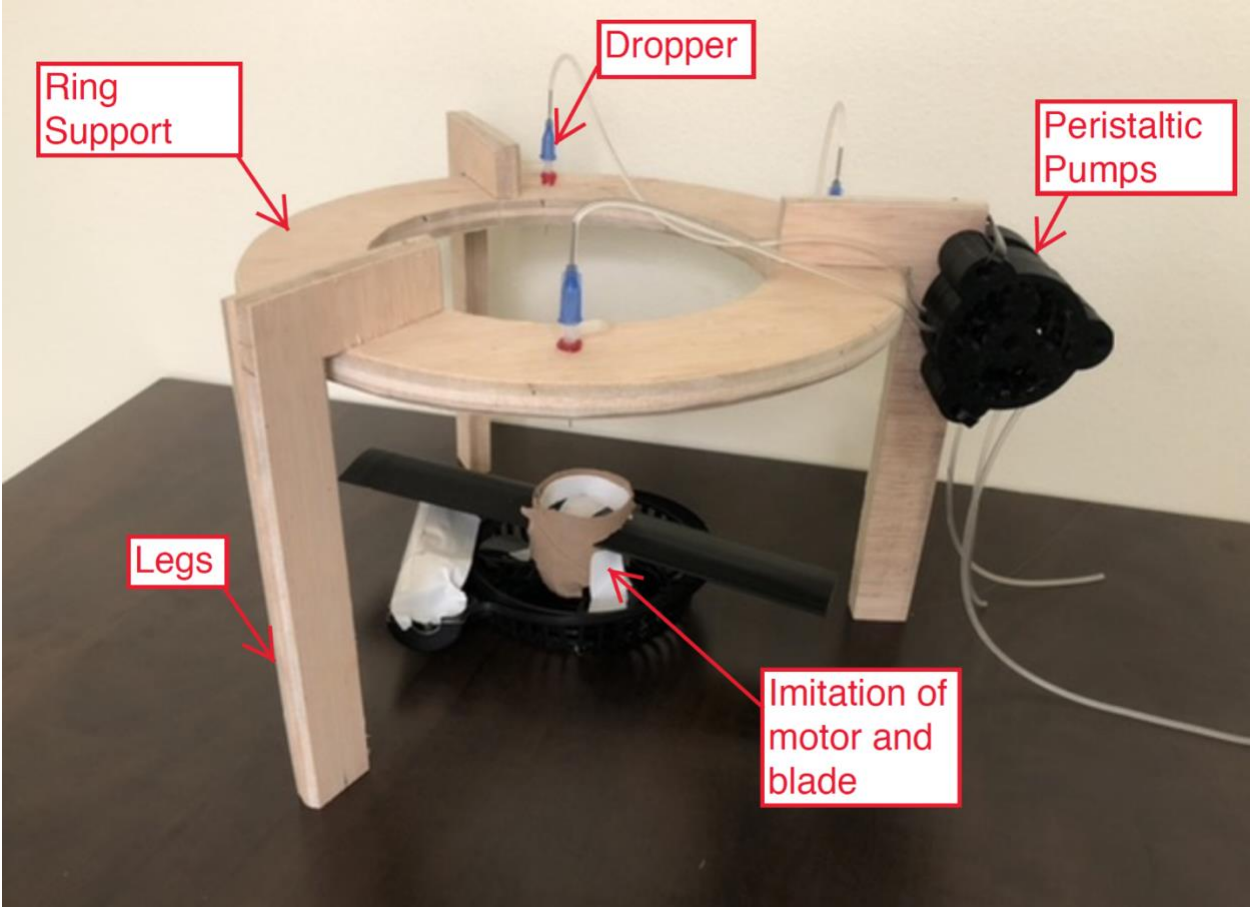


Figure 11. Concept model prototype

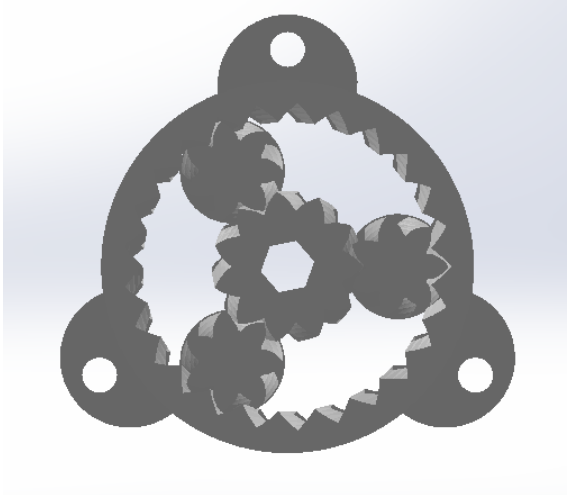


Figure 12. CAD model of a peristaltic pump

While testing this concept model we were able to determine which factors of the design were successful and which needed more attention. The structure and dropper system proved to be successful concepts. The structure was strong and stable, and the droppers delivered consistent drop sizes at specific locations. The location of the motor mount showed need for more attention. Operating the pump motor while it is mounted to the support structure allows vibrations from the motor to transfer into the structure. To avoid vibrations in the structure holding the nozzles we will separate the pump motor from the structure and keep the tubing connection from the pump to the nozzles. Due to the preliminary analysis that we have done, we are reasonably confident that our design can deliver the desired performance. With this desired performance there are inherent hazards. Since we shall be manufacturing the water delivery system, we shall remain focused on the hazards of that particular system, but for a full list of hazards and the way we would attempt to combat them, see the Hazard Checklist in Appendix G. The main hazards of the water delivery system involve getting water into electrical systems or potentially flooding the room in which the machine is operating.

5. Final Design

Our final design for our blade coating erosion testing machine is made up of two systems. These systems are the Fluid Delivery System and the Rotating Blade System. Figure 13 shows an isometric view of our design in SolidWorks. Next, we go over the two systems and the main components of each system.

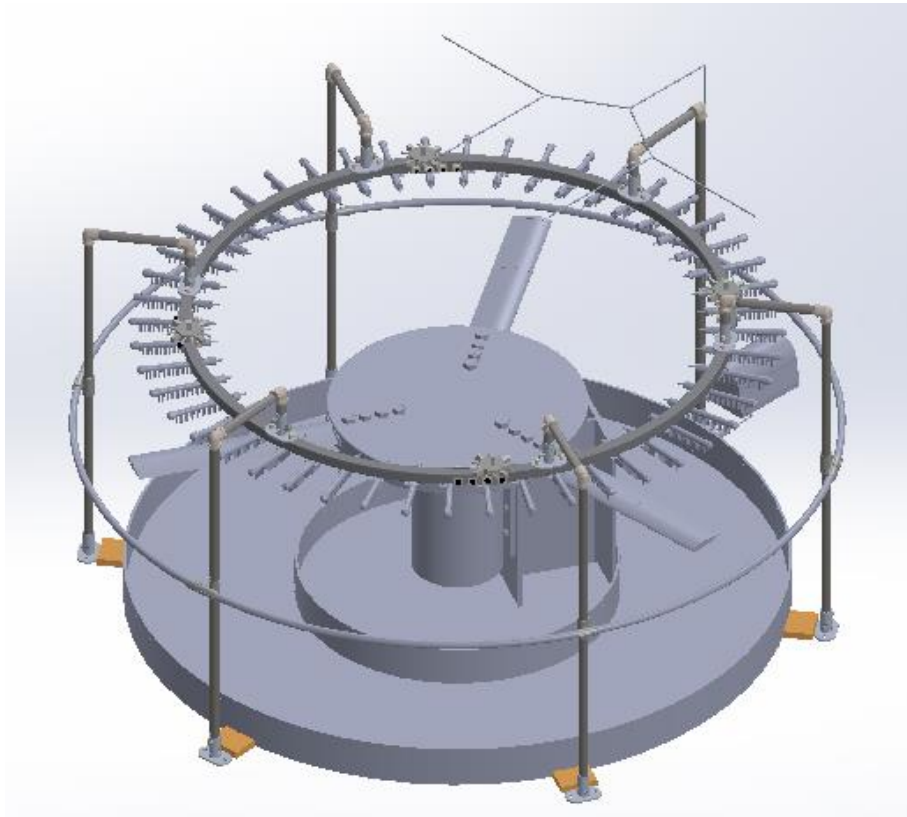


Figure 13. CAD assembly drawing

5.1 Fluid Delivery System Structure Design

Support Structure

The support structure consists of a ring held up by 6 equally spaced legs that can also be fixed to the ground. The legs are attached to the ring via two-bolt flanges. The support structure supports the tubing and fittings, and holds the dropper configurations over the rotating blade. It also supports the $\frac{3}{4}$ " PVC rail that goes around the outside of the legs to hold up our spray capturing curtain. The structural support design CAD model is shown in Figure 14.

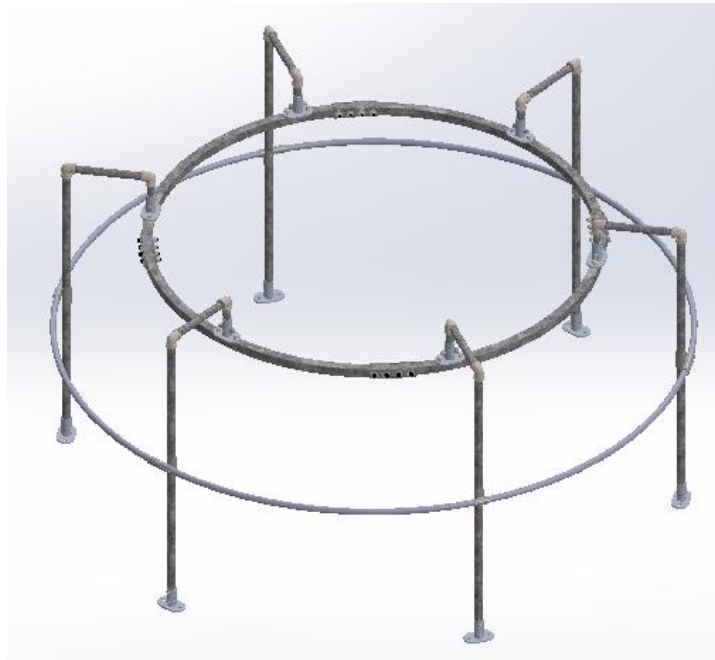


Figure 14. Support Structure design

Legs

The 6 legs are made of galvanized steel pipes and 90° fittings. They hold the dropper configurations over the rotating blade at the specification height and locations. The flanged feet allow the support system to be bolted to the ground, so no movement occurs during testing. An image of the leg design can be seen in Figure 15. A detailed list of the parts and materials that make up the leg is in the technical drawings in Appendix V.

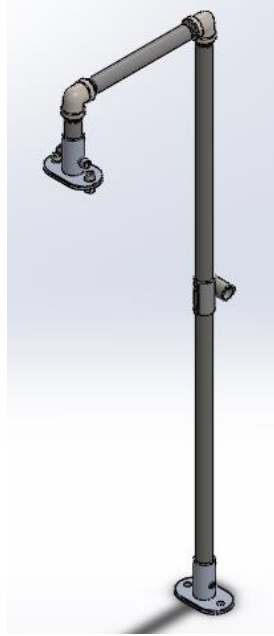


Figure 15. Leg design for structural support

We performed FEA on the legs to ensure they can handle design loads. We used a conservative load estimate of 50lbf load on each of the legs. The result of the study shows little deflection and acceptable stresses on the legs. Below, in Figure 16 and 17, are snapshots of the results of our study.

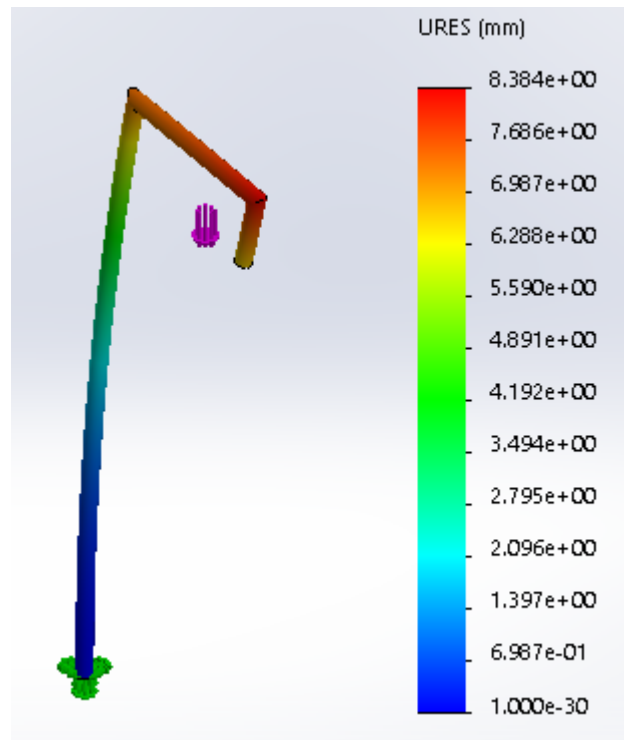


Figure 16. Crude leg FEA with conservative 50lbf load per leg

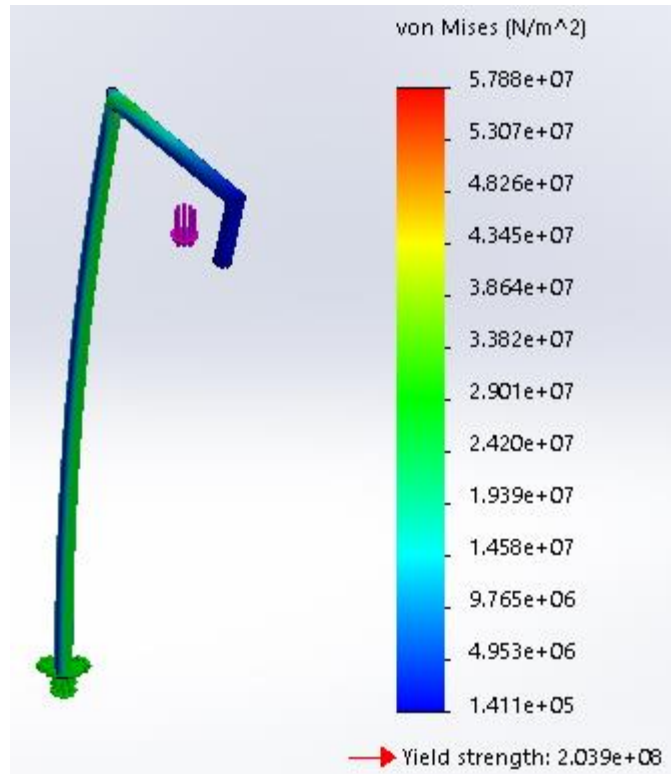


Figure 17. Crude leg FEA with conservative 50lbf load per leg

Ring

The ring holds the dropper configurations in the correct locations above the rotating blade. It is made of four 90° curved struts bolted together with curved brackets. This allows for disassembly for transportation or part replacement. The struts and brackets are made of zinc-plated steel which allow some corrosion resistance. However, some parts may need to be replaced if corrosion eventually occurs. The ring is connected to the legs via the same two-bolt flange used for the leg feet. An image of the ring design can be seen in Figure 18. A detailed list of the parts and materials that make up the ring is in the technical drawings in Appendix V.



Figure 18. Support ring dimensions

We performed FEA on the ring to ensure it can handle design loads. We used a conservative load estimate of 200lbf load on the ring. The result of the study shows little deflection and acceptable stresses on the ring. Below in Figures 19 and 20 are snapshots of the results of our study.

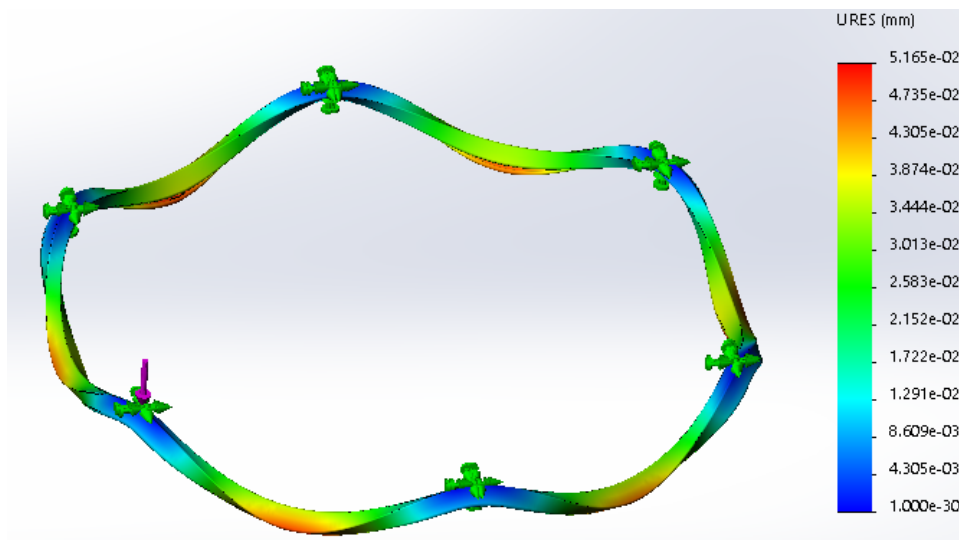


Figure 19. Crude Ring FEA with conservative 200lbf load

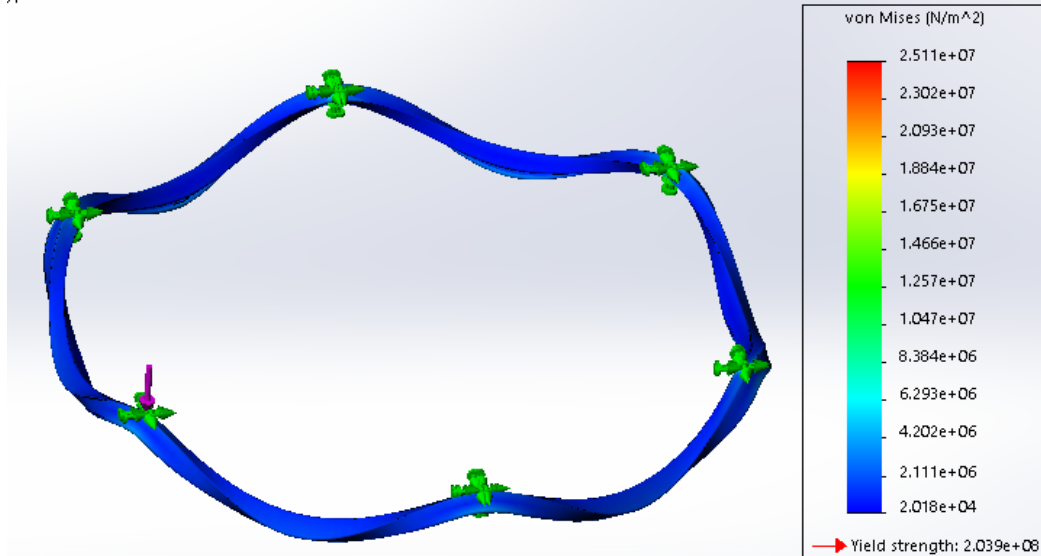


Figure 20. Crude Ring FEA with conservative 200lbf load

Table 4. Summary of results from Crude Structural FEA

	Max. Deflection Normal Conditions (mm)	Max. Stress Normal Conditions (MPa)	Yield Strength (MPa)	Factor of Safety
Ring	0.052	25.1	204	8.13
Leg	8.4	57.9	204	3.52

5.2 Fluid Path Design

We have chosen to use a peristaltic pump, as shown in Figure 21, to move the fluid throughout the fluid delivery system. The pump works by squeezing the tubing as the roller rotates. This pump is a positive displacement pump and it will work by drawing fluid from our reservoir and pumping that fluid at a constant flow rate to the nozzles. The pump depicted was specifically selected because it has variable speed capability, it has an adequate pressure rating, and it meets our design flow rate requirement.

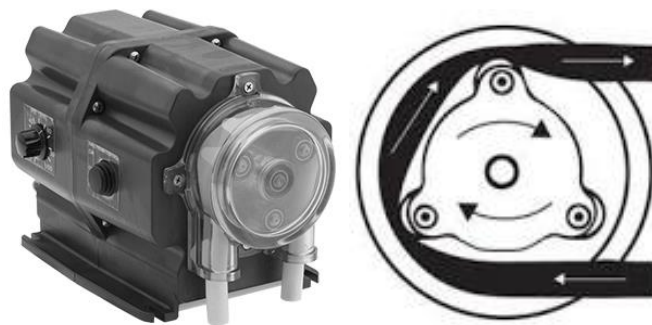


Figure 21. Peristaltic pump and inside view

The pump draws fluid through a hole in the wall of the reservoir, then through ¼" flexible tubing and an in-line filter. The filter is shown in Figure 22.



Figure 22. In-line tubing filter

The ¼" tubing is connected to the inlet of the pump with a barbed reducer fitting as shown in Figure 23.



Figure 23. Barbed reducer tubing fitting

The outlet of the pump is connected with another barbed reducer fitting to another length of ¼" tubing. This tubing is routed up the nearest leg to the top face of the ring assembly. There, it splits into two, and then four lengths of ¼" flexible tubing with 3 total barbed Y-connectors. The barbed Y-connectors are shown in Figure 24.



Figure 24. Barbed Y-connector

The four new lengths of ¼" tubing each go to the inlet of a 1:12 flow splitter. The 1:12 flow splitters are made of a custom 6061 aluminum body with thirteen ¼" tubing to ¼" NPT threaded male adapters. A 1:12 flow splitter is shown in Figure 25.

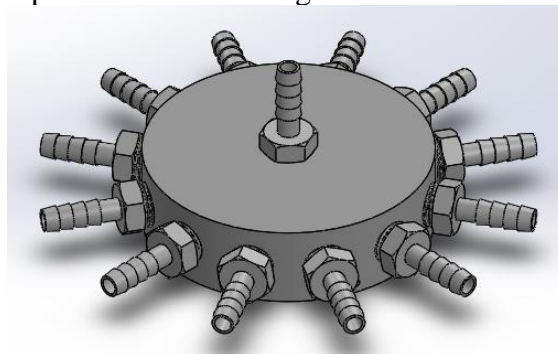


Figure 25. 1:12 flow splitter

These adapters allow ¼" tubing to attach to the 1:12 splitter body. The inlet of the 1:12 flow splitter is on the top face of the body. In the design, flow from the inlet ¼" tubing enters the body and splits evenly 12 ways before exiting each of the 12 outlet ¼" tubing lengths. Each of these outlet ¼" tubing lengths routes to a dropper configuration assembly.

Dropper Configuration

The dropper configuration assembly is shown below in Figure 26.

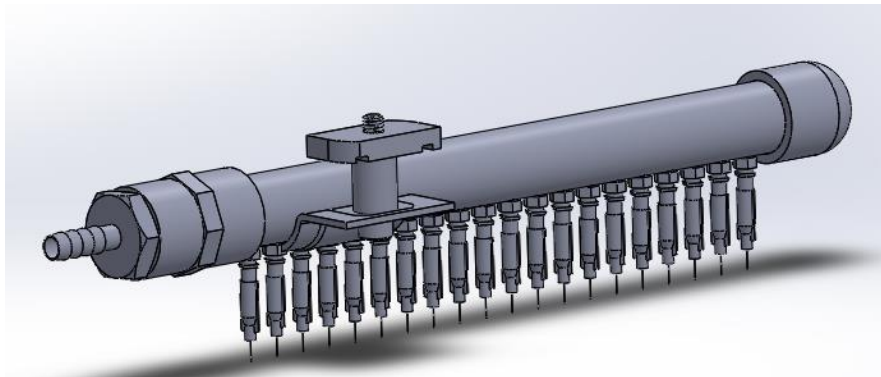


Figure 26. Dropper configuration

A detailed list of the components that make up the dropper assembly is in the technical drawings Appendix V. The ¼" tubing that comes from an outlet of the 1:12 flow splitter is connected to the inlet of the dropper configuration. This inlet is a ¼" tubing to ½" NPT threaded male adapter as shown in Figure 27, which is connected via threads to the dropper assembly PVC. This part is shown in Figure 28.

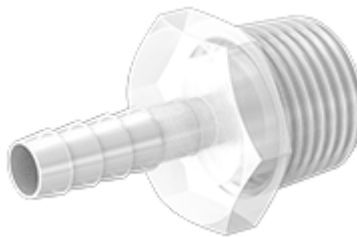


Figure 27. ¼" tubing to ½" NPT male adapter

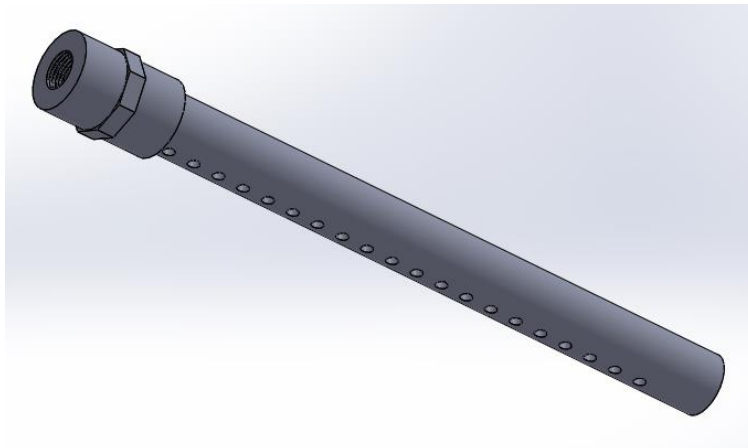


Figure 28. Dropper Assembly PVC

The dropper assembly PVC has a PVC end cap to prevent flow from escaping the end of the pipe. The dropper assembly PVC also has 20 threaded holes in line along its length. Each of these holes will be joined via threads with a thread to luer lock adapter as shown in Figure 29.



Figure 29. Thread-to-luer lock adapter

These adapters allow a connection from the PVC pipe to our nozzles. A nozzle is shown in Figure 30.



Figure 30. 32 Ga nozzle

The nozzles are fit on the end of the adapters via luer lock connections.

The dropper configurations are held in place along the ring with a pipe clamp connection. The components of this connection are detailed in the technical drawing package in Appendix V. This clamp connection is shown in Figure 31.

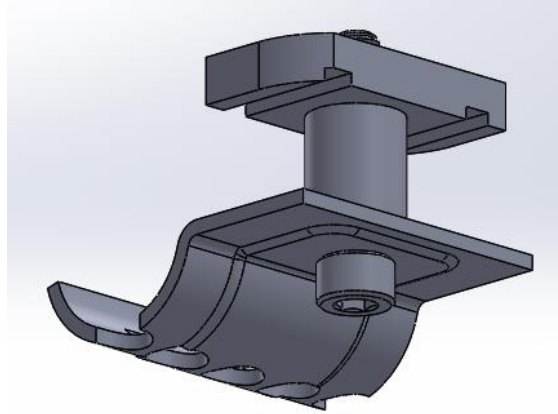


Figure 31. Dropper clamp connection

The clamp has holes in it where the dropper nozzles fit into the clamp. The center clamp hole has the 4th dropper nozzle from the inlet side of the dropper PVC going through it. This ensures vertical alignment between the droppers and the exposure zone of the rotating blade system.

Spray Collection Curtains

The spray collection curtains will hang from the $\frac{3}{4}$ " PVC rail that is connected to the outside of the legs with through-hole reducers as shown in Figure 32.



Figure 32. PVC rail

The PVC rail is made up of three lengths of $\frac{3}{4}$ " schedule 40 PVC pipe. For assembly, each of these lengths are fed through a through-hole reducer and flexed to fit into the through hole reducer on a neighboring leg. Once each $\frac{3}{4}$ " PVC pipe is held by two through-hole reducers, the ends of the PVC pipes are connected with $\frac{3}{4}$ " PVC fittings to create a circular rail. The four waterproof curtains are clipped onto the PVC rail with the designated clips and grommet holes. The curtains are pulled tight and connected to the inside face of the outer wall of the reservoir with plastic rivets. This allows captured spray from droplet impacts to be funneled into the reservoir. The curtains can be trimmed along the bottom to eliminate extra length.

5.3 Reservoir Design

The reservoir holds the water that has been captured from falling drops and supplies that water back to the peristaltic pump. The reservoir also has holes around the top of the walls for the spray curtains to be attached with plastic rivets. An image of the reservoir assembly is shown in Figure 33.

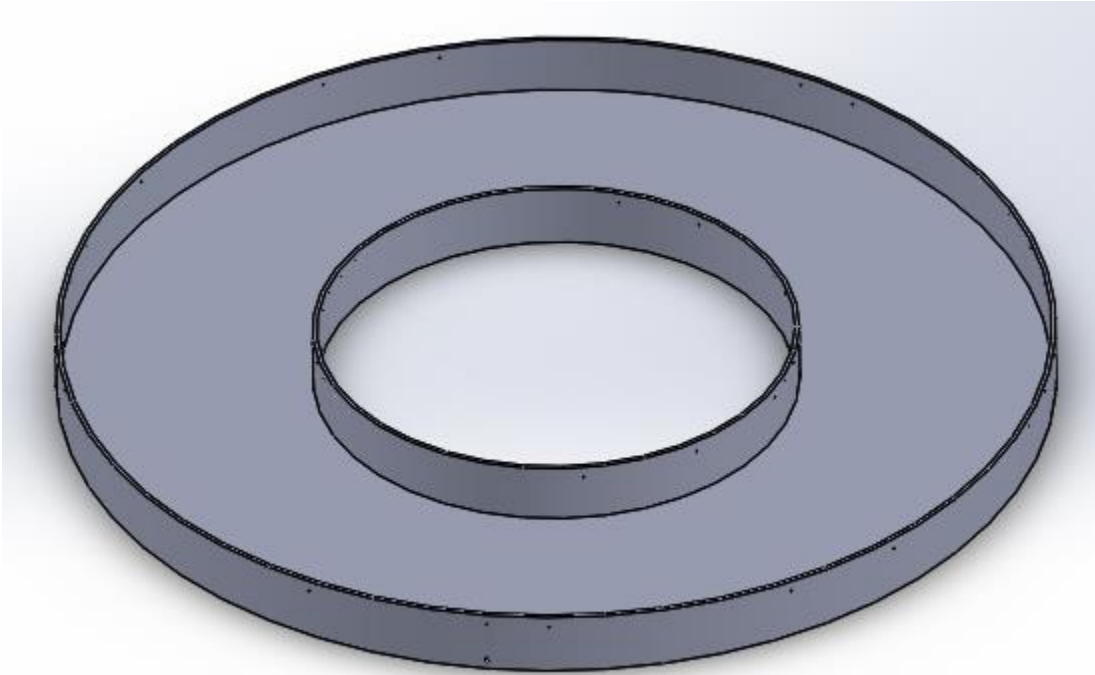


Figure 33. Reservoir

We believe that a plastic pool or tank with similar dimensions would be a good starting point for manufacturing this component. We were unable to find a pool or tank that fit the cost and geometric criteria for this project during the time we had available. Therefore, we did not select a stock part or raw materials to construct the reservoir from. Once a stock part is obtained, we recommend using stiff plastic sheeting and caulk to create a water-tight wall along the inside diameter of the reservoir.

5.4 Rotating Blade System

The Rotating Blade System seen below in Figure 34 consists of four main components, the disk, the blades, the sheaths, and the motor. We made the decision to have a large central disk as a mounting port for both safety and rotor balance reasons. The larger the disk, the smaller the blades need to be which decreases the chance that they are going to fly out of their mounts. And one of the most easily balanced rotating objects is a circular disk.

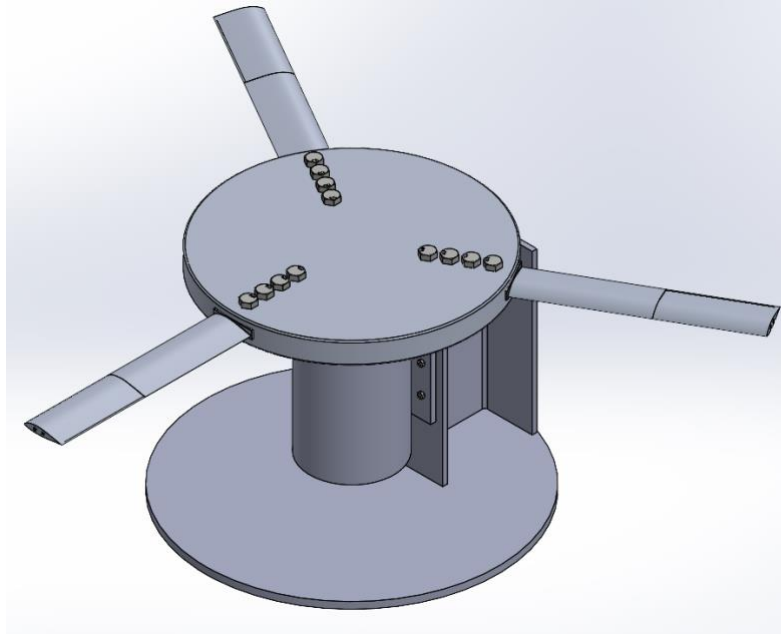


Figure 34. Rotating Blade System

We needed a secure method to spin three sizable aluminum airfoil blades as seen in Figure 35 up to 100 m/s, so we needed to design a system that had very secure connections. Large tabs at the mounting side of the blade allows for easy alignment and for four 30 mm diameter bolts to attach each blade to the disk.

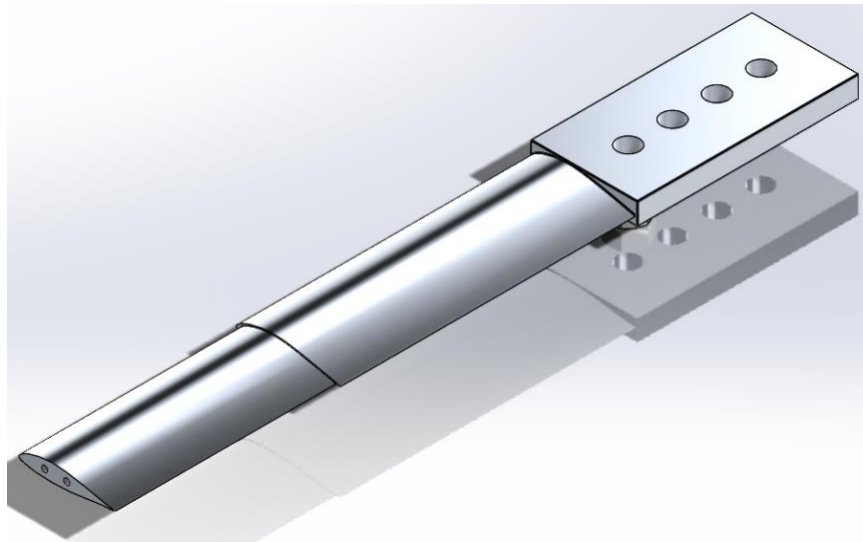


Figure 35. DU 96-W-180 6061 aluminum airfoil blade

Those mounting locations line up with holes in the central disk 36, which has three ports spaced 120° from each other. The disk is shown below in Figure 36.



Figure 36. Central mounting disk

We decided on three ports and three blades with the input of our sponsor, TTP because that is what wind turbines have, it would allow for more testing, and a three blade system is more easily balanced than a two blade system. The last 30 cm of each blade is slightly smaller than the portion closer to the disk, to allow for a mounting sheath to be attached. The sheath is shown below in Figure 37.

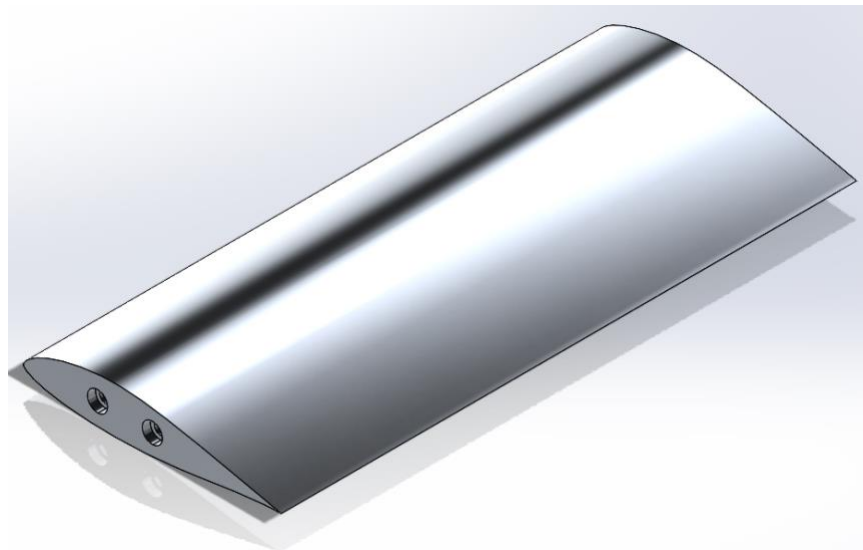


Figure 37. Blade sheath

This sheath can be detached from the main blade so that they can have fiberglass or carbon fiber layups on them more easily. It is a requirement from DNVGL that the LE solution be applied to the material that is similar to what the wind turbine blade is made of, so we need to be able to have some kind of layup easily applied to the sheath, so we made it detachable.

All of these components need to be spun up to a very high speed, so the final main component of our system is the motor. Our desired elements were that it could provide a constant speed of 955 RPM (100 rad/s), had 5 hp, was waterproof, and could be mounted with the shaft in a vertical orientation. We needed it to provide 5 hp because the blades will be impacting water drops at a very high speed, which is an impact the motor must constantly overcome. Our calculations had several unverifiable assumptions, but it was agreed with our sponsor that a 5 hp motor would have enough power to overcome the constant impact of water and air resistance. Finding a motor that has a variable speed drive between 900 RPM and 1000 RPM that could also provide 5 hp was not possible if we wanted to be anywhere near our price range. We therefore settled for a 900 RPM motor and chose the cheapest motor that was also described as ‘drip-proof’ (none are truly waterproof, but drip-proof means they are fine to be used in applications where they are getting wet), the PEWWE5-9-254T from Worldwide Electric.

A necessity of the system is that the motor needs to have the shaft vertically oriented. In order to achieve that we used a combination of inch thick steel plate and W14x90 I-beam. These were used to ensure that little to no deflection occurs at the motor. The remaining components are to ensure that all of these components are attached properly. Analysis of the bolted connections can be found in the Design Verification section.

5.5 Safety and Maintenance

Our design for the Water Delivery System has minimal issues with potential safety hazards. The only moving part is the peristaltic pump, which the sponsor would purchase as a finished product from a manufacturer. The tip-over risk is very minimal as the design is so wide and not very high off the ground. For a more complete look at the potential areas of concern and what we have done to address them, we performed a Failure Modes and Effects Analysis that can be found in Appendix P.

The key to maintaining this device will be periodic inspection of everything to ensure that there will be no operating issues. There should be regular checks on the in-line filter to make sure that it has not become saturated with particulates. The filter should be examined after each use. The nozzles should also be checked for any build up every time that the filter is replaced. This can be done by removing the nozzle and visually inspecting the metal end. If there is a build-up, then there are two options: clean the nozzles by immersing them in a solution of vinegar and water and then scrubbing them clean, or purchasing new nozzles.

The Rotating Blade System has much greater risk of potential safety hazards. Given the motor will be spinning the system at 900RPM, if any of the bolts in the system were to fail there would be a dramatic and catastrophic failure. The way to prevent anyone from potentially getting hurt is to set the machine to running and then vacate the room.

Due to these bolts being so critical, consistent inspections and replacements will be required. Every 100 hours of operation we recommend inspection of every bolt and replacing them if wear is evident.

5.6 Cost Overview

We have done our best to source materials from cheap locations and find the simplest assembly process for our sponsors to assemble. Broken down into subsystems in Table 5 below is the cost, with the total at the bottom. A more detailed description of the cost breakdown can be seen in the indented BOM in Appendix L.

Table 5. Summarized Bill of Materials

Description	Qty	Cost	Total Cost
Leg Assembly	6	\$ 171.43	\$ 1,028.57
Ring Assembly	1	\$ 435.07	\$ 435.07
Reservoir Assembly	1	\$ 2.58	\$ 2.58
Fluid Path Assembly	1	\$ 906.08	\$ 906.08
Dropper Assembly	1	\$ 843.59	\$ 843.59
Curtain Hanging Parts	1	\$ 125.56	\$ 125.56
Rotating Blade Assembly	1	\$ 13,038.55	\$ 13,038.55
Purchased Parts Total			\$ 16,380.00

This is well over our initial budget of \$1000, so we are slightly disappointed with this cost. That said, we have had our scope expanded to include the rotating blade system. Even without the rotating blade system, our price is over the \$1000 mark because we want to have the system be as durable as possible. The rotating blade system was not given an initial budget and was always going to be far more expensive than the water delivery system due to the custom machining of the disk, blades, and sheathes.

6. Manufacturing

This section outlines the steps we took to construct our verification prototype and includes procurement, manufacturing, assembly, and outsourcing. Our verification prototype is a cost-effective design for one dropper arm configuration which is supplied the design flowrate directly by a smaller capacity peristaltic pump drawing from a small reservoir.

6.1 Procurement

We purchased materials and components during Fall quarter 2020. These include ¼" flexible tubing, 20 count of 10 different sizes of blunt needle tips ranging in size from 30Ga to 16Ga, a 12" long by ½" diameter PVC pipe threaded at one end, all-plastic bonding glue, various tubing fittings, 1mL syringes, test tubes, and a small peristaltic pump. These were purchased at ACE hardware and through Amazon for very little cost.

6.2 Manufacturing

The verification prototype is shown below. It was constructed with mostly stock parts and fittings assembled as shown in Figure 38.

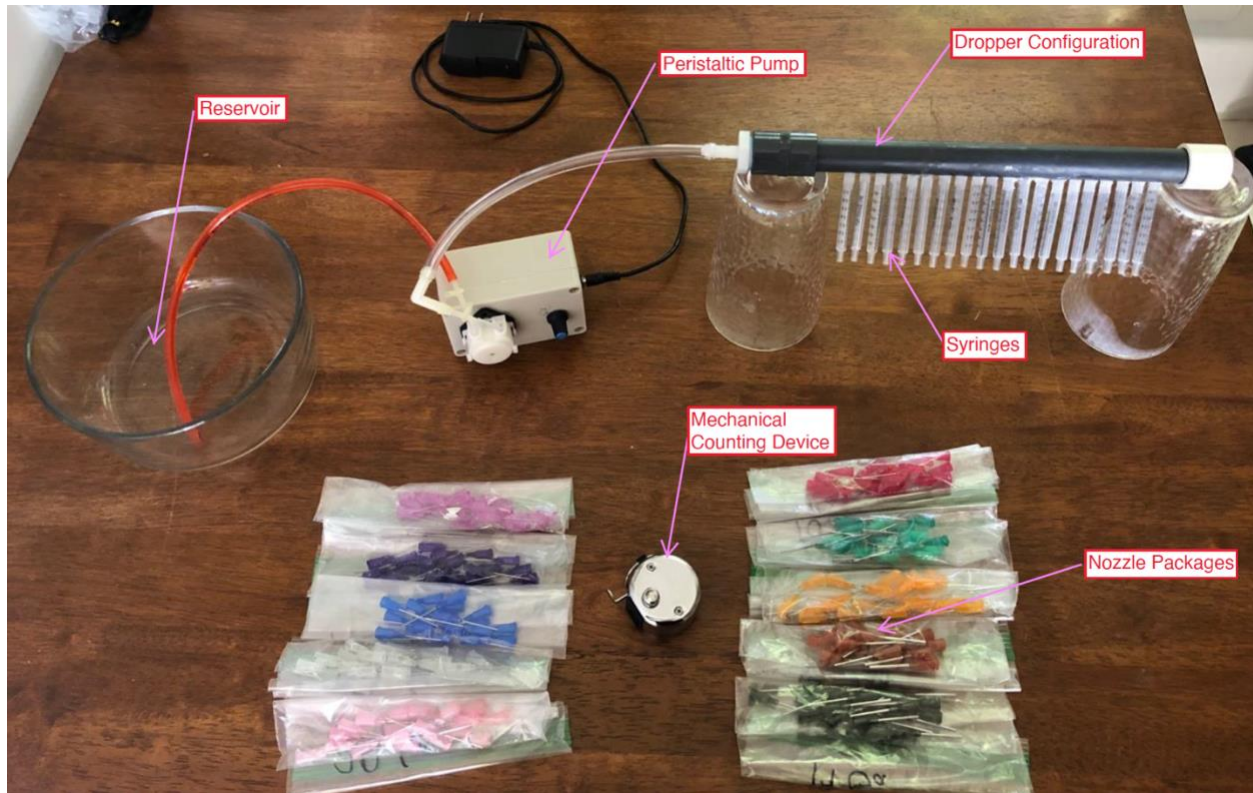


Figure 38. Verification prototype for nozzle sizing test.

The only custom part of our verification prototype is our dropper configuration which is made from 20 1mL syringe bodies compression fit and glued into $\frac{1}{4}$ " holes along the PVC pipe spaced at 1cm apart. The custom dropper configuration can be seen in Figure 39. These syringe bodies made up the outlets from the PVC pipe and can easily attach to our dropper nozzles via luer lock connection. The manufacturing steps for this custom part were as follows:

1. Drilled 20 count $\frac{1}{4}$ " holes spaced at 1cm apart center-to-center along the length of the $\frac{1}{2}$ " PVC pipe.
2. Completely cleaned the plastic debris out of the holes and $\frac{1}{2}$ " pipe.
3. Cut the handle end off of 20 syringes. Sanded the ends until they snugly fit into the $\frac{1}{4}$ " holes.
4. Used all-plastics glue to secure and seal the syringes into the drilled holes in the PVC pipe.
5. Applied Loctite sealing threadlocker to $\frac{1}{2}$ " PVC endcap. Pushed endcap onto non-threaded end of PVC pipe.
6. Applied Loctite sealing threadlocker to external threads of $\frac{1}{2}$ " thread to $\frac{1}{4}$ " tubing adapter. Installed external threaded end of adapter into internal threaded end of PVC pipe.
7. Installed the appropriate nozzle size onto each of the syringe outlets via luer lock connection.



Figure 39. Custom dropper configuration.

Our verification prototype worked for our testing purposes, but it is not capable of handling the longevity demanded by our final design specifications. The parts and manufacturing of the final dropper configuration assembly will be described with the rest of the custom parts we designed in our Final Design section.

6.3 Assembly

Our verification prototype is a system that moves water from a small reservoir via a peristaltic pump to the manufactured dropper assembly, out the nozzles, and into collection test tubes. The assembly steps for our verification prototype were as follows:

1. Filled a large bowl with water. This was the reservoir for the verification prototype.
2. Connected the inlet tube of the peristaltic pump to one end of the short flexible 1/8" tubing piece with a straight fitting.
3. Submerged the other end of the short flexible 1/8" tubing piece into the bowl.
4. Connected the outlet tube of the peristaltic pump to one end of the long flexible 1/4" tubing piece with a 1/8" to 1/4" expander fitting.
5. Connected the other end of the long flexible 1/4" tubing piece to the 1/4" tubing fitting end of the thread to tubing adapter on the custom dropper configuration.
6. Installed the appropriate nozzle size onto each of the syringe outlets via luer lock connection.
7. Arranged test tubes and collection cups under nozzles. Ensured that test tubes only collect from one dropper nozzle throughout any tests.

For testing, the peristaltic pump was calibrated to the design flowrate of a single dropper configuration. During the test, we counted and collected drops from individual nozzles in test tubes. We were able to take the mass of the fluid collected and solve for the average diameter of the drops produced. Multiple tests of this experiment with different nozzle sizes allowed us to develop the curve fit, shown in Figure 41, for drop size produced from our nozzles versus nozzle diameter and solve for the appropriate nozzle size for our design. Figure 40 below shows the testing configuration.



Figure 40. Experimental setup for drop collection with our verification prototype.

6.4 Outsourcing

We did no outsourcing for producing our prototype. Due to COVID-19, our sponsors requested that we do not build the final design and instead do design work for the rotating blade system. All of the manufacturing for the final designs shall be done by TTP. More information about manufacturing and assembly of the custom components of our design is located in the Final Design section.

7. Design Verification Chapter

We were able to test our structural prototype to verify the drop size and rainfall intensity design specifications for our fluid delivery system. We discuss the results of testing in this section, while the detailed test procedure and data collected during the test can be found in Appendix T. We show that our design meets the remaining specifications through design analysis, mainly FEA. All of these parameters can be found in our Design Verification Plan in Appendix M.

7.1 Dropper Configuration Verification

The specifications that we were able to test are the production of consistent 2 mm diameter rain drops from the nozzles, and a total rainfall intensity of 32.5 mm/hr. The test method that we utilized to verify these specifications included calibrating our peristaltic pump to the design flow rate for one dropper configuration. This calibrated design flow rate is $1/48^{\text{th}}$ of the total flow rate necessary to meet our 32.5 mm/hr rainfall intensity across the specification 20 cm exposure zone. It is $1/48^{\text{th}}$ of the total design flow rate because our structural prototype dropper configuration is 1 of 48 total dropper configurations in our full fluid delivery system design. With the successful

operation of one dropper configuration at 1/48th of the total design flow rate, we proved our prototype’s ability to meet the total rainfall intensity specification of 32.5 mm/hr.

We were able to test the diameter of drops produced by different nozzle sizes. During our first experiment we ran 9 total trials while operating our structural prototype at the calibrated flow rate. These trials covered 5 different nozzle sizes. As we progressed through our experiment, we realized that the drops produced by even the smallest nozzle sizes we had access to at the time were too big according to our specification. As a result, we decided to focus our tests on the smaller nozzle sizes we had access to. With the data we collected we were able to create a trend line that estimates what nozzle size we will need in order to achieve our drop diameter specification. A 2nd order polynomial trend line seems to best represent our data. According to the trend in the data collected in our first experiment and the desired specification drop diameter, we projected that we need nozzles with an ID of 0.08 mm. For our second experiment we were able narrow in on the correct dropper nozzle ID using the previous projection. We ran 5 trials for 32Ga nozzles and 5 trials for 34Ga nozzles. The results from all of our trials from experiment 1 and 2 are shown in Figure 41.

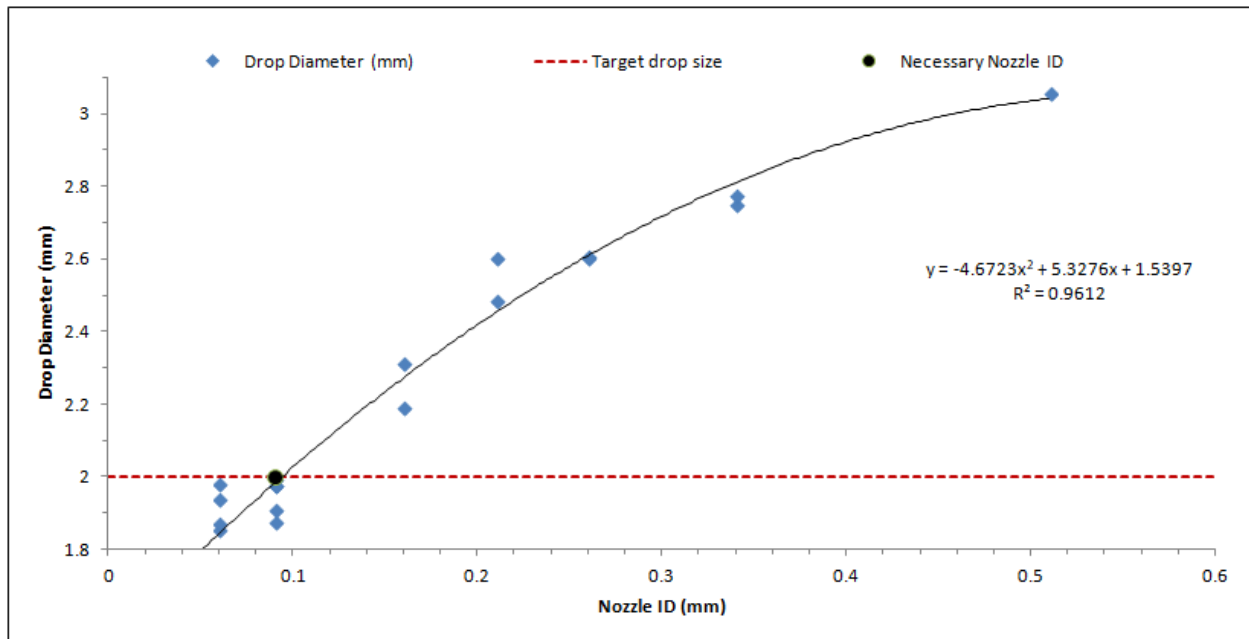


Figure 41. Average drop size results and trendline from all trials in experiments 1 & 2

Table 6 shows the results of our statistical analysis of our experimental data. These results are calculated in an Excel file which is in Appendix T.

Table 6. Statistical results for each nozzle size

Nozzle Size (Ga)	ID (mm)	Drop Diameter (mm)
23	0.34	2.7646 + 0.0831 - 0.0884
25	0.26	2.6058 + 0.0124 - 0.0126
27	0.21	2.5547 + 0.3231 - 0.4359
30	0.16	2.2518 + 0.3344 - 0.4826
32	0.09	1.9412 + 0.0753 - 0.0817
34	0.06	1.8809 + 0.1557 - 0.1869

Due to our relatively few trials with each nozzle size during the first experiment, our uncertainties in the results for drop diameter produced have large uncertainties when solving for 90% significance. During our first experiment we performed 2 trials per nozzle size for the 23Ga, 25Ga, 27Ga, and 30Ga nozzle sizes. During our second experiment we performed 5 trials per nozzle size for the 32Ga and 34Ga nozzle sizes. It is also important to note the reason why the uncertainty numbers are not bilaterally symmetrical. We measured drop size using mass of collected drops, so our mass uncertainties are bilaterally symmetrical. This symmetry in drop mass uncertainties does not transmit to drop diameter uncertainties. As a sphere grows, adding more mass to it results in smaller changes in diameter. Therefore, the absolute value of the positive diameter uncertainty will always be a little less than that of the negative diameter uncertainty.

We saw these uncertainties shrink when we increased the number of trials with each nozzle size during our second experiment. The statistical analysis of our second experiment data shows that we should move forward with the 32Ga nozzle size in our final design.

Another valuable result of our test of our structural prototype was the realization that we needed a more robust design for our final prototype design. Overall, our structural prototype worked well for our experiment needs. However, during the setup and practice trials of our experiment we found a couple of leaks in the compression fit between the PVC pipe and syringe bodies of our custom dropper configuration. We were able to seal these leaks for the remaining tests, but they indicated that the design and manufacturing method of our custom dropper configuration would not meet the longevity specification for our fluid delivery system. This led to a more robust design of the dropper configuration design which is discussed in the Final Design section.

7.2 Finite Element Analysis

In order to ensure that the components of the rotating blade system would not fail in use, we conducted finite element analysis (FEA) on each component and analyzed the yielding factor of safety for each component. The component we did the most extensive analysis on was the bolts fastening the blade to the rotating disk. We believe the bolts to require the most analysis because

we anticipated the most stress on them while the tester is in use and because they would cause the most possible harm if a failure was to occur. For our FEA we focused on the series of four bolts, with the center of each bolt on the midplane of the blade's width, assembled to one of the aluminum blades. The parameters for the bolts and blade are shown in Table 7.

Table 7. Bolt and Blade Parameters

Steel Bolts		6061 Aluminum Blade	
Yield Strength (MPa)	420	Yield Strength (MPa)	310
Young's Modulus (GPa)	200	Young's Modulus (GPa)	69
Poisson's Ratio	0.3	Poisson's Ratio	0.35
Material Density (kg/m ³)	8,050	Material Density (kg/m ³)	2,710
Bolt Spacing (mm)	60	Thickness (mm)	22
Diameter (mm)	30	Length (mm)	1000
Number of Bolts	4	Airfoil Shape	DU96-W-180

The free body diagram with the forces on the rotating blade are shown in Figure 42.

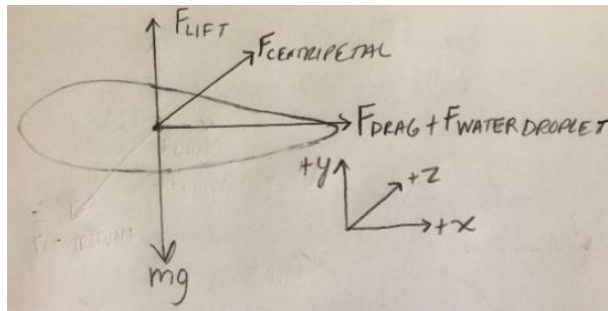


Figure 42. Blade FBD

In our analysis, we were only concerned with the in-plane shear stress on the bolts as it pertains to the X-Z plane shown in Figure 42. Therefore, the forces of concern in the study were drag force and centrifugal force. A table of the values for the force magnitudes is shown in Table 8. We were able to calculate that the total centrifugal force on the blade spinning at 100 rad/s was 50,901.6 N using the excel spreadsheet in Appendix Q.

Table 8. Bolt Forces

Forces on Bolt	
Centrifugal (N)	50,901.6
Drag (N)	0.7

We were able to calculate the stress on the four bolts depending on the in-plane forces and the positions of the bolts and applied forces relative to an arbitrary origin. These calculations are shown in Appendix R and were based on the loading of the system shown in Figure 43.

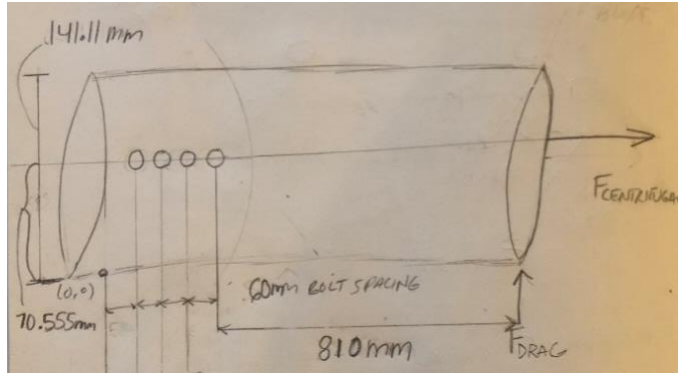


Figure 43. System Loading

The particular FEA we conducted was for a snapshot of the rotating blade system when the blade is rotating at the desired angular velocity of 100 rad/s. Therefore, we used a steady state, linear, static analysis for our Abaqus Modeling. The assembly we used in our analysis was one blade with four bolts as shown in Figure 44.

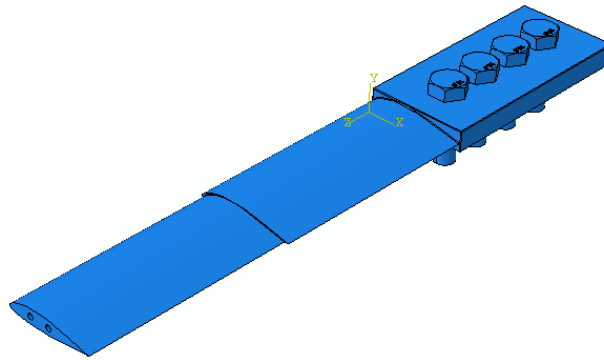


Figure 44. Blade/Bolt Assembly

We ended up making two different FEA models to ensure that both were yielding similar results. The only difference between the two models was the Abaqus loading functionality that we used to model the centrifugal force. In both models, we applied the drag force as a point load on the farthest point at the end of the leading edge to receive a conservative estimate. In the first model, we applied the centrifugal force as a body force by converting the force to a force/volume. Therefore, knowing the centrifugal force was 50,901.6 N and the volume of the blade was 0.002707 m³, we applied a 18,803,705 N/m³ body force over the entire blade. The centrifugal body force loading of the first model is shown in Figure 45.

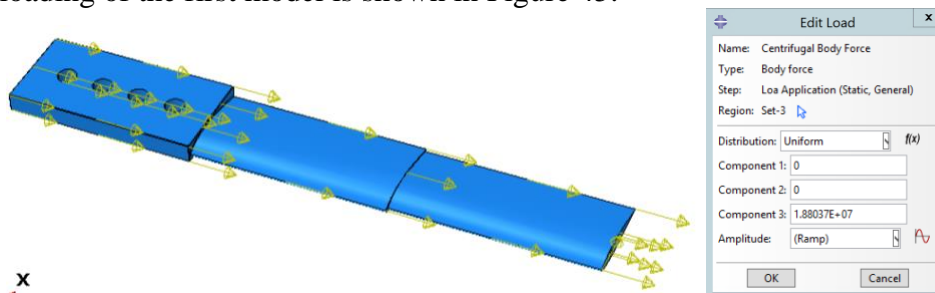


Figure 45. Model 1 Centrifugal Body Force Loading

Our second model used Abaqus's centrifugal rotational body force loading function. In this case, we didn't need to enter a force value and only needed to select the entire blade, input two points on the axis of rotation, and 100 rad/sec for angular velocity. The centrifugal rotational body force loading of the second model is shown in Figure 46.

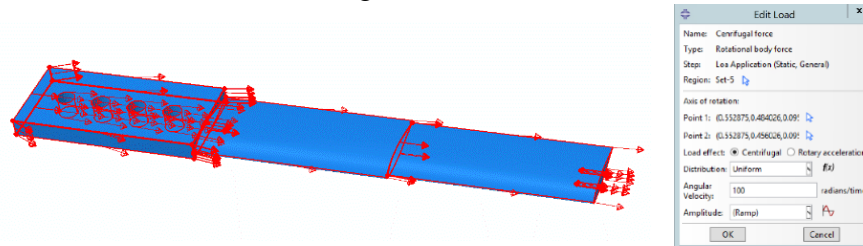


Figure 46. Model 2 Centrifugal Rotational Body Force Loading

We modeled the boundary conditions for both models by selecting the cross sections at the bottom and top of the bolt and constricted linear displacement in the X, Y, and Z directions. The boundary conditions used for both models is shown in Figure 47.

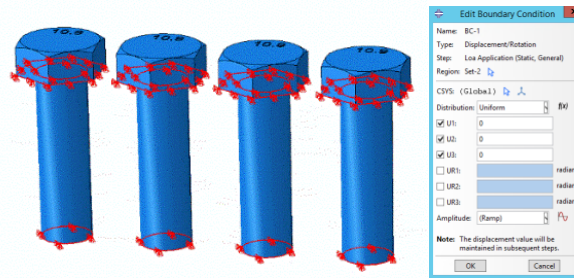


Figure 47. Bolt Boundary Conditions

For both models, we used standard, 3D stress, tetrahedral, quadratic elements. Our first model that used a body force to model the centrifugal force, had 59,913 degrees of freedom. Our meshed model 1 assembly is shown in Figure 48.

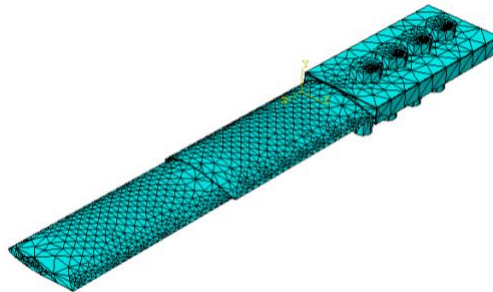


Figure 48. Meshed Model 1 Assembly

There were no warning messages regarding the quality of the mesh we used. Therefore, we concluded that the mesh had sufficient quality because it passed the aspect ratio and min/max angle criteria Abaqus checks for. When conducting the mesh convergence study, we checked the following node shown as a red dot in Figure 49.

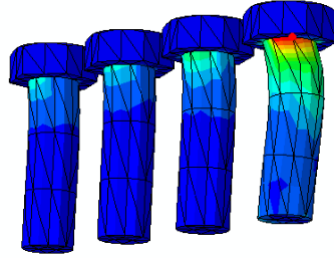


Figure 49. Node Checked for Model 1 Mesh Convergence Study

The mesh convergence plot showing resulting max Von Mises stresses in the bolts versus degrees of freedom ranging from 35,148 to 58,913 degrees of freedom is shown in Figure 50.

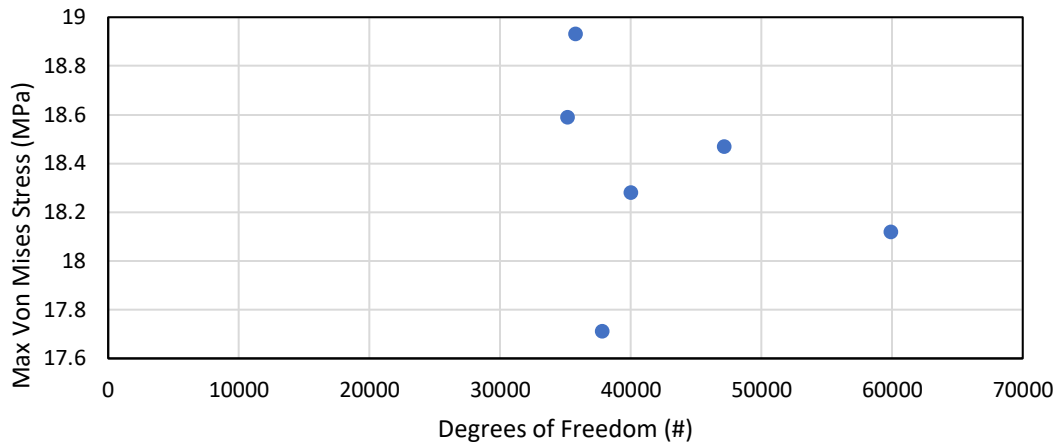


Figure 50. Model 1 Mesh Convergence Plot

It is important to note that anything less than around 35,000 degrees of freedom did not have a dense enough mesh for Abaqus to yield a result. In addition, as the model's degrees of freedom increased beyond 60,000, the Von Mises stress results exponentially increased, which was exaggerated by the continually decreasing element edge lengths. This is noted by the fact that 350,000 degrees of freedom gave a result of 38.34 MPa. Therefore, we concluded that the model had converged at 59,913 degrees of freedom because anything larger produced stress values that were drastically outside the range of the first 6 plots. In addition, this conclusion was supported by the fact that our hand calculations gave an expected stress of 18.02MPa, which was very close to the max stress of our converging model. However, in order to be even more certain of this convergence, we analyzed the previously mentioned second model that instead used the rotational body force to model the centrifugal force. The second model we used for our results had 159,330 degrees of freedom. Our meshed model 2 assembly is shown in Figure 51.

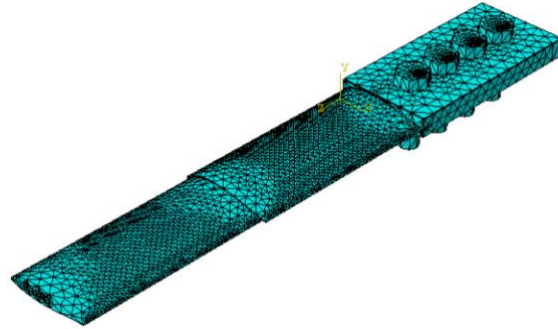


Figure 51. Meshed Model 2 Assembly

There were no warning messages regarding the quality of the mesh for our second model either. Therefore, we concluded that the mesh we used for our second model also had sufficient quality. When conducting the mesh convergence study, we checked the following node shown as a red dot in Figure 52.

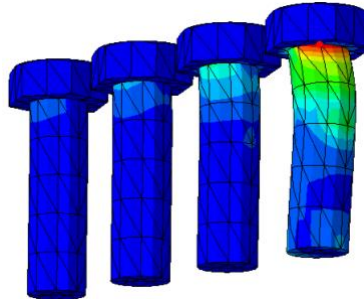


Figure 52. Node Checked for Model 2 Mesh Convergence Study

The mesh convergence plot showing the max Von Mises stress in the bolts ranging from 40,011 to 159,330 degrees of freedom is shown in Figure 53.

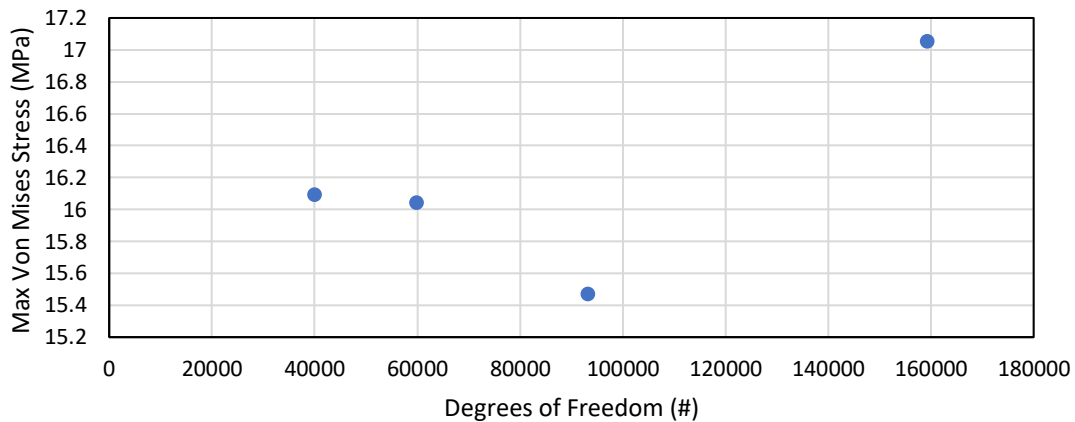


Figure 53. Model 2 Mesh Convergence Plot

Any model with around less than 40,000 degrees of freedom did not have a dense enough mesh for Abaqus to yield a solution. We concluded that the model converged because the numbers had slight increases and decreases between points and the model was also quite dense at 159,330 degrees of freedom. After 159,330 degrees of freedom, we likewise ran into a similar issue as

model 1, where the continually decreasing element edge lengths began to yield stress values that continually grew in a rapid manner.

One warning that we received when running our FEA models stated that some of the elements in our model were distorted. Another warning we received said that some nodes that were part of my tie constraint were “either missing intersection with their respective master surface or are outside the adjust zone.” We decided that these warnings were not of concern because after analyzing the physical displacement of the model, it became clear that the FEA model was predicting an accurate deflection shape of what we expected to occur. For example, this expected deflection included that the first bolt would take the most load and have the largest deflection and this pattern continued to decrease down the line of the bolts. These deflections in meters are shown in Figure 54.

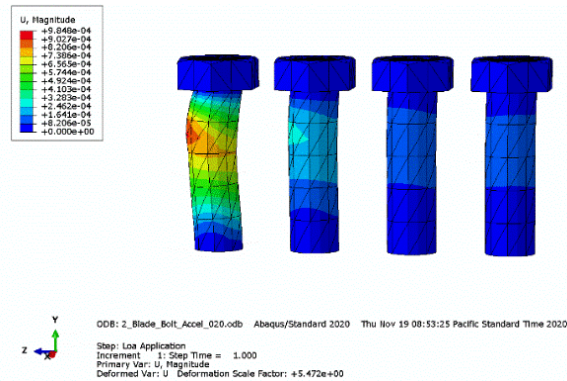


Figure 54. Bolt Deflection Contour Plot

In addition to the realistic physical deflections of the model, we believe that the warnings did not significantly affect the results because the resulting Von Mises stresses of both models were close to our initial hand calculations. Lastly, we decided the listed distorted elements were not of major concern because none of them were at the interface between the bolts and the blade where most of the stress occurred.

The resulting bolt Von Mises stress contour plot for the first model in units of Pa is shown in Figure 55.

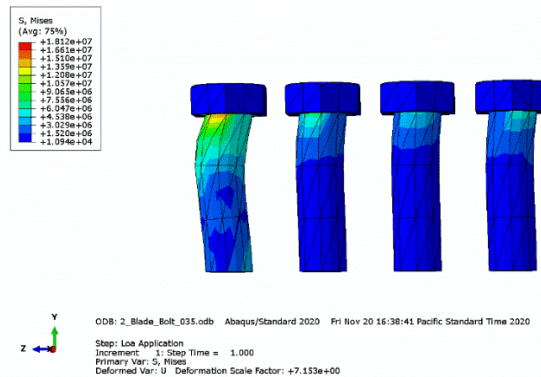


Figure 55. Model 1 Bolt Von Mises Stress Contour Plot

The max bolt Von Mises stress from model 1 is 18.12 MPa, which is extremely close to our hand calculation value of 18.02 MPa. The resulting bolt Von Mises stress contour plot for the second model in units of Pa is shown in Figure 56.

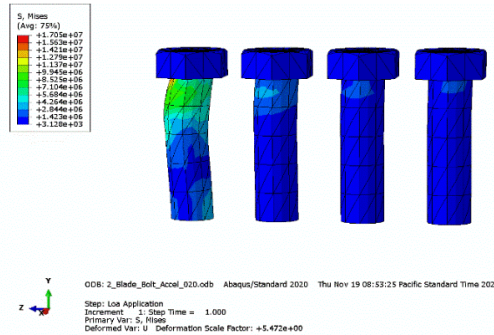


Figure 56. Model 2 Bolt Von Mises Stress Contour Plot

A summary table, listing each method used and the resulting max Von Mises stress on the bolts and yielding F.O.S. is shown in Table 9. The yielding F.O.S were calculated using the ratio of yield strength, which is 420 MPa for the steel bolts, to the max Von Mises stress that occurred in the bolts.

Table 9. Resulting Max Von Mises bolt stresses and F.O.S.

Method	Max Von Mises Bolt Stress (MPa)	F.O.S
Hand Calculations	18.02	23.3
FEA Model 1	18.12	23.2
FEA Model 2	17.05	24.6

The results of our hand calculations and two FEA models confirm that the use of 4, 30 mm diameter bolts to fasten the rotating disk and blade would satisfy the requirement of having a yielding F.O.S greater than 10. Therefore, the results of this study confirm that the use of 4, 30 mm diameter steel bolts would ensure the safety of any users or spectators of the wind turbine tester. We were happy with the results of our FEA models because they were both quite close to our initial hand calculations. We believe that the discrepancy between my model 1 and 2 results can be attributed to the fact that the first model used a body force that distributed a constant force gradient across the entire volume of the blade, when in fact the force values should increase and be the greatest at the points farthest away from the axis of rotation. Therefore, we believe that our model 1 results are a conservative estimate of the actual stress that would occur at the bolts because they are assuming slightly higher forces at the points closer to the bolts. Another discrepancy we noted between my two FEA models and our hand calculations were that our hand calculations estimates the max stress in all of the bolts and had the same max stress in all of the bolts. Therefore, our hand calculations did not take into consideration the fact that the first bolt would take the most load and less load would be taken on each additional bolt after. With that being said, we believe that the FEA results proved to show a more realistic response and deflection of the bolts.

From the same two FEA models we were able to find the max Von Mises stresses in the blade. The contour plot of the Von Mises stress in the blade from model 1 is shown in Figure 57. The max Von Mises stress in the blade is 27.74 MPa.

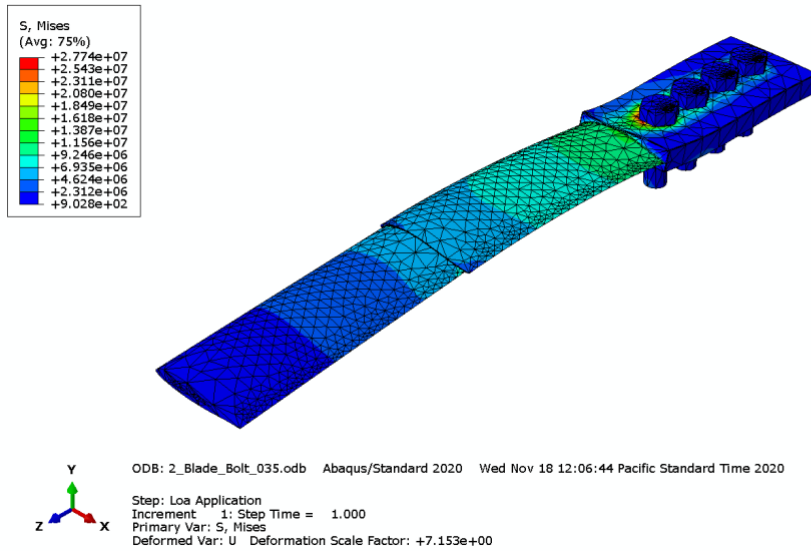


Figure 57. Model 1 Blade Von Mises Stress Contour Plot

The contour plot of the Von Mises stress in the blade from model 2 is shown in Figure 58. The max Von Mises stress in the blade is 43.97 MPa.

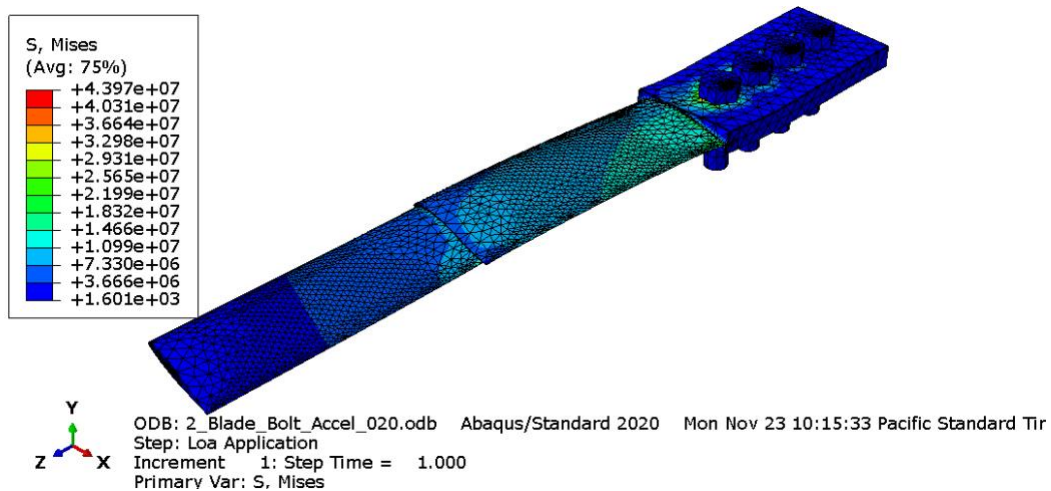


Figure 58. Model 2 Blade Von Mises Stress Contour Plot

If we were to take the yielding factor of safety for both of these results, we would receive a best case yielding F.O.S. of 11.18, and worst case yielding F.O.S. of 7.05.

Our next FEA model analyzed the assembly of the sheath and sheath bolts. This assembly is shown in Figure 59.

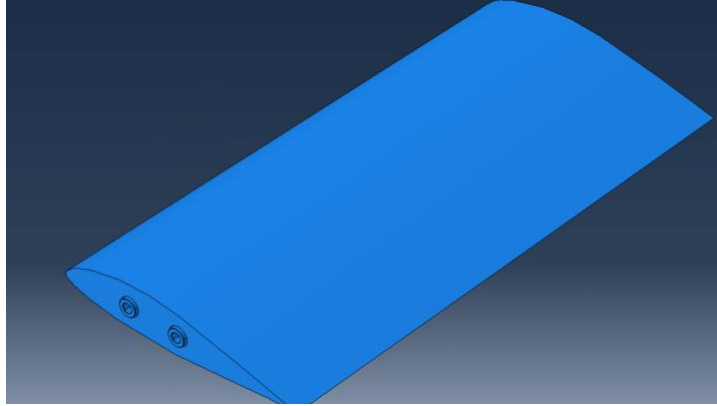


Figure 59. Sheath and Sheath Bolt Assembly

The material properties used in FEA modeling for the bolts and sheath are shown in Table 10.

Table 10. Material Properties for Bolts and Sheath

Steel Bolts		6061 Aluminum Sheath	
Yield Strength (MPa)	420	Yield Strength (MPa)	310
Young's Modulus (GPa)	200	Young's Modulus (GPa)	69
Poisson's Ratio	0.3	Poisson's Ratio	0.35

We were able to calculate a conservative estimate of the centrifugal force by assuming that the sheath was a point mass rotating around the center of the disk. Therefore, we used the following formula:

$$F_{centrifugal} = m\omega^2r$$

In this equation, m is the 0.37266kg mass of the sheath, ω is the 100 rad/sec angular velocity, and r is the 1.15 m distance from center of rotation on the disk to the point mass located at the end of the sheath. From this formula we calculated the centrifugal force of the sheath to be 4,285.59 N. Using this centrifugal force, we calculated a body force that we could apply to the entire volume of the sheath using the following formula:

$$Body\ Force = \frac{F_{centrifugal}}{V_{sheath}}$$

Using this formula and knowing that the volume of the sheath was $0.00013897\ m^3$, we were able to calculate that the body force on the sheath was $30,838,238.47\ N/m^3$. Next, we applied this body force and the 0.7 N drag force to our Abaqus FEA model as shown in Figure 60.

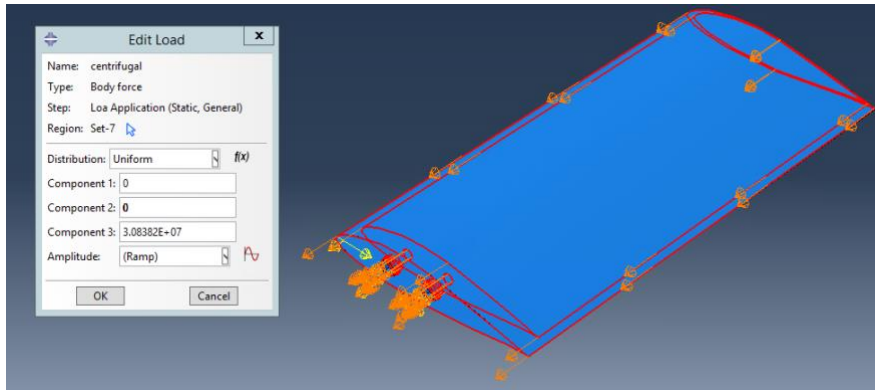


Figure 60. Body Centrifugal Force Load on Sheath

Next, we applied a boundary condition restricting displacement along the entire threaded region of the bolts because these bolts would be physically restricted to displace in this region by the interface with the blade. The boundary condition made in Abaqus are shown in Figure 61.

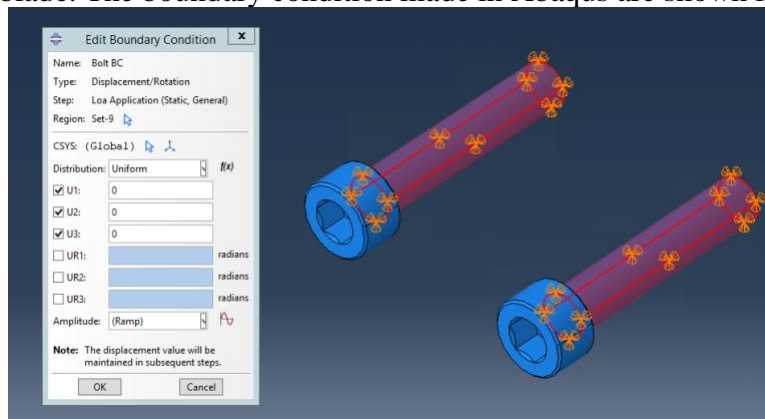


Figure 61. Boundary Condition on Bolts

The resulting contour plot of the Von Mises stresses on the bolts are shown in Figure 62.

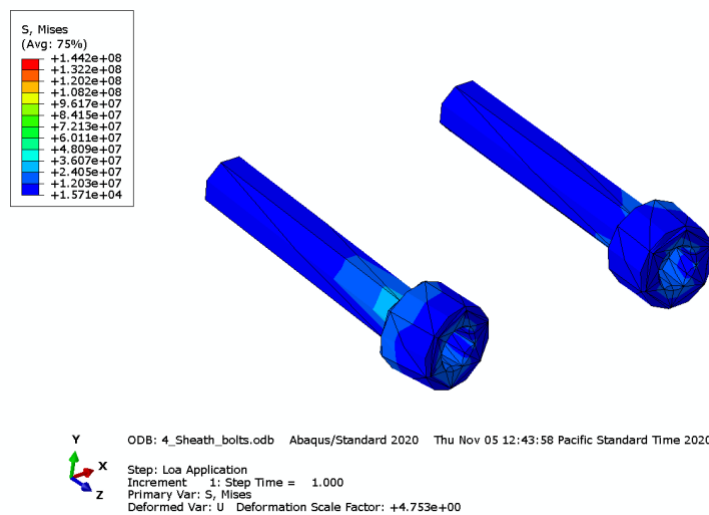


Figure 62. Contour Plot of Von Mises Stress on Sheath Bolts

The resulting contour plot of the Von Mises stresses on the sheath are shown in Figure 63.

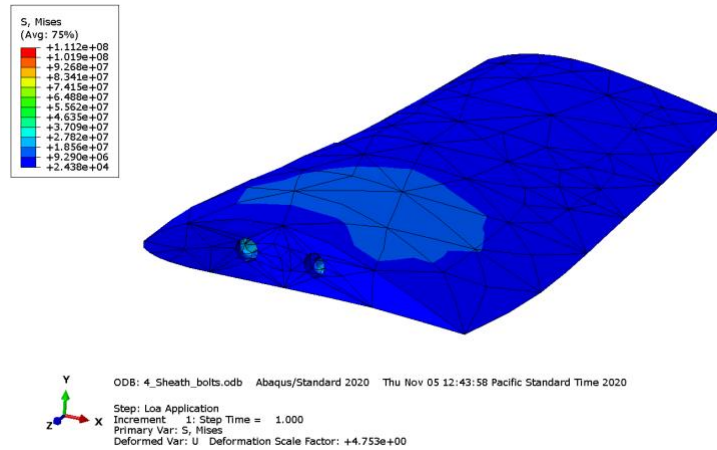


Figure 63. Contour Plot of Von Mises Stress on Sheath

Noting that the max Von Mises stress was 144.2 MPa on the bolts and 111.2 MPa on the sheath, we were able to calculate the yielding factor of safety using the following equation:

$$F.O.S. = \sigma_{ult} / \sigma_{actual}$$

The resulting max Von Mises stresses and F.O.S. of the bolts and sheath are shown in Table 11.

Table 11. Max Von Mises Stress and F.O.S. for Sheath and Bolts

Component	Max Von Mises Bolt Stress (MPa)	F.O.S
Bolts	144.2	2.91
Sheath	111.2	2.79

The last assembly we modeled in Abaqus was the disk and bolt assembly in order to find the Von Mises stress that occur in the disk as a result of the blade rotating at 100 rad/s. The assembly is shown in Figure 64.

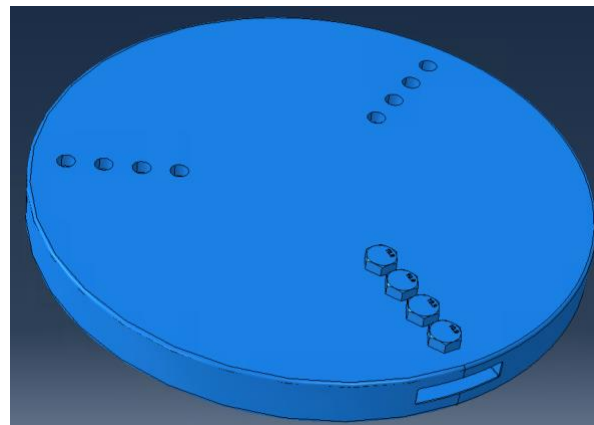


Figure 64. Disk and Bolt Assembly

In this model we applied the centrifugal force of the blade that we previously calculated and applied that force as a body force on the bolts. Knowing that the volume of the bolts was 0.00041931 m^3 , and the centrifugal force was $50,901.63 \text{ N}$, we calculated that the centrifugal body force on the bolts was $121,393,789.8 \text{ N/m}^3$. The body force loading on the bolts is shown in Figure 65.

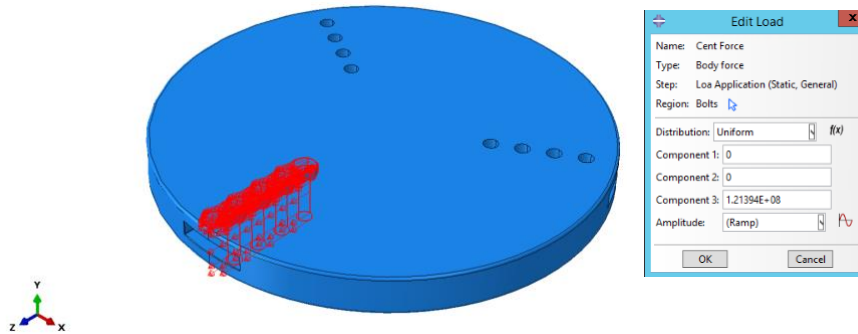


Figure 65. Centrifugal Body Force Loading on Bolts

For the boundary conditions, we restricted the displacement of all surfaces on the disk that were in contact with the bolts in the x, y, and z directions. The boundary conditions are shown in Figure 66.

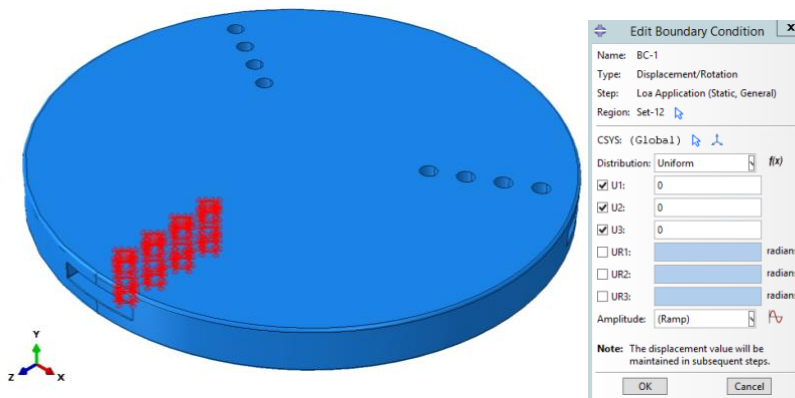


Figure 66. Boundary Conditions on Disk

The resulting disk Von Mises stress contour plot is shown in Figure 67.

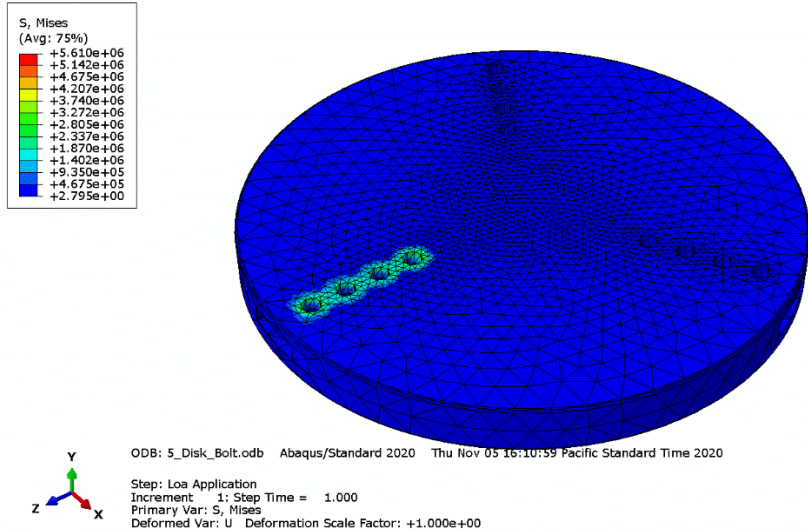


Figure 67. Disk Von Mises Stress Contour Plot

Using the max Von Mises stress from the contour plot and the yielding F.O.S. equation previously mentioned, we were able to calculate the yielding F.O.S. of the disk. The max Von Mises stress and yielding factor of safety for the disk are listed in Table 12.

Table 12. Disk Max Von Mises Stress and Yielding F.O.S.

Component	Max Von Mises Bolt Stress (MPa)	F.O.S
Disk	5.610	55.26

8. Project Management

This section will discuss the main project deliverables, when they were due, and how we attempted to stay organized in order to adhere to our timeline. Throughout the duration of this project, we were in a constant battle to keep our Gantt up to date with our changes and updates to the Scope of Work. We did not commence building and testing of the finalized design during Fall quarter. Due to the COVID-19 pandemic we were instead tasked with designing the rotating blade system.

Table 13. Key Deliverables

Deliverable	Description	Due Date
Scope of Work (SOW)	Document outlining scope of project	2/3/20
Preliminary Design Review (PDR)	First major review of all initial designs of solution	3/2/20
Critical Design Review (CDR)	Detailed review of all components, costs, analysis, and updated solution	5/25/20
Initial Test Plan and Operator's Manual	Detailed testing plan for components and system, a user's guide detailing how to operate the system and all potential safety hazards	5/30/20
Manufacturing Test and Review	Status of component manufacturing, updated test plan, and updated schedule of project completion	6/4/20
Prototype*	Confirmation Prototype Review	10/20/20
Operators Manual	Complete operator's manual detailing all safety hazards, all use cases, and general troubleshooting	11/10/20
Final Design Review (FDR)	Final design report, showcase of project expo website	11/24/20

*Not complete due to the pandemic

8.1 Completed Analysis

Since the completion of the *Critical Design Review*, our team has completed the following action items:

- Design Analysis
- Detailed CAD Drawing Package
- Manufacturing Plan
- Design Verification Plan
- Safety Review
- Continued Testing

8.2 Purchases

We only tested on one portion of the Water Delivery System, to see what the correct diameter of needle would be needed to produce 2.0mm water drops at our desired flowrate. To do that we bought

- Small fish tank peristaltic pump
- Tubing
- Needles ranging in size from 12Ga to 34Ga

A cost prediction for the entire system is included with the indented Bill of Materials (iBOM). The iBOM is a document which lists all of the purchases that would need to be made for both the Water Delivery System and the Rotating Blade System to be built and can be found in Appendix L.

8.3 Effectiveness of Planning

We maintain that the method of planning that we used was successful. The use of the Gantt chart, found in Appendix I, to monitor large scale progress worked very well to keep us on schedule. The use of Weekly Status Reports was very helpful in reminding us what we needed to achieve each week in order to keep up with the Gantt chart.

9. Conclusions and Recommendations

Unfortunately, due to the COVID-19 pandemic, our senior project was not able to complete the manufacturing of much more than a single testing section. Instead of building the water delivery system which was the scope of our project up to Fall quarter 2020, we spent the remainder of our time designing the rotating blade system. Both systems are integrated and fulfill the majority of requirements. The biggest requirement that we were not able to meet was the initial budget estimate, mainly due to the additional system that requires custom machining processes. We are confident that the water delivery system will be able to work well for an extended period of time, given it is well maintained. One possible potential issue is the pressure rating of the peristaltic pump. The pump is rated to 20psi operating pressure, and we estimate that our system will have a maximum operating pressure of 15.8 psi. See Appendix U for the MatLab script we used to calculate this pressure estimate. This leaves us with a smaller factor of safety than we would have liked, however a pump that achieves that factor of safety would be more costly. One actual shortcoming was that we did not meet the weight requirement for the fluid delivery system. This portion of the project was overweight by a small margin. This missed specification was partially due to balancing material and component costs and weight. It was also an ambitious and fairly low-priority specification from the start of the project.

If we could do this project differently, we would have worked towards a more solidified scope from the start of the project. We would have clarified this with TTP so that we did not have to scramble to redesign and add new specifications to the project later on. This issue was partially due to the pandemic. Our scope for this project went through two major changes. One was when we realized the rotating blade system was going to be too dangerous to manufacture on campus, and one when the pandemic threatened to close the machine shops on campus. Overall, we have really enjoyed working with TTP. They have set aside a lot of time for us to talk with them and review designs and ideas. We really appreciate all of their help and support.

Next Steps

We are confident that the rotating blade system will be a success, but due to complications with the motor manufacturer, we were unable to get information until late in the quarter. If someone were to spend additional time refining our designs, we would recommend focusing on the connection between motor and disk. The disk and blade and connections were thoroughly investigated, and we are confident that they will hold up under the loads we predicted them to be under. All systems would need to be tested to ensure that the whole system follows our analysis.

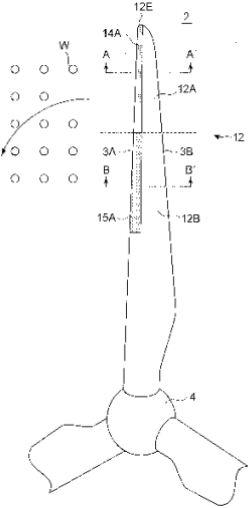
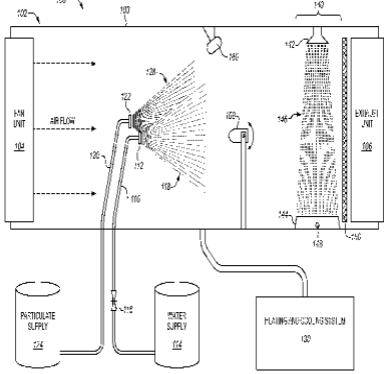
Those tests would follow similar template to how we tested the single dropper branch. It is incredibly vital that all precautions are taken with the rotating blade system as if failure were to occur then there would be rapidly moving projectiles that would be dangerous to anyone in the vicinity.

Another necessary next step is to find a place to set up and operate the system. We envisioned an enclosed testing area with extra safety precautions in case of accidents.

References:

- [1] Xu J Z 2011 A study on performance influences of airfoil aerodynamic parameters and evaluation indicators for the roughness sensitivity on wind turbine blade
- [2] Ashby M F, Shercliff H and Cebon D Materials: Engineering, Science, Processing and Design
- [3] Bartolome, Luis. Prospective challenges in the experimentation of the rain erosion on the leading edge of wind turbine blades. Wind Energy
- [4] Gohardani O 2011 Impact of erosion testing aspects on current and future flight conditions
- [5] Pritchard, Philip. Fox and McDonald's Introduction to Fluid Mechanics
- [6] Field P R, Hand W, Cappelluti G and McMillan A 2012 Hail threat standardization
- [7] de Vries, Eize. SGRE brings leading-edge protection as retrofit. Wind Power Monthly
- [8] Sareen A, Chinmay S A and Selig M S 2013 Effects of leading edge erosion on wind turbine blade performance Wind Energy
- [9] Kumar B G, Singh B G and Nakamura T 2002 Degradation of carbon fiber-reinforced epoxy composites by ultraviolet radiation and condensation Compos. Mater.
- [10] Maniaci, David. Leading Edge Erosion. Sandia Laboratory
- [11] DNVGL – RP0171. Testing of rotor blade erosion protection systems
- [12] ASTM International 2011 Standard Test Method for Liquid Impingement Erosion Using Rotating Apparatus
- [13] Diarkis 2013 San and Rain Erosion Testing. Available:
<http://diarkis.com/index.php/analytics/sandrain-erosion-testing>
- [14] Dear J P and Field J E 1988 High-speed photography of surface geometry effects in liquid/solid impact
- [15] Gurit 2013 Guid to composites. Available:
www.gurit.com/files/documents/Gurit_Guide_to_Composites.pdf.
- [16] Keegan, M. H. On Erosion Issues Associated with the Leading Edge of Wind Turbine Blades
- [17] 3M 2011 Wind Energy. Available:
http://solutions.3m.com/wps/portal/3M/en_US/Wind/Energy
- [18] Dalili, N. A Review of Surface Engineering Issues Critical to Wind Turbine Performance. Renewable and Sustainable Energy Reviews
- [19] University of Dayton Research Institute 2013 Rain erosion test facility. Available:
www.udri.udayton.edu/NONSTRUCTURALMATERIALS/COATINGS/Pages/RainErosionTestFacility.aspx
- [20] Elert G and Volynets I 2001 Diameter of a raindrop. Available:
<http://hypertextbook.com/facts/2001/IgorVolynets.shtml>
- [21] Plenzer, Ryszard. Elastic and Strength Properties of OSB Layers

Appendix A: Relevant Patents

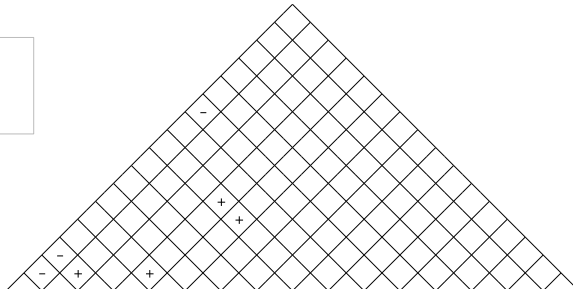
PATENT NO.	PATENT NAME	DESCRIPTION	IMAGE
US20140186188A1	Wind turbine blade and wind turbine generator having the same	Wind turbine blades mounted on rotor with test protective coating on blades.	 <p>The diagram shows a perspective view of a wind turbine blade assembly. A central hub (4) is connected to three blades. One blade is shown in a cross-sectional view with various parts labeled: 12E at the tip, 14A and 12A along the upper surface, 3A and 3B along the lower surface, and 15A and 12B along the root. Section lines A-A' and B-B' are indicated. A rotor (2) is shown at the top, and a wind direction (W) is indicated by an arrow.</p>
US20160363505A1	Wind Tunnel for Erosion Testing	Wind tunnel that exposes test subjects to high winds and water damage.	 <p>The schematic diagram shows a wind tunnel system for erosion testing. It includes a fan unit (100) on the left, a nozzle (102) that directs a flow of air (104) through a test chamber (106). A spray of water (108) is directed at the test subject (110) inside the chamber. A water supply (112) and a particulate supply (114) are connected to the system. A pressure transducer (116) is used to measure the flow. The test chamber is connected to a collector unit (118) and a fan unit (120) on the right.</p>
WO2010046299A3	Airfoil and blade for a turbine, and method for directly determining the progress of erosion of a turbine blade airfoil	Sensor element (2) is integrated into the material of the turbine blade airfoil (1) in order to directly determine the progress of erosion of the turbine blade airfoil.	N/A

PATENT NO.	PATENT NAME	DESCRIPTION	IMAGE
EP2674740A1	A fatigue testing device for a wind turbine blade	Application of cyclical loads to a relatively long wind turbine blade during blade testing.	<p>Fig. 5</p>
US7686571B1	Bladed rotor with shear pin attachment	Airfoil portion formed from a single crystal material and two platforms attached to the ends of the airfoil by shear pins that fit within slots formed between the platform and airfoil.	

Appendix B: Quality Function Deployment

Correlations	
Positive	+
Negative	-
No Correlation	
Relationships	
Strong	●
Moderate	○
Weak	▽
Direction of Improvement	
Maximize	▲
Target	◇
Minimize	▼

QFD House of Quality
 Project: Wind Turbine Testing
 Revision Date: _____



Row #	WHO: Customers								HOW: Engineering Specifications (Tress)								NOW: Curr. Products									
	Weight Chart	Relative Weight	TPP	Customers	End Energy Producers	Tester operators	Maximum Relationship	Direction of Improvement	Total Weight	Test Arm length	Blade tip Speed	Rain (mm/h): 30-35	Droplet Size (mm)	Temperature (C)	single person operated	provides constant UV light	Humidity range	number of cycles	airfall measurements	Size of Gauge Zone Length	Our Current Product	Competitor #1: University of Barcelona Test Machine	Competitor #2: R&D test system for LM wind power	Competitor #3: poly Tech tester	Oran W. Nicks Low Speed Wind Tunnel at Texas A&M University	
1	2%	8	0	0	0	0	9	▼	●	●	▽	○	○	○	○	○	○	○	○	○	○	6	1	0	5	1
2	5%	8	8	0	0	0	9	▼	▽	○	▽	●	●	●	○	▽	▽	▽	▽	▽	0	8	8	4	2	
3	6%	9	9	0	0	0	9	▼	○	●	▽	▽	▽	○	○	▽	▽	○	○	○	10	10	10	2	3	
4	6%	9	10	0	0	0	9	▼	▽	▽	▽	▽	▽	●	○	○	○	○	○	○	0	10	10	7	4	
5	13%	9	4	8	5	9	9	○	○	○	▽	▽	▽	▽	▽	▽	▽	●	○	○	8	8	9	8	5	
6	7%	9	4	8	0	0	9	○	○	○	▽	▽	▽	▽	▽	▽	▽	○	○	○	8	8	9	8	6	
7	6%	8	2	9	0	0	9	○	○	●	○	○	○	○	▽	○	○	○	○	○	5	1	1	1	7	
8	15%	4	8	5	8	9	9	○	○	●	▽	▽	▽	▽	▽	▽	○	○	○	○	10	8	10	10	8	
9	7%	10	0	10	0	0	9	▼	●	●	●	●	●	○	○	○	○	○	○	○	4	10	10	1	9	
10	17%	10	0	10	10	0	9	○	○	●	▽	▽	▽	●	▽	▽	○	○	○	○	10	9	10	9	10	
11	6%	4	2	9	0	0	9	○	▽	○	○	○	○	○	●	○	○	○	○	○	7	3	4	2	11	
12	5%	9	8	0	0	0	9	▼	▽	▽	▽	▽	▽	○	○	○	○	○	○	○	0	2	6	7	12	
13	5%	9	8	0	0	0	9	▼	▽	▽	▽	▽	▽	○	○	○	○	○	○	○	0	0	0	0	13	
14	0%																								14	
15	0%																									15
16	0%																									16

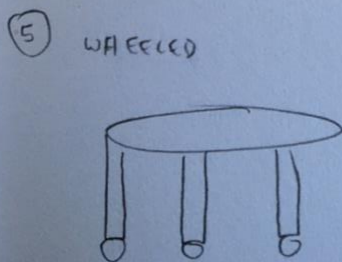
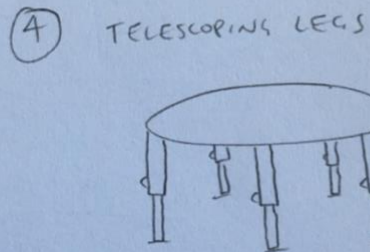
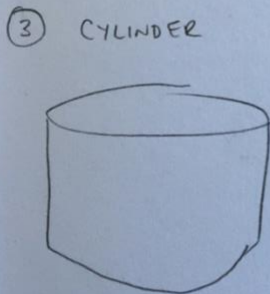
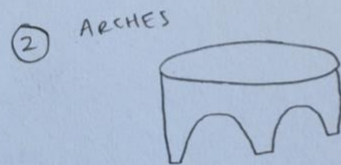
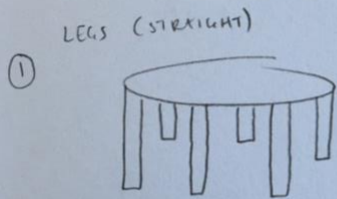
Appendix C: All Ideas from Ideation

Moving Water/Water supply	Measure Drop Rate	Protect User
Peristaltic pump	Bucket collector	Cover top
Syringe with lead screw	Monitor flowrate	Safety rules for operation
Fine mesh filter	Drop rate camera	Use of a key required for operation
Prosthetic udder	Impact sensor on blade	Water catchment system to prevent flooding
Jet modulated by sound	Drop rate controller	Bulletproof glass surroundings
Jet into spoon		Waterproof electronics
Rotating plate with holes in it to break up jet		Lightweight arms
Weight mounted on syringe		Automatic shutoff timer
Elastic powered syringe		Speed sensors
Rack and pinion driven syringe		Strain gauges
Chain driven syringe		Allow operation from a distance
Timed paddle rotation to block satellite drops		Personal protective equipment
Central sprinkler with circular spray pattern		
Plastic bag with holes poked into it		
Pressure driven dropper tube		

Appendix D: Pugh Matrices

1. Support Water Delivery System




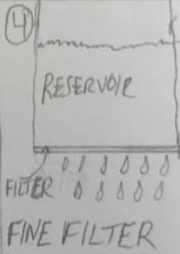



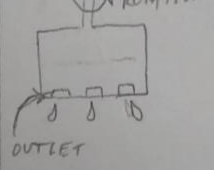

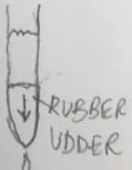
CONCEPT CRITERIA	1	2	3	4	5	6
STABILITY	D	+	+	-	+	S
PORTABILITY	A	-	-	+	+	S
SAFETY	T	+	+	S	S	+
INTEGRATEABILITY	U	S	+	+	S	S
HEIGHT CHANGE	M	S	S	F	S	S
$\Sigma +$	-	2	3	3	1	1
$\Sigma -$	-	1	1	1	1	0
ΣS	-	2	1	1	3	4



2. Create Water Droplets

CONCEPT	1	2	3	4	5	6	7	8	9	10
CRITERIA										
WEIGHT		-	-	-	-	-	-	-	-	-
COST		-	-	-	-	-	-	-	-	-
CONTINUOUS OPERATION TIME LENGTH	D	+	S	+	S	+	S	+	S	S
EASE OF ACHIEVING 32.5 mm/hr RAINFALL	A	+	S	+	S	+	S	+	S	S
EASE OF ACHIEVING 2mm RAIN DROPS	T	+	+	+	+	+	+	-	+	-
CONSTANT FLOW RATE	U	+	+	+	+	+	S	-	+	-
EASE OF OPERATING WITH 2 PERSON	M	+	+	+	+	+	+	+	+	-
SAFETY		-	-	-	-	-	-	-	-	S
EASE OF VARYING DROP RATE		+	+	-	+	-	+	+	+	S
EASE OF VARYING DROP SIZE		+	+	-	+	-	+	S	+	S
$\Sigma+$		7	5	5	5	5	4	4	5	8
$\Sigma-$		3	3	5	3	5	3	5	3	5
ΣS		0	2	0	2	0	3	1	2	5

1st

<p>① WATER DROPPER</p> 	<p>② PERISTALTIC PUMP</p> 	<p>③ SYRINGE W/ LEAD SCREW</p> 	<p>④</p>  <p>RESERVOIR</p> <p>FIBER</p> <p>FINE FILTER</p>	<p>⑤ SYRINGE W/ RACK & PINION</p>  <p>PINION DRIVING RACK</p>
<p>⑥ PRESSURE DRIVEN DROPPER TUBE</p>  <p>INLET</p>	<p>⑦ WEIGHT DRIVEN SYRINGE</p>  <p>WEIGHT</p>	<p>⑧ CENTRAL ROTATING SPRINKLER</p>  <p>ROTATION</p> <p>OUTLET</p>	<p>⑨ BELT/CHAIN DRIVEN SYRINGE</p> 	<p>⑩ PROSTHETIC UDDER</p>  <p>RUBBER UDDER</p>

Appendix E: Morphological Matrix

Number	Sub-Function	Concepts				
		Option 1	Option 2	Option 3	Option 4	Option 5
1	Transport Water	Peristaltic Pump	Air Pressure-Driven	Rotating Paddle	Peristaltic Pump	Air Pressure-Driven
2	Create Water Drop	Nozzle	Nozzle	Nozzle	Nozzle	Nozzle
3	Support Water Delivery System	Straight Legs	Arched Legs	Cylinder Container	Telescoping Legs	Wheeled Legs

Appendix F: Weighted Decision Matrix

	Ideas	1	2	3	4	5	6	7
Criteria	Criteria Weights (0-5)	Straight Legs with Peristaltic Pump	Arches with Pressure Driven Dropper	Cylinder with Rotating Paddle to Block Satellite Drops	Telescoping Legs with Peristaltic Pump	Wheeled Legs with Pressure Driven Dropper	Hydraulic shock absorbing legs with Peristaltic pump	Damping Table and Peristaltic pump
Stability	4	4	5	5	3	2	5	5
Portability	3	3	2	1	4	5	3	3
Safety of Supports	5	3	4	5	3	3	5	5
Integrability	5	3	3	3	4	3	5	5
Height Change of Supports	2	2	2	2	5	1	4	5
Weight of materials	1	2	4	2	2	4	2	3
Cost	4	3	4	2	3	4	2	3
Continuous operation time	5	5	5	5	5	5	5	5
Ability to achieve 32.5 mm/hr	5	5	5	5	5	5	5	5
Ability to achieve 2mm dia. Drops	5	5	4	5	5	4	5	5
Constant flow rate	4	5	4	5	5	4	5	5
Ease of operation by 1 person	4	5	5	4	5	5	5	5
Safety of Dropper	5	4	5	5	4	5	4	5
Ease of varying drop rate	4	5	4	3	5	4	5	5
Ease of varying drop size	2	5	3	5	5	3	5	5
Drop location accuracy	5	5	4	5	5	4	5	5
Ease of setup calibration	2	5	4	2	5	4	5	5
Manufacturability	3	5	5	2	5	5	5	5
Totals		288	281	270	298	271	312	324

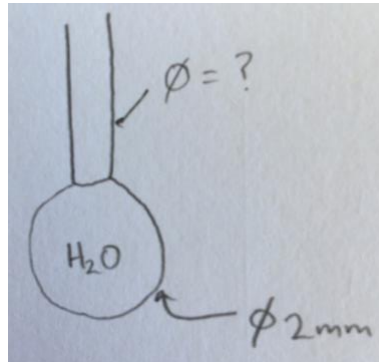
Appendix G: Design Hazard Checklist

Y	N	
Y		1. Will any part of the design create hazardous revolving, reciprocating, running, shearing, punching, pressing, squeezing, drawing, cutting, rolling, mixing or similar action, including pinch points and sheer points?
Y		2. Can any part of the design undergo high accelerations/decelerations?
Y		3. Will the system have any large moving masses or large forces?
Y		4. Would it be possible for the system produce a projectile?
Y		5. Would it be possible for the system to fall under gravity creating injury?
	N	6. Will a user be exposed to overhanging weights as part of the design?
Y		7. Will the system have any sharp edges?
	N	8. Will any part of the electrical systems not be grounded?
Y		9. Will there be any large batteries or electrical voltage in the system above 40 V?
	N	10. Will there be any stored energy in the system such as batteries, flywheels, hanging weights or pressurized fluids?
	N	11. Will there be any explosive or flammable liquids, gases, or dust fuel as part of the system?
	N	12. Will the user of the design be required to exert any abnormal effort or physical posture during the use of the design?
	N	13. Will there be any materials known to be hazardous to humans involved in either the design or the manufacturing of the design?
Y		14. Can the system generate high levels of noise?
	N	15. Will the device/system be exposed to extreme environmental conditions such as fog, humidity, cold, high temperatures, etc?
Y		16. Is it possible for the system to be used in an unsafe manner?
Y		17. Will there be any other potential hazards not listed above? If yes, please explain on reverse.

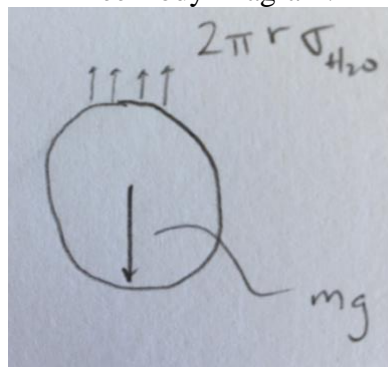
Description of Hazard	Planned Corrective Action
Crushed fingers in peristaltic pump	Do not touch when in use
Decapitation, limb severing, severe bruising or laceration from rapidly moving blades	Stay far away when machine is in use. Have operation station separate from physical machine.
Flying attachments striking user	Stay far away when machine is in use. Have operation station separate from physical machine.
Tip over	Ensure machine is fully stable for use. User mount samples of appropriate weight.
Electrocution	Using heavy duty motor to spin heavy blades and also using electricity to power peristaltic pumps
Potential loud noise	User wears ear protection
Catching tubing in rotating blade	Zip tie or affix tubing so that it stays well away from the moving blades
Flooding	Use large basin to catch any excess water or overflow. Use over a drain so that room does not flood

Appendix H: Preliminary Calculations

Determining the size of the needle based off of Tate's Method:



Free Body Diagram:



$$\sum F = 0$$

$$2\pi r_{needle}\sigma_{water} - m_{water}g = 0$$

$$2\pi r_{needle}\sigma_{water} = (\rho_{water}V_{drop})g$$

$$r_{needle} = \frac{\rho_{water} \frac{4}{3}\pi R_{water}^3 g}{2\pi\sigma_{water}}$$

$$r_{needle} = \frac{2\rho_{water}R_{water}^3 g}{3\sigma_{water}}$$

$$d_{needle} = \frac{4 \left(1000 \frac{kg}{m^3}\right) \left(9.81 \frac{m}{s^2}\right) (0.001m)^3}{3(0.072 \frac{kg}{s^2})}$$

$$d_{needle} = 0.182m$$

Finding velocity of water drop at blade surface:

For droplet sizes of 0.1mm to 3mm, the terminal velocity of the drop may be defined using the empirical relation in ASTM G73-10:

$$v_{drop,max} = 4.0d^{0.56} \left(\frac{m}{s}\right)$$

Using the above equation and other relations from ASTM G73-10 seen below,

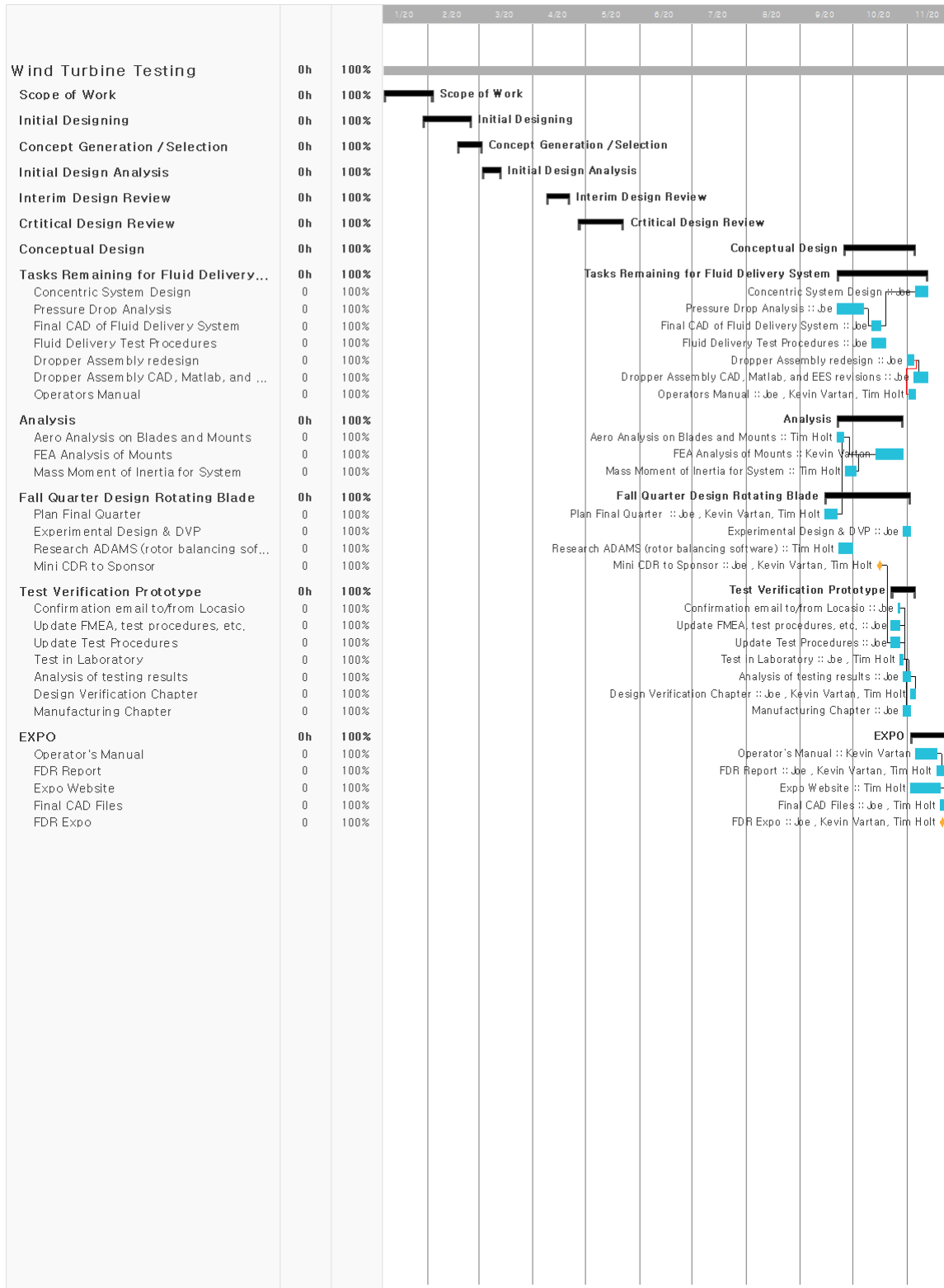
$$x(t) = v_{drop,max}t + \frac{v_{drop,max}^2}{g} \left(e^{-\frac{gt}{v_{drop,max}}} - 1 \right)$$

$$v(t) = v_{drop,max} \left(1 - e^{-\frac{gt}{v_{drop,max}}} \right)$$

We find that the velocity of the drop, regardless of its diameter, will be less than 2 m/s when it makes contact with the blade. A numerical solution in Excel was used to find the table below.

d [mm]	v_drop_max [m/s]	v (x = 20cm) [m/s]
0.5	2.713	1.532
1.0	4.000	1.696
1.5	5.020	1.754
2.0	5.897	1.773
2.5	6.682	1.809
3.0	7.400	1.835

Appendix I: Gantt Chart



Appendix J: Concept Model Build Day Images

Concept Model	Image
Parastaltic pump to syringe tip	 A photograph showing a hand holding a syringe tip over a black parastaltic pump. A tube is connected to the pump and leads to a red cup. Another red cup is placed next to it. The setup is on a white surface.
Jet broken up by sound	 A close-up photograph of a black jet nozzle. A stream of liquid is being emitted from the nozzle. A hand is holding a small object near the nozzle, possibly demonstrating the effect of sound on the jet.
Rack and Pinion driven syringe	 A photograph showing a hand holding a syringe. A rack and pinion mechanism is attached to the plunger, demonstrating a mechanical drive system for the syringe.

Timed Paddle rotation to block satellite drops



Plastic Bag with hole in it



Appendix K: DVP&R Fluid Delivery System:

Senior Project DVP&R												
Date: 11/24/2020		Team: Wind Turbine		Sponsor: Turbine Technology Partners		Description of System: Fluid Delivery System				DVP&R Engineer: Joe Blakewell		
TEST PLAN						TEST REPORT						
Item No	Specification #	Test Description	Acceptance Criteria	Test Responsibility	Test Stage	SAMPLES TESTED		TIMING		TEST RESULTS		NOTES
						Quantity	Type	Start date	Finish date	Quantity Pass	Quantity Fail	
1	2.1	Weight of Water Distribution System (empty)	<220 lbs.	N/A	Design	1		10/15/2020	11/20/2020	0	1	The achievement of this specification was determined by CAD analysis. SolidWorks estimates total weight to be about 260lbs. This is a cost vs importance of specification tradeoff
2	2.2	Radial area of dropper exposure zone	R = 0.80m to 1.10m	All	Design	1		10/15/2020	11/20/2020	1	0	The achievement of this specification was determined by CAD analysis.
3	2.3	Drop Intensity: We operated our verification prototype at the design flow rate while testing nozzle sizes	9 OE-4 m/s	All	Design	1		10/28/2020	10/28/2020	1	0	More information about the verification of this specification can be found in our Design Verification Report
4	2.4	Drop Diameter: We tested 7 different nozzle sizes to find which one produced 2mm drop diameters at our design flowrate	2.0x0.5mm	All	Design	7	Sub	10/28/2020	11/16/2020	1	0	More information about the verification of this specification can be found in our Design Verification Report
5	2.5	Number of Operators	1	All	Design	1		10/11/2020	11/20/2020	1	0	The achievement of this specification is to be determined by analysis.

Rotating Blade System:

Senior Project DVP&R													
Date: 11/24/2020		Team: Wind Turbine		Sponsor: Turbine Technology/ Partners		Description of System: Rotating Blade System			DVP&R Engineer: Tim Holt				
TEST PLAN						TEST REPORT							
Item No	Specification #	Test Description	Acceptance Criteria	Test Responsibility	Test Stage	SAMPLES TESTED		TIMING		Test Result	TEST RESULTS		NOTES
						Quantity	Type	Start date	Finish date		Quantity Pass	Quantity Fail	
1	3.1	Weight of Rotating Blade System	<1500 lbs.	All	Design	1		#####	11/20/2020	CAD software estimates designed system to weigh 1303 lbs.	1	0	The achievement of this specification was determined by analysis
2	3.2	Test arm length (blade tip rotation radius)	>1.10 meters	All	Design	3		#####	10/15/2020				The achievement of this specification was determined by analysis
3	3.3	Blade Tip Speed	>100 m/s	All	Design	3		11/11/2020	11/11/2020	Motor speed means tip speed is approx. 108 m/s	3	0	The achievement of this specification was determined by analysis
4	3.4	DU 96-W-180 Airfoil Shape	Airfoil shape must be DU 96-W-180	All	Design	3		#####	11/24/2020	Designed to be this shape	3	0	The achievement of this specification was determined by analysis
5	3.5	Lifespan	>100 testruns	All	Design	1		TBD			0	0	The achievement of this specification was not determined by analysis. This must be performed by future project engineers.
6	3.6	Size of Gauge Zone	20.0±0.6cm	All	Design	48		#####	11/24/2020	Designed to be 20cm long	48	0	The achievement of this specification was determined by analysis
7													

Appendix L: Indented Bill of Materials

Indented Bill of Material (BOM) Wind Turbine Tester Assembly

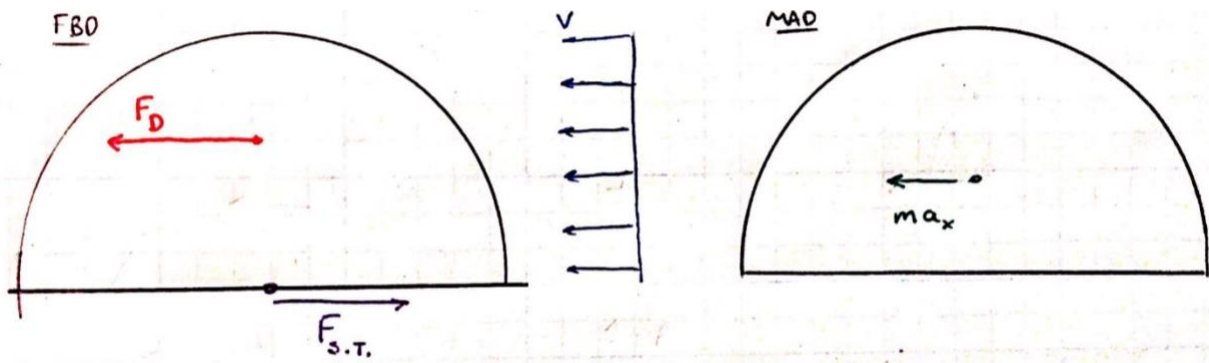
Assy Level	Part Number	Description	Matl	Vendor	Qty	Cost	Ttl Cost
		Lvl0 Lvl1 Lvl2 Lvl3					
0	100000	Final Assembly					
1	101000	Leg Assembly		----	6		
2	101001	90° elbow for 1" Sch. 40	Galvanized Pipe	McMaster	2	\$ 6.53	\$ 78.36
2	101002	1" Schedule 40 60" long	Galvanized Pipe	McMaster	1	\$ 60.06	\$ 360.36
2	101003	1" Schedule 40 12"	Galvanized Pipe	McMaster	1	\$ 17.37	\$ 104.22
2	101004	1" Schedule 40 6"	Galvanized Pipe	McMaster	1	\$ 7.79	\$ 46.74
2	101005	Through-hole reducer	Aluminum	McMaster	1	\$ 19.00	\$ 114.00
2	101006	1" Floor Mounting Flange	Aluminum	McMaster	2	\$ 21.91	\$ 262.92
2	101007	1/2"-13 bolt, 2 1/2" long (5pk)	Zinc-plated Steel	McMaster	2	\$ 8.30	\$ 16.60
2	101008	1/2"-13 Locknut (50pk)	Zinc-plated Steel	McMaster	1	\$ 10.07	\$ 10.07
2	101009	M12x1.75mm, 30mm long (10pk)	Zinc-plated Steel	McMaster	2	\$ 7.32	\$ 14.64
2	101010	M12 Washer (25pk)	316 Stainless Steel	McMaster	1	\$ 7.14	\$ 7.14
2	101011	M12x1.75mm Locknut (10pk)	18-8 Stainless Steel	McMaster	2	\$ 6.76	\$ 13.52
1	102000	Ring Assembly		----	1		
2	102001	Curved Struts (type 1 and 2)	Zinc-plated Steel	McMaster	4	\$ 95.05	\$ 380.20
2	102002	Strut Brackets (inner and outer)	Zinc-plated Steel	McMaster	8	\$ 2.17	\$ 17.36
2	102003	1/2"-13, 3" Long (5pk)	18-8 Stainless Steel	McMaster	4	\$ 5.42	\$ 21.68
2	102004	Washer for 1/2" (50pk)	18-8 Stainless Steel	McMaster	1	\$ 6.25	\$ 6.25
2	102005	1/2"-13 Locknut (10pk)	18-8 Stainless Steel	McMaster	2	\$ 4.79	\$ 9.58
1	103000	Reservoir Assembly		----	1		
2	103001	Plastic Pool	Plastic	?	1	?	
2	103002	Sealing caulk or epoxy	Caulking	Home Depot	1	\$ 2.58	\$ 2.58
1	104000	Fluid Path Assembly		----	1		
2	104001	Peristaltic Pump	Many	McMaster	1	\$ 577.83	\$ 577.83
2	104002	Cable Ties (100pk)	Nylon	McMaster	1	\$ 15.62	\$ 15.62
2	104003	Flexible tubing (per foot)	Rubber	McMaster	200	\$ 0.97	\$ 194.00
2	104004	Y-Connectors (10pk)	Nylon	McMaster	1	\$ 16.26	\$ 16.26
2	104005	Threads-to-barb adapter for 1:12 flow splitter (10pk)	Nylon	McMaster	6	\$ 4.81	\$ 28.86
2	104006	Reducer, for 3/8"x1/4" Tube ID (10pk)	Nylon	McMaster	1	\$ 5.29	\$ 5.29
2	104007	In-line tubing filter	Nylon	McMaster	1	\$ 30.49	\$ 30.49
2	104008	Al. stock for 1:12 flow divider	Aluminum	McMaster	1	\$ 37.73	\$ 37.73
1	105000	Dropper Assembly			1		
2	105001	Dropper PVC Pipe	PVC	ACE	48	\$ 2.99	\$ 143.52
2	105002	1/4" Tube ID x 1/2 NPT Adapter (10pk)	Nylon	McMaster	5	\$ 5.35	\$ 26.75
2	105003	1/2" pipe cap	PVC	McMaster	48	\$ 0.28	\$ 13.44
2	105004	10-32 MUNF to Luer adapter	Nylon	ISM	960	\$ 0.16	\$ 153.60
2	105005	0.09mm ID nozzle (50pk)	Many	Amazon	20	\$ 14.89	\$ 297.80
2	105006	Strut Mount Clamp	Zinc-plated Steel	McMaster	48	\$ 1.31	\$ 62.88
2	105007	M6x1mm 30mm Long (50pk)	Zinc-plated Steel	McMaster	1	\$ 7.84	\$ 7.84
2	105008	M6 Spacer, 17mm long	Aluminum	McMaster	48	\$ 1.52	\$ 72.96
2	105009	M6 Strut Channel Nut (5pk)	Zinc-plated Steel	McMaster	10	\$ 6.48	\$ 64.80
1	106000	Curtain Hanging Parts			1		
2	106001	Shower Curtains	Vinyl Plastic	McMaster	4	\$ 23.02	\$ 92.08
2	106002	3/4" PVC pipe	PVC	McMaster	3	\$ 5.67	\$ 17.01
2	106003	3/4" PVC fittings	PVC	McMaster	3	\$ 0.28	\$ 0.84
2	106004	Curtain Hooks (100pk)	Zinc-plated Steel	McMaster	1	\$ 9.73	\$ 9.73
2	106005	Plastic Rivets (25pk)	Nylon	McMaster	2	\$ 2.95	\$ 5.90
1	107000	Rotating Blade System		----	1		
2	107001	Rotor Disk	AL-6061	Machine Shop	1	\$ 2,000.00	\$ 2,000.00
2	107002	Airfoil Blade	AL-6061	Machine Shop	3	\$ 2,000.00	\$ 6,000.00
2	107003	Airfoil Sheath	AL-6061	Machine Shop	3	\$ 1,000.00	\$ 3,000.00
2	107004	M30 x 3.5 mm thread x 110 mm Long Hex Bolt	Zinc Yellow-Chromate Plated St	McMaster	12	\$ 17.09	\$ 205.08
2	107005	M30 x 3.5 mm Thread Hex Nut	Zinc-Plated Steel	McMaster	12	\$ 4.04	\$ 48.48
2	107006	M6 x 0.75 mm Thread, 30 mm Long Bolt	Black-Oxide Alloy Steel	McMaster	6	\$ 3.91	\$ 23.46
2	107007	Split-Tapered Bushing	Steel	McMaster	1	\$ 24.37	\$ 24.37
2	107008	1/2"-20 Thread Size, 2-1/4" Long Hex Bolt	Zinc Yellow-Chromate Plated St	McMaster	6	\$ 14.69	\$ 88.14
2	107009	1/2"-20 Thread Size Hex Nut	Zinc Yellow-Chromate Plated St	McMaster	6	\$ 0.17	\$ 1.02
2	107010	PEWWES-9-254T900 RPM Motor	Many	Worldwide Electric	1	\$ 1,648.00	\$ 1,648.00
						Purchased Parts Total:	\$ 16,380.00

Appendix M: Design Verification Plan

Date:		Team:		Sponsor:		Description of System:		DVP&R Engineer:					
5/5/2020		Wind Turbine		Turbine Technology Partners		Water Delivery System		Joe Blakevell					
TEST PLAN					TEST REPORT								
Item No	Specification #	Test Description	Acceptance Criteria	Test Responsibility	Test Stage	SAMPLES Quantity	SAMPLES TYPE	TIMING Start date	TIMING Finish date	Test Result	TEST RESULTS Quantity Pass	Quantity Fail	NOTES
1	2.1	Weight of Water Distribution System (empty)	<220 lbs.	All	Design	1		TBD					The achievement of this specification is dependent on a test we will perform when a sample from TTP arrives in the mail.
2	2.2	Radius of Support Ring	1.00±0.01 m	All	SP/FP	1		TBD					The achievement of this specification will be evaluated after construction of our structural prototype is complete. This has been put off until fall quarter due to the ban on use of power tools
3	2.3	Drop Intensity	9.0E-6 m/s	All	SP	1		TBD					The achievement of this spec. will be evaluated after construction of our structural prototype and testing of our peristaltic pump. See notes for item No. 2 for progress update.
4	2.4	Drop Diameter	2.0±0.5mm	All	SP/FP	1	Sub	TBD					The achievement of this spec. will be evaluated after flowrate is determined and dropper nozzle selection is being tested. See item No. 1 for progress.
5	2.5	Number of Operators	1	All	FP	1		TBD					The achievement of this spec. will be verified after construction of the final prototype is completed.

Appendix N: Water Drop Spacing Calculations

We had to perform this test because an equation based approach to this problem would be close to impossible without having an initial starting point for the analysis. The starting point that we ended up with is an air speed of 9m/s, found by using the pressure in the canister and considering it as the dynamic pressure of the air coming out of the canister, and a time it took to leave the drop's initial location of 0.029s. Using the Free Body Diagram below and Newton's Second Law, we were able to find an approximation for the acceleration of the water drop.



JUST IN X-DIR, $(\sum F_x)_{FBD} = (\sum F_x)_{MAD}$

$$F_{s.t.} - F_D = -ma_x$$

$$F_{s.t.} - \frac{C_D A \rho V^2}{2} = -ma_x$$

$F_D = C_D A \frac{\rho V^2}{2}$

$F_{s.t.} \equiv$ FORCE FROM SURF. TENSION/
FRICTIONAL INTERACTION
AT CONTACT WITH MATERIAL

\uparrow
?

We know that the drag force (F_D) on the water drop is what causes it to move, and the frictional force at the intersection of the drop and the surface is caused by some surface tension (F_{st}). We will assume that this F_{st} is relatively constant (does not depend on velocity of the water drop). This is a much more complicated problem than what is being shown here, but this simplified analysis will allow us to make a conservative estimate about how far apart the dropper locations must be in order for the blade to be dry before the drops from a subsequent dropper location hit the blade.

$$\sum F_x = ma_{drop,x}$$

$$F_{st} - F_D = -ma_{drop,x}$$

$$F_D = \frac{C_D A (\rho_{air} (V_{air} - V_{drop})^2)}{2}$$

$$a_{drop,x} = \frac{C_D A (\rho_{air} (V_{air} - V_{drop})^2)}{2m} - \frac{F_{st}}{m}$$

$$\int a_{drop,x} dt = \int \frac{C_D A (\rho_{air} (V_{air} - V_{drop})^2)}{2m} - \frac{F_{st}}{m} dt$$

$$V_{drop,f} - V_{drop,i} = \frac{C_D A \rho_{air}}{2m} \int (V_{air} - V_{drop})^2 dt - \frac{F_{st}}{m} \Delta t$$

From this equation it is impossible to draw any conclusions because it is a nonlinear differential equation. We shall therefore make the simplifying assumption that the difference between the velocity of the air (V_{air}) and the velocity of the drop (V_{drop}) will remain approximately constant. We shall assume that

$$V_{air} - V_{drop} \cong 0.9V_{air}$$

From this assumption, we can resolve the equation to be

$$V_{drop,f} = \left(\frac{C_D A \rho_{air}}{2m} (0.9V_{air}) - \frac{F_{st}}{m} \right) \Delta t$$

Even having made all of these simplifying assumptions, we still have many unknowns. For example, the shape of the water drop changes when it is hit with air, and in unpredictable ways. This means that both the C_D and the A will be changing. The water drop also leaves a trail of water as it moves along the blade, meaning that its mass is continuously changing. This is also forgetting that there is also an impact that we have completely neglected. Based off of all of these unmodelable parameters, we cannot predict the spacing of the droppers with any certainty. We have therefore decided that we shall base our spacing off of what we have seen in photos from machines already in use in the industry, and to charge whosoever uses this machine to verify that our assumptions were correct, and change the spacing if not.

Appendix O: Links to each Part

Description	Material	Vendor	Link
1" 90° Elbow (tapped both ends)	Galvanized Malleable Iron	Home Depot	https://www.homedepot.com/b/Mueller-Global-1-in-Galvanized-Malleable-Iron-90-degree-FIT-FIT-4-FIT-51C-0055HV/100202648
1" Schedule 40 (0.8m) (31.5") long pipe (one end threaded)	Galvanized Pipe	Home Depot	https://www.homedepot.com/b/1-in-x-10-ft-Galvanized-Steel-Pipe-565-1200HC/100576422
1" Schedule 40 (0.23m) (9") long pipe (both ends threaded)	Galvanized Pipe	Home Depot	https://www.amazon.com/Eventhrow-Supplies-NRGU-1090-Galvanized-Diameter-1/80167680DZ/ref=sr_1_8?dclid=1&keywords=1%24%24kanterde+pipe+8%24+long&qid=1588275276&sr=8-8
1" Floor Mounting Flange	Galvanized Iron	Home Depot	https://www.homedepot.com/b/ODK-Industries-1-in-Galvanized-Iron-Floor-Flange-311-L-1/100537306
1/2 Ring (1/2 in. x 4 ft. x 8 ft.)	OSB (Oriented Strand Board)	Home Depot	https://www.homedepot.com/b/Oriented-Strand-Board-Common-15-32-in-x-4-ft-x-8-ft-Aqua-0-451-in-x-47-75-in-x-95-75-in-512977/202084681
1-1/4 in. Construction Screw	Steel (Zinc Plated)	Home Depot	https://www.homedepot.com/b/Grp-Blue-1-1-4-in-Construction-Screw-114GCS1/204982329
Hinge	Steel	Home Depot	https://www.homedepot.com/b/Eventhll-4-in-Satin-Nickel-5-8-in-Radius-Door-Hinge-15002/202558089
Fiberglass	Fiberglass	Poly Composites Lab	
Plastic Pool	Plastic		
Sealing caulk or epoxy	Caulking	Home Depot	https://www.homedepot.com/b/DNA-Alex-Plus-10-1-oz-White-Acrylic-Latex-Caulk-Plus-Silicone-18103/100097524
Brin Water Filters	Mary	Brin	https://www.brin.com/replacement-filter/
Shower Curtain	Plastic	Amazon	https://www.amazon.com/Design-Plastic-Resistant-Curtain-Bathroom/dp/B00AVLVOZ/ref=sr_1_6?dclid=1&keywords=shower%2Bcurtain%2Bbrin&qid=1588277593&sr=8-6&th=1
Peristaltic Pump	Mary	Amazon	https://www.amazon.com/Kemmer-K-5TP-Peristaltic-Pump/dp/B07D087GV/ref=sr_1_12?dclid=1&keywords=peristaltic-pump&qid=1590090338&sr=8-12
Flexible tubing	Rubber	Amazon	https://www.amazon.com/Rain-Bird-122-2505-irrigation-distribution/dp/B00499JMYX/ref=sr_1_5?dclid=1&keywords=drfo-irrigation+tubing&qid=1588278361&sr=8-5
Y-connectors	Plastic	Amazon	https://www.amazon.com/Kalibin-Connectors-Irrigation-Universal-Fit/dp/B070G3G5B4/ref=sr_1_8?dclid=1&keywords=drfo-irrigation+tubing+y-connectors&qid=1588279579&sr=8-8
Nozzles	Plastic and metal	Amazon	https://www.amazon.com/Needles-Dispensing-Syringe-Needle-Placer/dp/B07C13Y5M4/ref=sr_1_18?dclid=1&keywords=shunt+needle+12+gauge&qid=1588277656&sr=8-18
16-Ga. Sheet metal (1x4' sheet)	Steel	Metals Depot	
1/4 in. -20 Hex Nuts	Steel	Home Depot	https://www.homedepot.com/b/1-4-in-20-x-3-4-in-Zinc-Plated-Hex-Bolt-100-Pack-8005580/204273598
1/4 in. -20 Hex Nuts	Steel	Home Depot	https://www.homedepot.com/b/Eventhll-1-4-in-20-Zinc-Plated-Hex-Nut-100-Pack-801730/204274089
1/4 in. Zinc Flat Washer	Steel	Home Depot	https://www.homedepot.com/b/Eventhll-1-4-in-Zinc-Flat-Washer-100-Pack-807210/204284538

Appendix P: FMEA

System / Function	Potential Failure Mode	Potential Causes of the Failure Mode	Current Preventive Activities	Current Detection Activities	Current Detection Efficiency	Recommended Action(s)	Responsibility & Target Completion Date	Actions Taken	Severity	Occurrence	Criticality	RPN
Professional Reservoir Retains Water	Provide precise drop size	plugged nozzles	filter in pump line	check drop sizes	3	verify drop size with high speed camera	All (First thing Fall quarter)	designed filter in final product, tested drop sizes	9	1	5	45
	Accurate Drop locations	Foreign object interference	fasten tubes	check tube mounts	1	verify drop target/landing area	All (First thing Fall quarter)	hold T/P to only test in test area	9	1	0	0
		flowrate too high	protect power source	test power source before use	2	size power source	Joe (5/13)	rechecked pump power source	4	2	4	32
		Loss of power	protect power source	test power source before use	2	size power source	Joe (5/13)	called out for reliable power source	10	1	1	10
	necessary flowrate	Pump Damages	size pump well	periodically disassemble sprayer/injector	3	size pump	Joe (5/13)	Sized pump well	4	4	4	64
		Spray water out of recirculation system	size of catchment system	Check volume in basin	3	Check for excess spray outside of machine	Tim (5/11)	designed curtains to catch spray	10	3	2	60
	Support System	Legs break	design for strength	check structure wear	1	size structural supports	Kevin (4/20)	structural CAD and FEA	10	1	6	60
		Circular support breaks	design for strength	check structure wear	1	size structural supports	Kevin (4/20)	structural sizing and FEA	2	1	2	4
	Secure Components	fasteners fail	reduce vibrations	measure vibrations while operating	3	test design for operating vibrations	Tim (10/30)	sized fasteners	9	1	3	27
	Look Professional	Materials rust	use stainless fasteners	visually inspect for rust	5	plan fastener materials	Tim (4/30)	used specific materials	3	4	2	24
Reservoir Retains Water	leak	size from travel, improper assembly	Assign checks in instructions	visually inspect for leaks	4	Design for easy and effective sealing	All (10/13)	manufacturing instructions	5	4	2	40

Appendix Q: Centrifugal Force Excel Calculation

A	B	C	D	E	F	G	H	I	J
		Breaking up blade into a bunch of small "point masses" to find the center of mass							
		m_blade	7.825	kg					
		R	1.15	m					
		R_0	0.15	m					
		dR	0.001	m					
		dm	0.007825	kg		F	50901.6	N	
		omega	100	rad/s		R_c	0.6505	m	
		F=m*r*omega^2				mass check	7.825	kg	
		dF=dm*r*omega^2							
		F=sum(dF)							
		R_c=F/(m_blade*omega^2)							
	m	N	kg						
	R	dF	dm						
1	0.151	11.8158	0.007825						
2	0.152	11.894	0.007825						
3	0.153	11.9723	0.007825						
4	0.154	12.0505	0.007825						
5	0.155	12.1288	0.007825						
6	0.156	12.207	0.007825						
7	0.157	12.2853	0.007825						
8	0.158	12.3635	0.007825						
9	0.159	12.4418	0.007825						
10	0.16	12.52	0.007825						
11	0.161	12.5983	0.007825						
12	0.162	12.6765	0.007825						
13	0.163	12.7548	0.007825						
14	0.164	12.833	0.007825						

The excel sheet has 2404 rows, so please reference attached excel file for equations and more detail

Appendix S: EES file for one dropper configuration

File is included in submission folder, but text is as follows:

"Model for 1 set of droppers"

"This system of equations is a rough model for one dropper configuration in our Fluid Delivery System Design"

"The purpose of this script is to prove that the flowrate difference between 20 droppers in a row drawing from one pipe is negligible"

"Flow rates from each dropper nozzle are boxed in solutions output. Since they are all very similar, the difference in dropper flowrate is negligible."

"Constants"

"density('Water', T=T_0, P=p_atm)"

rho=1.93 [slug/ft^3] "density of water"

T_0=70 [F]

p_atm = 2116.8 [lbf/ft^2] "atmospheric pressure"

g=32.2 [ft/s^2]

d=(1/48) [ft] "diameter of tubing"

d_nozzle = 0.000295 [ft] "ID of nozzles"

q_0 = 4.0163*10^(-4) "flow rate for 1 dropper configuration (ft^3/s)"

K_elbow = 0.3

K_nozzleexit = 1.0 "loss coeff for nozzle exit"

"kinematicviscosity(Water, T=T_0, P=p_atm)"

v_kin = 1.0503*10^(-5)

l_0_0_1 = 2 + 4.64 [ft]

l_nozzle = 1/24 "length of nozzle (ft)"

l_btwn droppers = 0.0328 [ft] "distance between droppers"

l_pump_0 = 5 [ft]

"Mass Balance"

q_1_2 = q_0 - q_1 "flow rate from spot 1 to 2 is the provided flowrate minus the rate out of nozzle 1, ft^3/s"

q_2_3 = q_1_2 - q_2 "ft^3/s"

q_3_4 = q_2_3 - q_3 "ft^3/s"

q_4_5 = q_3_4 - q_4 "ft^3/s"

q_5_6 = q_4_5 - q_5 "ft^3/s"

q_6_7 = q_5_6 - q_6 "ft^3/s"

$$q_{7_8} = q_{6_7} - q_7 \text{ "ft}^3/\text{s"}$$

$$q_{8_9} = q_{7_8} - q_8 \text{ "ft}^3/\text{s"}$$

$$q_{9_10} = q_{8_9} - q_9 \text{ "ft}^3/\text{s"}$$

$$q_{10_11} = q_{9_10} - q_{10} \text{ "ft}^3/\text{s"}$$

$q_{11_12} = q_{10_11} - q_{11}$ "flow rate from spot 11 to 12 is the provided flowrate minus the rate out of nozzle 1, ft³/s"

$$q_{12_13} = q_{11_12} - q_{12} \text{ "ft}^3/\text{s"}$$

$$q_{13_14} = q_{12_13} - q_{13} \text{ "ft}^3/\text{s"}$$

$$q_{14_15} = q_{13_14} - q_{14} \text{ "ft}^3/\text{s"}$$

$$q_{15_16} = q_{14_15} - q_{15} \text{ "ft}^3/\text{s"}$$

$$q_{16_17} = q_{15_16} - q_{16} \text{ "ft}^3/\text{s"}$$

$$q_{17_18} = q_{16_17} - q_{17} \text{ "ft}^3/\text{s"}$$

$$q_{18_19} = q_{17_18} - q_{18} \text{ "ft}^3/\text{s"}$$

$$q_{20} = q_{18_19} - q_{19} \text{ "ft}^3/\text{s"}$$

"Velocities"

$v_0 = (4/\pi) * q_0 / (d^2)$ "solving for velocity through nozzle from flow rate through nozzle, ft/s"

$$v_1 = (4/\pi) * q_1 / (d_{\text{nozzle}}^2) \text{ "ft/s"}$$

$$v_2 = (4/\pi) * q_2 / (d_{\text{nozzle}}^2) \text{ "ft/s"}$$

$$v_3 = (4/\pi) * q_3 / (d_{\text{nozzle}}^2) \text{ "ft/s"}$$

$$v_4 = (4/\pi) * q_4 / (d_{\text{nozzle}}^2) \text{ "ft/s"}$$

$$v_5 = (4/\pi) * q_5 / (d_{\text{nozzle}}^2) \text{ "ft/s"}$$

$$v_6 = (4/\pi) * q_6 / (d_{\text{nozzle}}^2) \text{ "ft/s"}$$

$$v_7 = (4/\pi) * q_7 / (d_{\text{nozzle}}^2) \text{ "ft/s"}$$

$$v_8 = (4/\pi) * q_8 / (d_{\text{nozzle}}^2) \text{ "ft/s"}$$

$$v_9 = (4/\pi) * q_9 / (d_{\text{nozzle}}^2) \text{ "ft/s"}$$

$$v_{10} = (4/\pi) * q_{10} / (d_{\text{nozzle}}^2) \text{ "ft/s"}$$

$$v_{11} = (4/\pi) * q_{11} / (d_{\text{nozzle}}^2) \text{ "ft/s"}$$

$$v_{12} = (4/\pi) * q_{12} / (d_{\text{nozzle}}^2) \text{ "ft/s"}$$

$$v_{13} = (4/\pi) * q_{13} / (d_{\text{nozzle}}^2) \text{ "ft/s"}$$

$$v_{14} = (4/\pi) * q_{14} / (d_{\text{nozzle}}^2) \text{ "ft/s"}$$

$$v_{15} = (4/\pi) * q_{15} / (d_{\text{nozzle}}^2) \text{ "ft/s"}$$

$$v_{16} = (4/\pi) * q_{16} / (d_{\text{nozzle}}^2) \text{ "ft/s"}$$

$$v_{17} = (4/\pi) * q_{17} / (d_{\text{nozzle}}^2) \text{ "ft/s"}$$

$$v_{18} = (4/\pi) * q_{18} / (d_{\text{nozzle}}^2) \text{ "ft/s"}$$

$$v_{19} = (4/\pi) * q_{19} / (d_{nozzle}^2) \text{ "ft/s"}$$
$$v_{20} = (4/\pi) * q_{20} / (d_{nozzle}^2) \text{ "ft/s"}$$

$v_{1_2} = (4/\pi) * q_{1_2} / (d^2) \text{ "Solving for velocity between nozzles from flow rate between nozzles, ft/s"}$

$$v_{2_3} = (4/\pi) * q_{2_3} / (d^2) \text{ "ft/s"}$$

$$v_{3_4} = (4/\pi) * q_{3_4} / (d^2) \text{ "ft/s"}$$

$$v_{4_5} = (4/\pi) * q_{4_5} / (d^2) \text{ "ft/s"}$$

$$v_{5_6} = (4/\pi) * q_{5_6} / (d^2) \text{ "ft/s"}$$

$$v_{6_7} = (4/\pi) * q_{6_7} / (d^2) \text{ "ft/s"}$$

$$v_{7_8} = (4/\pi) * q_{7_8} / (d^2) \text{ "ft/s"}$$

$$v_{8_9} = (4/\pi) * q_{8_9} / (d^2) \text{ "ft/s"}$$

$$v_{9_10} = (4/\pi) * q_{9_10} / (d^2) \text{ "ft/s"}$$

$$v_{10_11} = (4/\pi) * q_{10_11} / (d^2) \text{ "ft/s"}$$

$$v_{11_12} = (4/\pi) * q_{11_12} / (d^2) \text{ "ft/s"}$$

$$v_{12_13} = (4/\pi) * q_{12_13} / (d^2) \text{ "ft/s"}$$

$$v_{13_14} = (4/\pi) * q_{13_14} / (d^2) \text{ "ft/s"}$$

$$v_{14_15} = (4/\pi) * q_{14_15} / (d^2) \text{ "ft/s"}$$

$$v_{15_16} = (4/\pi) * q_{15_16} / (d^2) \text{ "ft/s"}$$

$$v_{16_17} = (4/\pi) * q_{16_17} / (d^2) \text{ "ft/s"}$$

$$v_{17_18} = (4/\pi) * q_{17_18} / (d^2) \text{ "ft/s"}$$

$$v_{18_19} = (4/\pi) * q_{18_19} / (d^2) \text{ "ft/s"}$$

"Flowrates"

"Reynolds Numbers"

"Note: for small Nozzle ID reynolds number may go >2300 and indicate turbulent flow which this file does not account for"

$re_0 = v_0 * d / v_{kin} \text{ "solving for Reynolds number for flow through nozzle"}$

$$re_1 = v_1 * d_{nozzle} / v_{kin}$$

$$re_2 = v_2 * d_{nozzle} / v_{kin}$$

$$re_3 = v_3 * d_{nozzle} / v_{kin}$$

$$re_4 = v_4 * d_{nozzle} / v_{kin}$$

$$re_5 = v_5 * d_{nozzle} / v_{kin}$$

$$re_6 = v_6 * d_{nozzle} / v_{kin}$$

$$re_7 = v_7 * d_{nozzle} / v_{kin}$$

$$re_8 = v_8 * d_{nozzle} / v_{kin}$$

$$re_9 = v_9 * d_{nozzle} / v_{kin}$$

$$re_{10} = v_{10} * d_{nozzle} / v_{kin}$$

$$re_{11} = v_{11} * d_{nozzle} / v_{kin}$$

$$re_{12} = v_{12} * d_{nozzle} / v_{kin}$$

$$re_{13} = v_{13} * d_{nozzle} / v_{kin}$$

$$re_{14} = v_{14} * d_{nozzle} / v_{kin}$$

$$re_{15} = v_{15} * d_{nozzle} / v_{kin}$$

$$re_{16} = v_{16} * d_{nozzle} / v_{kin}$$

$$re_{17} = v_{17} * d_{nozzle} / v_{kin}$$

$$re_{18} = v_{18} * d_{nozzle} / v_{kin}$$

$$re_{19} = v_{19} * d_{nozzle} / v_{kin}$$

$$re_{20} = v_{20} * d_{nozzle} / v_{kin}$$

$$re_{1_2} = v_{1_2} * d / v_{kin} \text{ "solving for Reynolds number for flow between nozzles"}$$

$$re_{2_3} = v_{2_3} * d / v_{kin}$$

$$re_{3_4} = v_{3_4} * d / v_{kin}$$

$$re_{4_5} = v_{4_5} * d / v_{kin}$$

$$re_{5_6} = v_{5_6} * d / v_{kin}$$

$$re_{6_7} = v_{6_7} * d / v_{kin}$$

$$re_{7_8} = v_{7_8} * d / v_{kin}$$

$$re_{8_9} = v_{8_9} * d / v_{kin}$$

$$re_{9_10} = v_{9_10} * d / v_{kin}$$

$$re_{10_11} = v_{10_11} * d / v_{kin}$$

$$re_{11_12} = v_{11_12} * d / v_{kin}$$

$$re_{12_13} = v_{12_13} * d / v_{kin}$$

$$re_{13_14} = v_{13_14} * d / v_{kin}$$

$$re_{14_15} = v_{14_15} * d / v_{kin}$$

$$re_{15_16} = v_{15_16} * d / v_{kin}$$

$$re_{16_17} = v_{16_17} * d / v_{kin}$$

$$re_{17_18} = v_{17_18} * d / v_{kin}$$

$$re_{18_19} = v_{18_19} * d / v_{kin}$$

$$re_{19_20} = v_{20} * d / v_{kin}$$

"Energy Equations"

$$p_{pump} - p_0 = \rho * (g * l_{pump_0}) + \rho * (f_0 * (l_{pump_0} / d) * (v_0^2) / 2) + \rho * (K_{elbow} * (v_0^2) / 2) \text{ "lbf/ft}^2\text{"}$$

$$p_{0_0} - p_{0_1} = \rho * (f_{0_0} * (1_{0_0_1} / d) * (v_{0_0}^2) / 2) + 2 * \rho * (K_{elbow} * (v_{0_0}^2) / 2) \text{ "lbf/ft}^2\text{"}$$

$$p_{0_1} - p_{atm} = \rho * (((v_{1_1}^2) - (v_{0_1}^2)) / (2)) + (f_{1_1} * 1_{nozzle} * v_{1_1}^2) / (d_{nozzle} * 2) + \rho * (K_{nozzleexit} * (v_{1_1}^2) / 2) \text{ "lbf/ft}^2\text{"}$$

$$p_{1_2} - p_{atm} = \rho * (((v_{2_2}^2) - (v_{1_2}^2)) / (2)) + (f_{2_2} * 1_{nozzle} * v_{2_2}^2) / (d_{nozzle} * 2) + \rho * (K_{nozzleexit} * (v_{2_2}^2) / 2) \text{ "lbf/ft}^2\text{"}$$

$$p_{2_3} - p_{atm} = \rho * (((v_{3_3}^2) - (v_{2_3}^2)) / (2)) + (f_{3_3} * 1_{nozzle} * v_{3_3}^2) / (d_{nozzle} * 2) + \rho * (K_{nozzleexit} * (v_{3_3}^2) / 2) \text{ "lbf/ft}^2\text{"}$$

$$p_{3_4} - p_{atm} = \rho * (((v_{4_4}^2) - (v_{3_4}^2)) / (2)) + (f_{4_4} * 1_{nozzle} * v_{4_4}^2) / (d_{nozzle} * 2) + \rho * (K_{nozzleexit} * (v_{4_4}^2) / 2) \text{ "lbf/ft}^2\text{"}$$

$$p_{4_5} - p_{atm} = \rho * (((v_{5_5}^2) - (v_{4_5}^2)) / (2)) + (f_{5_5} * 1_{nozzle} * v_{5_5}^2) / (d_{nozzle} * 2) + \rho * (K_{nozzleexit} * (v_{5_5}^2) / 2) \text{ "lbf/ft}^2\text{"}$$

$$p_{5_6} - p_{atm} = \rho * (((v_{6_6}^2) - (v_{5_6}^2)) / (2)) + (f_{6_6} * 1_{nozzle} * v_{6_6}^2) / (d_{nozzle} * 2) + \rho * (K_{nozzleexit} * (v_{6_6}^2) / 2) \text{ "lbf/ft}^2\text{"}$$

$$p_{6_7} - p_{atm} = \rho * (((v_{7_7}^2) - (v_{6_7}^2)) / (2)) + (f_{7_7} * 1_{nozzle} * v_{7_7}^2) / (d_{nozzle} * 2) + \rho * (K_{nozzleexit} * (v_{7_7}^2) / 2) \text{ "lbf/ft}^2\text{"}$$

$$p_{7_8} - p_{atm} = \rho * (((v_{8_8}^2) - (v_{7_8}^2)) / (2)) + (f_{8_8} * 1_{nozzle} * v_{8_8}^2) / (d_{nozzle} * 2) + \rho * (K_{nozzleexit} * (v_{8_8}^2) / 2) \text{ "lbf/ft}^2\text{"}$$

$$p_{8_9} - p_{atm} = \rho * (((v_{9_9}^2) - (v_{8_9}^2)) / (2)) + (f_{9_9} * 1_{nozzle} * v_{9_9}^2) / (d_{nozzle} * 2) + \rho * (K_{nozzleexit} * (v_{9_9}^2) / 2) \text{ "lbf/ft}^2\text{"}$$

$$p_{9_{10}} - p_{atm} = \rho * (((v_{10_{10}}^2) - (v_{9_{10}}^2)) / (2)) + (f_{10_{10}} * 1_{nozzle} * v_{10_{10}}^2) / (d_{nozzle} * 2) + \rho * (K_{nozzleexit} * (v_{10_{10}}^2) / 2) \text{ "lbf/ft}^2\text{"}$$

$$p_{10_{11}} - p_{atm} = \rho * (((v_{11_{11}}^2) - (v_{10_{11}}^2)) / (2)) + (f_{11_{11}} * 1_{nozzle} * v_{11_{11}}^2) / (d_{nozzle} * 2) + \rho * (K_{nozzleexit} * (v_{11_{11}}^2) / 2) \text{ "lbf/ft}^2\text{"}$$

$$\begin{aligned}
p_{11_12} - p_{atm} &= \rho * (((v_{12}^2) - (v_{11_12}^2)) / (2)) + (f_{12} * l_{nozzle} * v_{12}^2) / (d_{nozzle}^2) + \rho * (K_{nozzleexit} * (v_{12}^2) / 2) \text{ "lbf/ft}^2\text{"} \\
p_{12_13} - p_{atm} &= \rho * (((v_{13}^2) - (v_{12_13}^2)) / (2)) + (f_{13} * l_{nozzle} * v_{13}^2) / (d_{nozzle}^2) + \rho * (K_{nozzleexit} * (v_{13}^2) / 2) \text{ "lbf/ft}^2\text{"} \\
p_{13_14} - p_{atm} &= \rho * (((v_{14}^2) - (v_{13_14}^2)) / (2)) + (f_{14} * l_{nozzle} * v_{14}^2) / (d_{nozzle}^2) + \rho * (K_{nozzleexit} * (v_{14}^2) / 2) \text{ "lbf/ft}^2\text{"} \\
p_{14_15} - p_{atm} &= \rho * (((v_{15}^2) - (v_{14_15}^2)) / (2)) + (f_{15} * l_{nozzle} * v_{15}^2) / (d_{nozzle}^2) + \rho * (K_{nozzleexit} * (v_{15}^2) / 2) \text{ "lbf/ft}^2\text{"} \\
p_{15_16} - p_{atm} &= \rho * (((v_{16}^2) - (v_{15_16}^2)) / (2)) + (f_{16} * l_{nozzle} * v_{16}^2) / (d_{nozzle}^2) + \rho * (K_{nozzleexit} * (v_{16}^2) / 2) \text{ "lbf/ft}^2\text{"} \\
p_{16_17} - p_{atm} &= \rho * (((v_{17}^2) - (v_{16_17}^2)) / (2)) + (f_{17} * l_{nozzle} * v_{17}^2) / (d_{nozzle}^2) + \rho * (K_{nozzleexit} * (v_{17}^2) / 2) \text{ "lbf/ft}^2\text{"} \\
p_{17_18} - p_{atm} &= \rho * (((v_{18}^2) - (v_{17_18}^2)) / (2)) + (f_{18} * l_{nozzle} * v_{18}^2) / (d_{nozzle}^2) + \rho * (K_{nozzleexit} * (v_{18}^2) / 2) \text{ "lbf/ft}^2\text{"} \\
p_{18_19} - p_{atm} &= \rho * (((v_{19}^2) - (v_{18_19}^2)) / (2)) + (f_{19} * l_{nozzle} * v_{19}^2) / (d_{nozzle}^2) + \rho * (K_{nozzleexit} * (v_{19}^2) / 2) \text{ "lbf/ft}^2\text{"} \\
p_{19_20} - p_{atm} &= \rho * (f_{20} * l_{nozzle} * v_{20}^2) / (d_{nozzle}^2) + \rho * (K_{nozzleexit} * (v_{20}^2) / 2) \text{ "lbf/ft}^2\text{"}
\end{aligned}$$

$$\begin{aligned}
p_{0_1} - p_{1_2} &= \rho * (((v_{1_2}^2) - (v_{0}^2)) / (2)) + (f_{1_2} * l_{btwndroppers} * v_{1_2}^2) / (d^2) \text{ "lbf/ft}^2\text{"} \\
p_{1_2} - p_{2_3} &= \rho * (((v_{2_3}^2) - (v_{1_2}^2)) / (2)) + (f_{2_3} * l_{btwndroppers} * v_{2_3}^2) / (d^2) \text{ "lbf/ft}^2\text{"} \\
p_{2_3} - p_{3_4} &= \rho * (((v_{3_4}^2) - (v_{2_3}^2)) / (2)) + (f_{3_4} * l_{btwndroppers} * v_{3_4}^2) / (d^2) \text{ "lbf/ft}^2\text{"} \\
p_{3_4} - p_{4_5} &= \rho * (((v_{4_5}^2) - (v_{3_4}^2)) / (2)) + (f_{4_5} * l_{btwndroppers} * v_{4_5}^2) / (d^2) \text{ "lbf/ft}^2\text{"} \\
p_{4_5} - p_{5_6} &= \rho * (((v_{5_6}^2) - (v_{4_5}^2)) / (2)) + (f_{5_6} * l_{btwndroppers} * v_{5_6}^2) / (d^2) \text{ "lbf/ft}^2\text{"} \\
p_{5_6} - p_{6_7} &= \rho * (((v_{6_7}^2) - (v_{5_6}^2)) / (2)) + (f_{6_7} * l_{btwndroppers} * v_{6_7}^2) / (d^2) \text{ "lbf/ft}^2\text{"}
\end{aligned}$$

$$p_{6_7} - p_{7_8} = \rho * (((v_{7_8}^2) - (v_{6_7}^2)) / (2)) + (f_{7_8} * 1_{btwndroppers} * v_{7_8}^2) / (d^2) \text{ "lbf/ft}^2\text{"}$$

$$p_{7_8} - p_{8_9} = \rho * (((v_{8_9}^2) - (v_{7_8}^2)) / (2)) + (f_{8_9} * 1_{btwndroppers} * v_{8_9}^2) / (d^2) \text{ "lbf/ft}^2\text{"}$$

$$p_{8_9} - p_{9_{10}} = \rho * (((v_{9_{10}}^2) - (v_{8_9}^2)) / (2)) + (f_{9_{10}} * 1_{btwndroppers} * v_{9_{10}}^2) / (d^2) \text{ "lbf/ft}^2\text{"}$$

$$p_{9_{10}} - p_{10_{11}} = \rho * (((v_{10_{11}}^2) - (v_{9_{10}}^2)) / (2)) + (f_{10_{11}} * 1_{btwndroppers} * v_{10_{11}}^2) / (d^2) \text{ "lbf/ft}^2\text{"}$$

$$p_{10_{11}} - p_{11_{12}} = \rho * (((v_{11_{12}}^2) - (v_{10_{11}}^2)) / (2)) + (f_{11_{12}} * 1_{btwndroppers} * v_{11_{12}}^2) / (d^2) \text{ "lbf/ft}^2\text{"}$$

$$p_{11_{12}} - p_{12_{13}} = \rho * (((v_{12_{13}}^2) - (v_{11_{12}}^2)) / (2)) + (f_{12_{13}} * 1_{btwndroppers} * v_{12_{13}}^2) / (d^2) \text{ "lbf/ft}^2\text{"}$$

$$p_{12_{13}} - p_{13_{14}} = \rho * (((v_{13_{14}}^2) - (v_{12_{13}}^2)) / (2)) + (f_{13_{14}} * 1_{btwndroppers} * v_{13_{14}}^2) / (d^2) \text{ "lbf/ft}^2\text{"}$$

$$p_{13_{14}} - p_{14_{15}} = \rho * (((v_{14_{15}}^2) - (v_{13_{14}}^2)) / (2)) + (f_{14_{15}} * 1_{btwndroppers} * v_{14_{15}}^2) / (d^2) \text{ "lbf/ft}^2\text{"}$$

$$p_{14_{15}} - p_{15_{16}} = \rho * (((v_{15_{16}}^2) - (v_{14_{15}}^2)) / (2)) + (f_{15_{16}} * 1_{btwndroppers} * v_{15_{16}}^2) / (d^2) \text{ "lbf/ft}^2\text{"}$$

$$p_{15_{16}} - p_{16_{17}} = \rho * (((v_{16_{17}}^2) - (v_{15_{16}}^2)) / (2)) + (f_{16_{17}} * 1_{btwndroppers} * v_{16_{17}}^2) / (d^2) \text{ "lbf/ft}^2\text{"}$$

$$p_{16_{17}} - p_{17_{18}} = \rho * (((v_{17_{18}}^2) - (v_{16_{17}}^2)) / (2)) + (f_{17_{18}} * 1_{btwndroppers} * v_{17_{18}}^2) / (d^2) \text{ "lbf/ft}^2\text{"}$$

$$p_{17_{18}} - p_{18_{19}} = \rho * (((v_{18_{19}}^2) - (v_{17_{18}}^2)) / (2)) + (f_{18_{19}} * 1_{btwndroppers} * v_{18_{19}}^2) / (d^2) \text{ "lbf/ft}^2\text{"}$$

$$p_{18_{19}} - p_{19_{20}} = \rho * (((v_{20}^2) - (v_{18_{19}}^2)) / (2)) + (f_{19_{20}} * 1_{btwndroppers} * v_{20}^2) / (d^2) \text{ "lbf/ft}^2\text{"}$$

"Friction Factors"

f_0 = 64/re_0 "solves for friction factor for nozzles from reynolds number for laminar flow"

$$f_1 = 64/re_1$$

$$f_2 = 64/re_2$$

$$f_3 = 64/re_3$$

$$f_4 = 64/re_4$$

$$f_5 = 64/re_5$$

$$f_6 = 64/re_6$$

$$f_7 = 64/re_7$$

$$f_8 = 64/re_8$$

$$f_9 = 64/re_9$$
$$f_{10} = 64/re_{10}$$

$$f_{11} = 64/re_{11}$$
$$f_{12} = 64/re_{12}$$
$$f_{13} = 64/re_{13}$$
$$f_{14} = 64/re_{14}$$
$$f_{15} = 64/re_{15}$$
$$f_{16} = 64/re_{16}$$
$$f_{17} = 64/re_{17}$$
$$f_{18} = 64/re_{18}$$
$$f_{19} = 64/re_{19}$$
$$f_{20} = 64/re_{20}$$

$f_{1_2} = 64/re_{1_2}$ "solves for friction factor between nozzles from reynolds number for laminar flow"

$$f_{2_3} = 64/re_{2_3}$$
$$f_{3_4} = 64/re_{3_4}$$
$$f_{4_5} = 64/re_{4_5}$$
$$f_{5_6} = 64/re_{5_6}$$
$$f_{6_7} = 64/re_{6_7}$$
$$f_{7_8} = 64/re_{7_8}$$
$$f_{8_9} = 64/re_{8_9}$$
$$f_{9_10} = 64/re_{9_10}$$

$$f_{10_11} = 64/re_{10_11}$$

$$f_{11_12} = 64/re_{11_12}$$
$$f_{12_13} = 64/re_{12_13}$$
$$f_{13_14} = 64/re_{13_14}$$
$$f_{14_15} = 64/re_{14_15}$$
$$f_{15_16} = 64/re_{15_16}$$
$$f_{16_17} = 64/re_{16_17}$$
$$f_{17_18} = 64/re_{17_18}$$
$$f_{18_19} = 64/re_{18_19}$$
$$f_{19_20} = 64/re_{19_20}$$

$$p_{pumprel} = p_{pump} - p_{atm}$$
$$p_{pumprelpsi} = p_{pumprel}/144$$

Appendix T: Screenshot of Excel File 'ME 430 Experiment Data'

Excel file is included in project submission folder

Experiment 2: Verify Design of Branch of Dropper									
Part 1: Predicting pump flowrate collection									
Trial	Run time (min)	Misc (g)	Pump rate (ml/min)	Expected pump rate (ml/min)					
Trial 1	1	13.3833	13.3833	12.564					
Trial 2	1	14.4851	14.4851	12.564					
Trial 3	1	14.4851	14.4851	12.564					
Trial 4	1	14.4851	14.4851	12.564					
Trial 5	1	14.4851	14.4851	12.564					

Part 2: Idealized drop size vs									
Month: oct-1									
Trial	Misc (g)	# of Drops	Drop diameter (mm)	Misc (g)	# of Drops	Drop diameter (mm)	Misc (g)	# of Drops	Drop diameter (mm)
Trial 1	0.0097	31	2.1803	0.6765	84	2.4867	1.0293	63	3.0607
Trial 2									
Trial 3									
Trial 4									
Trial 5									

Experiment day 2									
Trial	Misc (g)	# of Drops	Drop diameter (mm)	Misc (g)	# of Drops	Drop diameter (mm)	Misc (g)	# of Drops	Drop diameter (mm)
Trial 1	0.0308	201	1.3765	0.1883	71	0.00246	1.8809		
Trial 2	0.0346	201	1.3765	0.4146	102	0.00382	1.8001		
Trial 3	0.0382	144	1.3765	0.2971	72	0.00382	1.8001		
Trial 4	0.0382	89	1.3765	0.2971	72	0.00382	1.8001		
Trial 5	0.0382	89	1.3765	0.2971	72	0.00382	1.8001		
Trial 6	0.0382	89	1.3765	0.2971	72	0.00382	1.8001		
Trial 7	0.0382	89	1.3765	0.2971	72	0.00382	1.8001		
Trial 8	0.0382	89	1.3765	0.2971	72	0.00382	1.8001		
Trial 9	0.0382	89	1.3765	0.2971	72	0.00382	1.8001		
Trial 10	0.0382	89	1.3765	0.2971	72	0.00382	1.8001		

Experiment day 2									
Trial	Misc (g)	# of Drops	Drop diameter (mm)	Misc (g)	# of Drops	Drop diameter (mm)	Misc (g)	# of Drops	Drop diameter (mm)
Trial 1	0.0038	13412	0.0025	1.8809					
Trial 2	0.0038	13412	0.0025	1.8809					
Trial 3	0.0038	13412	0.0025	1.8809					
Trial 4	0.0038	13412	0.0025	1.8809					
Trial 5	0.0038	13412	0.0025	1.8809					
Trial 6	0.0038	13412	0.0025	1.8809					
Trial 7	0.0038	13412	0.0025	1.8809					
Trial 8	0.0038	13412	0.0025	1.8809					
Trial 9	0.0038	13412	0.0025	1.8809					
Trial 10	0.0038	13412	0.0025	1.8809					

Appendix U: MatLab Script for fluid Pathway through FDS

The script is pasted in below. It is also included in the project submission folder.

File Name: ME430maxpressureshowerorientation.m

Script:

```
% Finding Max. Pressure in 'splitting tubes' fluid delivery system
```

```
%% Estimating Reynold's Number for quarter inch tubing before 1st split (48 qtr  
inch tubes worth of flow)
```

```
mu = 8.90*10^(-4); % Dynamic Viscosity of water (Pa*s)
```

```
Dtube = 0.00635; % ID of 1/4" tubing (0.25in = 0.00635m)
```

```
rhowater = 1000; % Density of water (kg/(m^3))
```

```
Ddrop = 0.002; % m , Drop Diameter = 2mm
```

```
numbrackets = 48; % number of brackets each tube goes to
```

```
numdroppersperbracket = 20; % number of droppers per dropper assembly
```

```
numdroppers = numbrackets*numdroppersperbracket; % total number of droppers
```

```
dropvolume = (4/3)*pi*(Ddrop/2)^3; % volume of each drop (m^3)
```

```
I = 9.05*10^(-6); % Drop Intensity Spec. from DNVGL-RP-0171
```

```
A = pi*((1.1^2)-(0.9^2)); % Exposure zone Area for rainfall (m^2)
```

```
P = I*A % Flow rate of water to reach spec. intensity (m^3/s)
```

```
dropfreq = P/(numdroppers*dropvolume); % Drop frequency (drops/sec)
```

```
tubearea = pi*(Dtube/2)^2; % tube cross section area (m^2)
```

```
Vavgatpumpoutlet = dropvolume*dropfreq*numdroppers/tubearea; % velocity of  
fluid at pump outlet (m/s)
```

```
Reqtrtubingatpumpoutlet = rhowater*Vavgatpumpoutlet*Dtube/mu; % reynolds  
number at pump outlet
```

```
%% Finding required Flowrate from pump outlet
```

```
qatpumpoutlet = Vavgatpumpoutlet*tubearea; % flow rate at pump outlet (m^3/s)
```

```
qatpumpoutletmlpermin = qatpumpoutlet*(6*10^7); % flow rate at pump outlet  
(ml/min)
```

```
%% Estimating Reynold's Number for quarter inch tubing after 1st split into 2  
tubes (24 dropper configurations worth of flow each)
```

```
numbrackets = 24; % number of brackets each tube supplies flow
```

numdroppers = numbrackets*numdroppersperbracket; % number of droppers each tube supplies flow

Vavgafter1stsplit = dropvolume*dropfreq*numdroppers/tubearea; % Average velocity in tube after 1st split (m/s)

Reqtrtubingafter1stsplit = rhewater*Vavgafter1stsplit*Dtube/mu; % Reynold's number after 1st split in tubing

%% Estimating Reynold's Number for quarter inch tubing after 2nd split (12 dropper configurations worth of flow each)

numbrackets = 12; % number of brackets each tube supplies flow

numdroppers = numbrackets*numdroppersperbracket; % number of droppers each tube supplies flow

Vavgafter2ndsplit = dropvolume*dropfreq*numdroppers/tubearea; % Average velocity in tube after 2nd split (m/s)

Reqtrtubingafter2ndsplit = rhewater*Vavgafter2ndsplit*Dtube/mu; % Reynold's number after 2nd split in tubing

%% Finding Flowrate for experiment with 1x 1:12 splitter

qafter2ndsplit = Vavgafter2ndsplit*tubearea; % flow rate after 2nd tubing split (m³/s)

qafter2ndsplitmlpermin = qafter2ndsplit*(6*10⁷); % flow rate after 2nd tubing split (converts m³/s to ml/min)

qafter12_1 = qafter2ndsplitmlpermin/12; % flow rate leaving 1:12 splitter (ml/min)

%% Estimating Reynold's Number for quarter inch tubing after 3rd split (1:12 splitter) (1 dropper configuration worth of flow each)

numbrackets = 1; % number of brackets each tube supplies flow

numdroppers = numbrackets*numdroppersperbracket; % number of droppers each tube supplies flow

Vavgafter3rdsplit = dropvolume*dropfreq*numdroppers/tubearea; % Average velocity in tube after 3rd split (m/s)

Reqtrtubingafter3rdsplit = rhewater*Vavgafter3rdsplit*Dtube/mu; % Reynold's number after 3rd split in tubing

%% Estimating Reynold's Number for nozzle

$D_{\text{nozzle}} = 0.00009$; % 0.09mm = 0.00009m
 $\text{dropvolume} = (4/3)*\pi*(D_{\text{drop}}/2)^3$; % volume of a drop (m³)
 $\text{nozzlearea} = \pi*(D_{\text{nozzle}}/2)^2$; % Cross sectional area of nozzle (m²)

$V_{\text{avgnozzle}} = \text{dropvolume}*\text{dropfreq}/\text{nozzlearea}$; % m/s

$R_{\text{nozzle}} = \rho_{\text{water}}*V_{\text{avgnozzle}}*D_{\text{nozzle}}/\mu$;

%% Total Expected Lengths of Tubing

$L_{\text{qtrtubingatpumpoutlet}} = 1.5$; % m, length of quarter inch tubing leaving pump outlet

$R_{\text{ring}} = 1.1$; % m

$C_{\text{ring}} = R_{\text{ring}}*2*\pi$; % m

$L_{\text{qtrtubingafter1stspl}} = R_{\text{ring}} + 1$; % m, length of quarter inch tubing after 1st split, from 1 tube to 2 tubes

$L_{\text{qtrtubingafter2ndspl}} = .5$; % m, length of quarter inch tubing after 2nd split, goes from 2 tubes to 4 tubes

$L_{\text{qtrtubingafter3rdspl}} = R_{\text{ring}} + 0.5$; % m, length of quarter inch tubing after 3rd split, goes from 4 tubes to 48 tubes

$L_{\text{nozzle}} = 0.0127$; % m, length of needle producing drop (0.50in)

%% Total Head Loss from Lengths of Tubing and nozzle

$f_{\text{qtrtubingatpumpoutlet}} = 0.058$; % Friction factor for quarter inch tubing with turbulent flow from moody diagram ($Re_q = 2600$, $e/D = 0.019$)

$f_{\text{qtrtubingafter1stspl}} = 64/Re_{\text{qtrtubingafter1stspl}}$; % Friction factor for quarter inch tubing with laminar flow

$f_{\text{qtrtubingafter2ndspl}} = 64/Re_{\text{qtrtubingafter2ndspl}}$; % Friction factor for quarter inch tubing with laminar flow

$f_{\text{qtrtubingafter3rdspl}} = 64/Re_{\text{qtrtubingafter3rdspl}}$; % Friction factor for quarter inch tubing with laminar flow

$f_{\text{nozzle}} = 64/R_{\text{nozzle}}$; % Friction factor for nozzle with laminar flow

$h_{\text{lmqtrtubingatpumpoutlet}} =$

$f_{\text{qtrtubingatpumpoutlet}}*(L_{\text{qtrtubingatpumpoutlet}}/D_{\text{tube}})*(V_{\text{avgatpumpoutlet}}^2)/2$;
% (m²)/(s²), head loss for quarter inch tubing from outlet of pump to 1st split

$h_{\text{lmqtrtubingafter1stspl}} =$

$f_{\text{qtrtubingafter1stspl}}*(L_{\text{qtrtubingafter1stspl}}/D_{\text{tube}})*(V_{\text{avgafter1stspl}}^2)/2$; %
(m²)/(s²), head loss for quarter inch tubing from 1st split to 2nd split

```

hlmqtrtubingafter2ndsplrit =
fqtrtubingafter2ndsplrit*(Lqtrtubingafter2ndsplrit/Dtube)*(Vavgafter2ndsplrit^2)/2;
% (m^2)/(s^2), head loss for quarter inch tubing from 2nd split to 1:12 splitter
hlmqtrtubingafter3rdsplrit =
fqtrtubingafter3rdsplrit*(Lqtrtubingafter3rdsplrit/Dtube)*(Vavgafter3rdsplrit^2)/2; %
(m^2)/(s^2), head loss for quarter inch tubing from 1:12 splitter to dropper config.
inlet

hlmnozzle = fnozzle*(Lnozzle/Dnozzle)*(Vavgnozzle^2)/2; % (m^2)/(s^2), head
loss for nozzle

%% Head loss from transition from quarter inch tubing to nozzle tubing
AR = nozzlearea/tubearea; % equals about 0.0016 so go with 0 => contraction loss
coeff: Kc = 0.5
Kc = 0.5;
hlmcontraction = Kc*(Vavgdroppertubing^2)/2;

%% Head loss from short lengths of PVC between tubing and nozzles
% negligible

%% Head loss from Y-connectors
Kteedividing = 0.9;
hlmteedividingqtr = 4*(Kteedividing*(Vavgatpumpoutlet^2)/2); % head loss for
2x Y-connectors, 1:12 flow divider, and in-line filter. conservative b/c using
average velocity at pump outlet for all 3

%% Total pressure loss from system
hlmtot = (2.5*9.81) + hlmqtrtubingatpumpoutlet + hlmteedividingqtr +
hlmqtrtubingafter1stsplrit + hlmqtrtubingafter2ndsplrit + hlmqtrtubingafter3rdsplrit +
hlmcontraction + hlmnozzle; % (m^2)/(s^2), total head loss for fluid path
PtotPa = hlmtot*rhowater; % Pa
Ptotpsi = PtotPa*(1/6894.8) % pressure pump must overcome to push fluid through
tubings (psi)
Pnozzle = hlmnozzle*rhowater*(1/6894.8); % pressure loss through nozzle (psi)

```

Appendix V: Technical Drawing Package

Technical Drawing Package is included in project submission folder

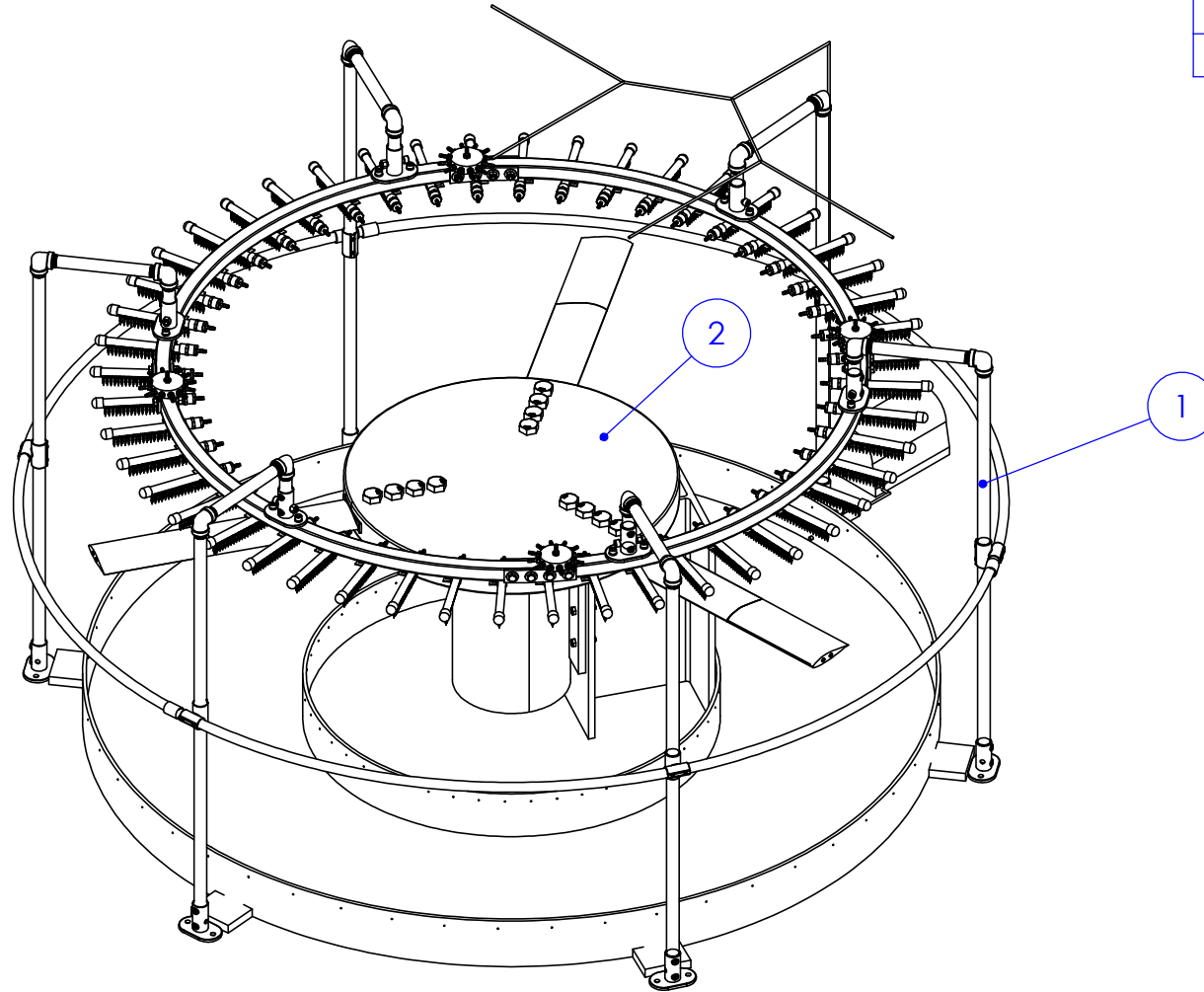
2

1

System #	System Name
1	Fluid Delivery System
2	Rotating Blade System

B

B



A

A

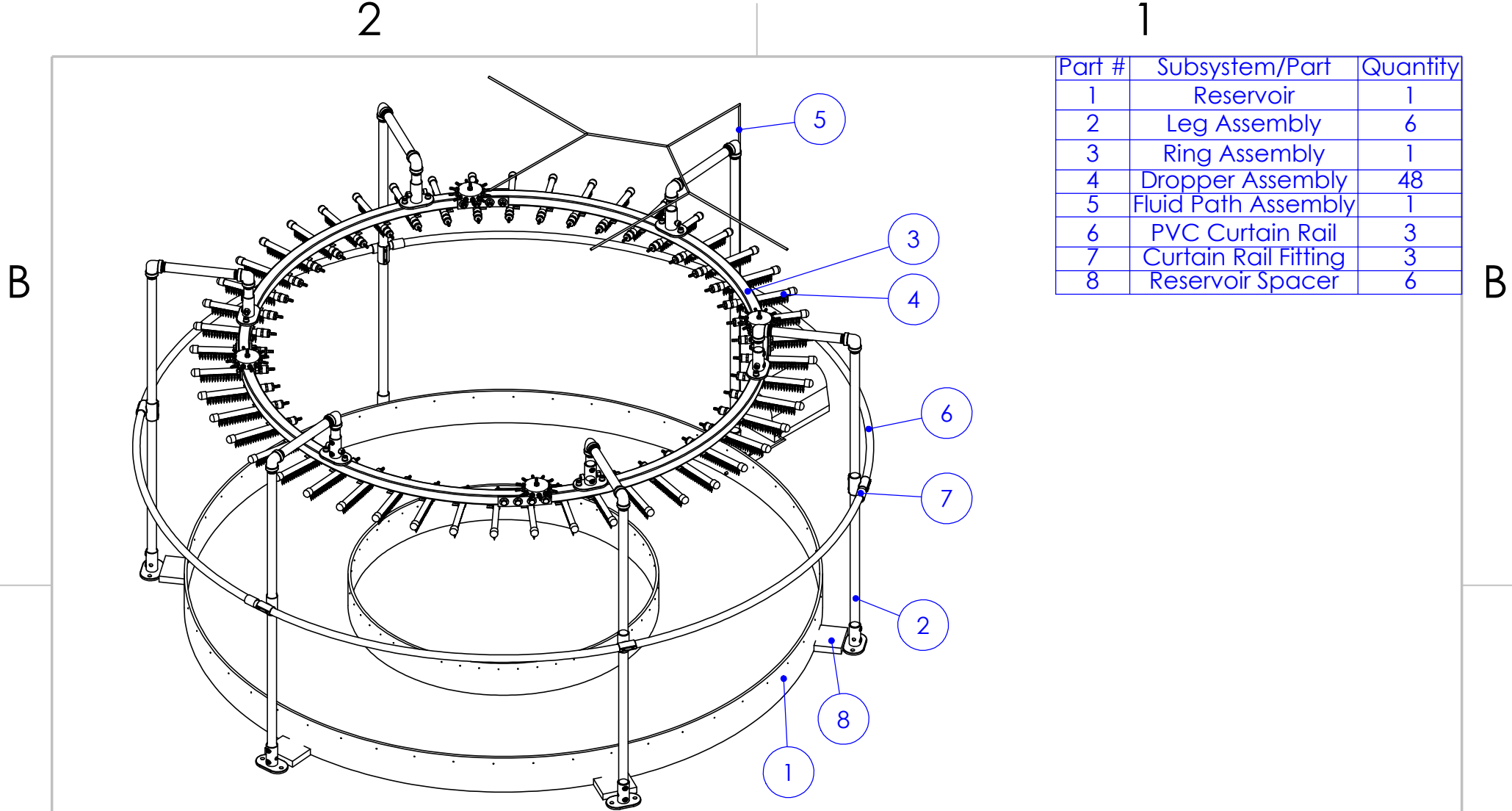
PROPRIETARY AND CONFIDENTIAL
 THE INFORMATION CONTAINED IN THIS DRAWING IS THE SOLE PROPERTY OF TURBINE TECHNOLOGY PARTNERS. ANY REPRODUCTION IN PART OR AS A WHOLE WITHOUT THE WRITTEN PERMISSION OF TURBINE TECHNOLOGY PARTNERS IS PROHIBITED.

		UNLESS OTHERWISE SPECIFIED: DIMENSIONS ARE IN CM UNLESS OTHERWISE SPECIFIED TOLERANCES: FRACTIONAL ANGULAR: MACH BEND TWO PLACE DECIMAL THREE PLACE DECIMAL		NAME	DATE
		INTERPRET GEOMETRIC TOLERANCING PER:	DRAWN	Joe B.	
		MATERIAL	CHECKED		
		FINISH	ENG APPR.		
NEXT ASSY	USED ON		MFG APPR.		
			Q.A.		
			COMMENTS:		
APPLICATION		DO NOT SCALE DRAWING			

TITLE:
Blade Coating Testing Design

SIZE	DWG. NO.	REV
A	Full Assembly	
SCALE: 1:20	WEIGHT:	SHEET 1 OF 19

1

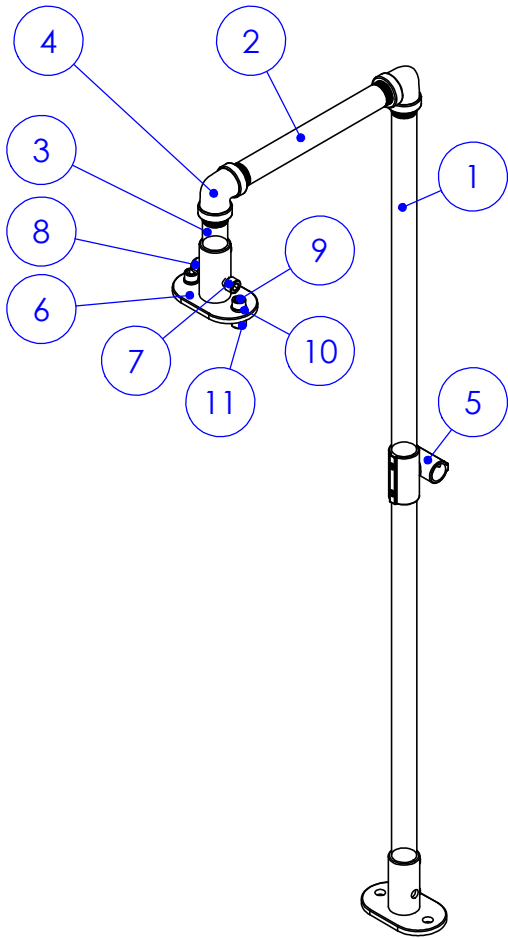


Part #	Subsystem/Part	Quantity
1	Reservoir	1
2	Leg Assembly	6
3	Ring Assembly	1
4	Dropper Assembly	48
5	Fluid Path Assembly	1
6	PVC Curtain Rail	3
7	Curtain Rail Fitting	3
8	Reservoir Spacer	6

<p>PROPRIETARY AND CONFIDENTIAL</p> <p>THE INFORMATION CONTAINED IN THIS DRAWING IS THE SOLE PROPERTY OF TURBINE TECHNOLOGY PARTNERS. ANY REPRODUCTION IN PART OR AS A WHOLE WITHOUT THE WRITTEN PERMISSION OF TURBINE TECHNOLOGY PARTNERS IS PROHIBITED.</p>			UNLESS OTHERWISE SPECIFIED: DIMENSIONS ARE IN CM UNLESS OTHERWISE SPECIFIED TOLERANCES: FRACTIONAL ANGULAR: MACH BEND TWO PLACE DECIMAL THREE PLACE DECIMAL		NAME	DATE	<p>TITLE:</p> <h2>Fluid Delivery System Assembly</h2>		
			INTERPRET GEOMETRIC TOLERANCING PER:	DRAWN	JOE B.				
			MATERIAL	CHECKED					
			FINISH	ENG APPR.					
				MFG APPR.					
	NEXT ASSY	USED ON		Q.A.			SIZE	DWG. NO.	REV
		APPLICATION	DO NOT SCALE DRAWING	COMMENTS:			A	FDS	
							SCALE: 1:20	WEIGHT:	SHEET 2 OF 19

2

1



Part #	Part Name/Manuf. #	Part Description	Quantity (per leg)	Material
1	1" Sch. 40 pipe, 52" long	1" Sch. 40 pipe, 52" long	1	Galvanized Steel
2	4549K625	1" Sch. 40 pipe, 12" long	1	Galvanized Steel
3	1" Sch. 40 pipe, 6" long	1" Sch. 40 pipe, 6" long	1	Galvanized Steel
4	4638K135	90° fitting for 1" Sch. 40	2	Galvanized Steel
5	4698T101	Through-hole reducer	1	Aluminum
6	Leg Foot	2 bolt flange/foot	2	Aluminum
7	90128A722	1/2"-13 bolt, 2 1/2" long	1	Zinc-plated Steel
8	95615A210	1/2"-13 Locknut	1	Zinc-plated Steel
9	90128A297	M12x1.75mm, 30mm long	2	Zinc-plated Steel
10	98690A116	M12 Washer	4	316 Stainless Steel
11	93625A400	M12x1.75mm Locknut	2	18-8 Stainless Steel

B

B

A

A

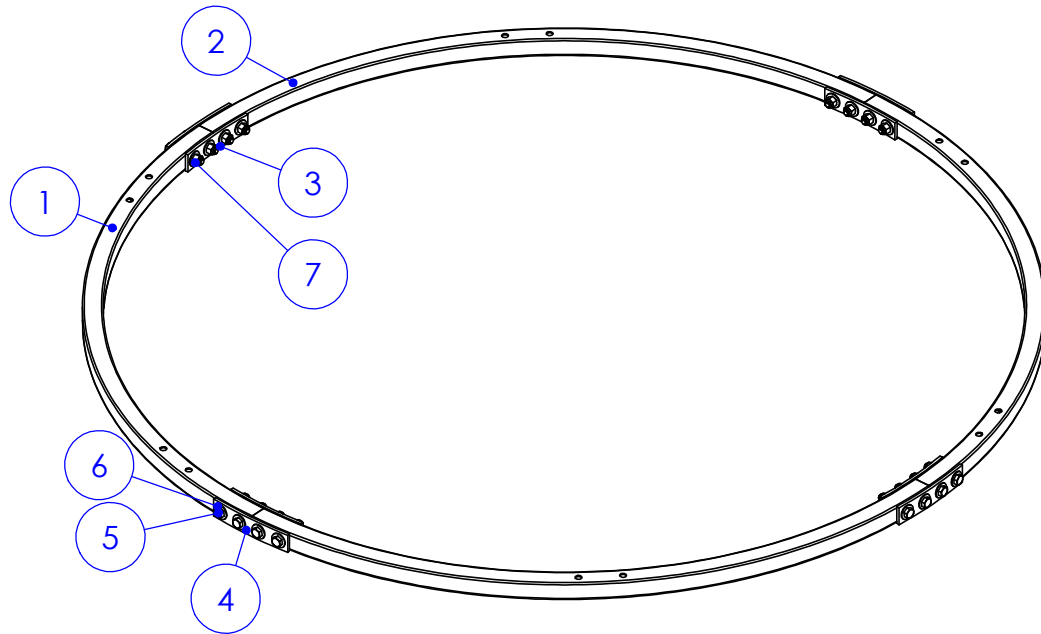
PROPRIETARY AND CONFIDENTIAL
 THE INFORMATION CONTAINED IN THIS DRAWING IS THE SOLE PROPERTY OF TURBINE TECHNOLOGY PARTNERS. ANY REPRODUCTION IN PART OR AS A WHOLE WITHOUT THE WRITTEN PERMISSION OF TURBINE TECHNOLOGY PARTNERS IS PROHIBITED.

		UNLESS OTHERWISE SPECIFIED: DIMENSIONS ARE IN CM UNLESS OTHERWISE SPECIFIED TOLERANCES: FRACTIONAL ANGULAR: MACH BEND TWO PLACE DECIMAL THREE PLACE DECIMAL		NAME	DATE
		INTERPRET GEOMETRIC TOLERANCING PER:			
		MATERIAL			
		FINISH			
NEXT ASSY	USED ON				
APPLICATION		DO NOT SCALE DRAWING			

TITLE: Leg Assembly		
SIZE A	DWG. NO. LEG	REV
SCALE: 1:10		WEIGHT:
SHEET 3 OF 19		

1

Part #	Part Name/Manuf. #	Part Description	Quantity	Material
1	Strut 1	90° curved strut, mounts to 2 legs	2	Zinc-plated Steel
2	Strut 2	90° curved strut, mounts to 1 leg	2	Zinc-plated Steel
3	Inner Strut Bracket	Curved, 4 holes	4	Zinc-plated Steel
4	Outer Strut Bracket	Curved, 4 holes	4	Zinc-plated Steel
5	92198A724	1/2"-13, 3" Long	16	18-8 Stainless Steel
6	92141A033	Washer for 1/2" bolt	32	18-8 Stainless Steel
7	91831A137	1/2"-13 Locknut	16	18-8 Stainless Steel



B

B

A

A

PROPRIETARY AND CONFIDENTIAL
 THE INFORMATION CONTAINED IN THIS DRAWING IS THE SOLE PROPERTY OF TURBINE TECHNOLOGY PARTNERS. ANY REPRODUCTION IN PART OR AS A WHOLE WITHOUT THE WRITTEN PERMISSION OF TURBINE TECHNOLOGY PARTNERS IS PROHIBITED.

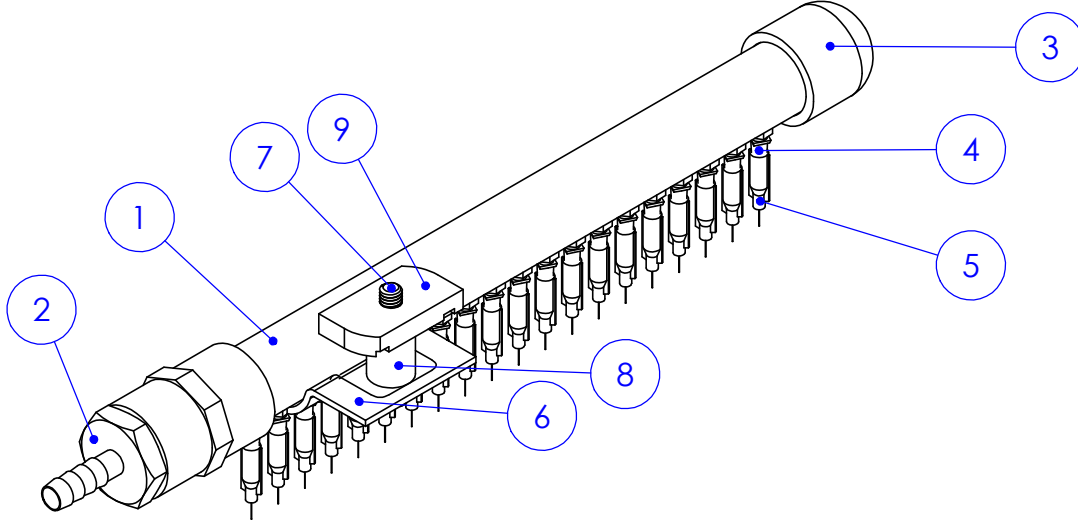
		UNLESS OTHERWISE SPECIFIED: DIMENSIONS ARE IN CM UNLESS OTHERWISE SPECIFIED TOLERANCES: FRACTIONAL ANGULAR: MACH BEND TWO PLACE DECIMAL THREE PLACE DECIMAL		NAME	DATE
		INTERPRET GEOMETRIC TOLERANCING PER:		JOE B.	
		MATERIAL	DRAWN		
		FINISH	CHECKED		
NEXT ASSY	USED ON		ENG APPR.		
			MFG APPR.		
			Q.A.		
			COMMENTS:		
APPLICATION		DO NOT SCALE DRAWING			

TITLE: Ring Assembly		
SIZE A	DWG. NO. RING	REV
SCALE: 1:15	WEIGHT:	SHEET 4 OF 19

Part #	Part Name/ Manuf. #	Part Description	Quantity (per assembly)	Material
1	Dropper PVC Pipe	Sch. 80 1/2" MPT x 1/2" Dia. FPT PVC	1	PVC
2	5372K114	1/4" Tube ID x 1/2 NPT	1	Nylon
3	4880K51	1/2" pipe cap	1	PVC
4	CIMLSTA-1032M-N	10-32 MUNF to Luer Adapter	20	Nylon
5	TE734025	0.08mm ID nozzle	20	Multiple
6	Strut Mount	Strut-Mount Clamp	1	Zinc-plated Steel
7	90128A266	M6x1 mm 30mm Long	1	Zinc-plated Steel
8	94669A352	M6 spacer, 17 mm Long	1	Aluminum
9	3259T33	M6 Strut Channel Nut	1	Zinc-plated Steel

B

B



A

A

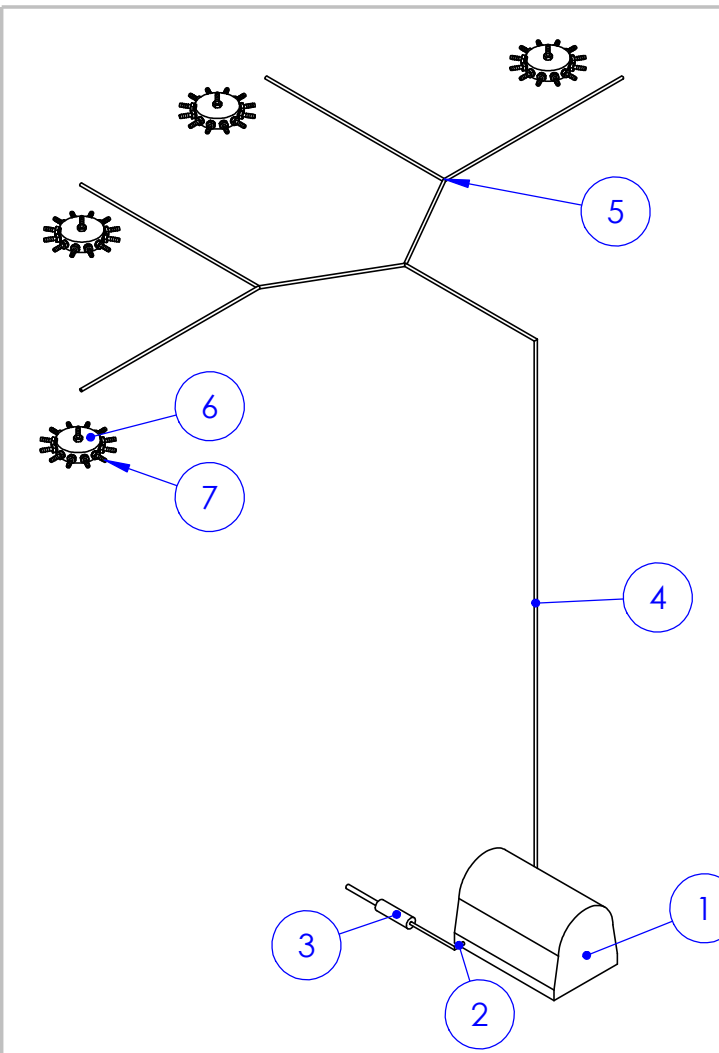
PROPRIETARY AND CONFIDENTIAL
 THE INFORMATION CONTAINED IN THIS DRAWING IS THE SOLE PROPERTY OF TURBINE TECHNOLOGY PARTNERS. ANY REPRODUCTION IN PART OR AS A WHOLE WITHOUT THE WRITTEN PERMISSION OF TURBINE TECHNOLOGY PARTNERS IS PROHIBITED.

		UNLESS OTHERWISE SPECIFIED: DIMENSIONS ARE IN CM UNLESS OTHERWISE SPECIFIED TOLERANCES: FRACTIONAL ANGULAR: MACH BEND TWO PLACE DECIMAL THREE PLACE DECIMAL		NAME	DATE
		INTERPRET GEOMETRIC TOLERANCING PER:		DRAWN	JOE B.
		MATERIAL		CHECKED	
		FINISH		ENG APPR.	
NEXT ASSY	USED ON			MFG APPR.	
				Q.A.	
APPLICATION		DO NOT SCALE DRAWING		COMMENTS:	

TITLE: Dropper Assembly		
SIZE A	DWG. NO. DROP	REV
SCALE: 1:2	WEIGHT:	SHEET 5 OF 19

B

B



Part #	Part Name/ Manuf. #	Part Description	Quantity	Material
1	43205K52	Peristaltic Pump	1	Multiple
2	5372K517	Reducer, for 3/8"x1/4" Tube ID	2	Nylon
3	4795K22	In-line Filter	1	Nylon
4	5195T67	1/4" tubing lengths	57	Polyurethane
5	5372K186	Y-connector	3	Nylon
6	1:12 Flow Divider Body	Flow Divider Body	4	Aluminum
7	5372K112	Adapter, for 1/4" Tube ID x 1/4 NPT Male	52	Nylon



A

A

PROPRIETARY AND CONFIDENTIAL
 THE INFORMATION CONTAINED IN THIS DRAWING IS THE SOLE PROPERTY OF TURBINE TECHNOLOGY PARTNERS. ANY REPRODUCTION IN PART OR AS A WHOLE WITHOUT THE WRITTEN PERMISSION OF TURBINE TECHNOLOGY PARTNERS IS PROHIBITED.

		UNLESS OTHERWISE SPECIFIED: DIMENSIONS ARE IN CM UNLESS OTHERWISE SPECIFIED TOLERANCES: FRACTIONAL ANGULAR: MACH BEND TWO PLACE DECIMAL THREE PLACE DECIMAL		NAME	DATE
		INTERPRET GEOMETRIC TOLERANCING PER:		DRAWN	JOE B.
		MATERIAL		CHECKED	
		FINISH		ENG APPR.	
NEXT ASSY	USED ON			MFG APPR.	
	APPLICATION	DO NOT SCALE DRAWING		Q.A.	
				COMMENTS:	

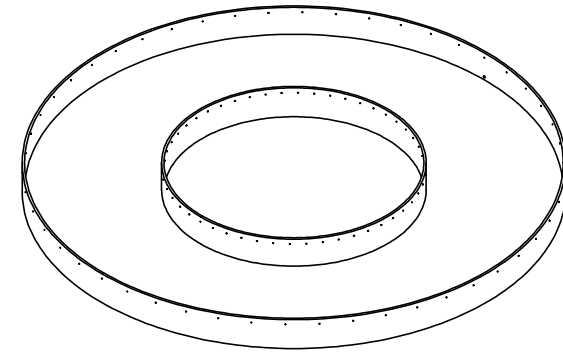
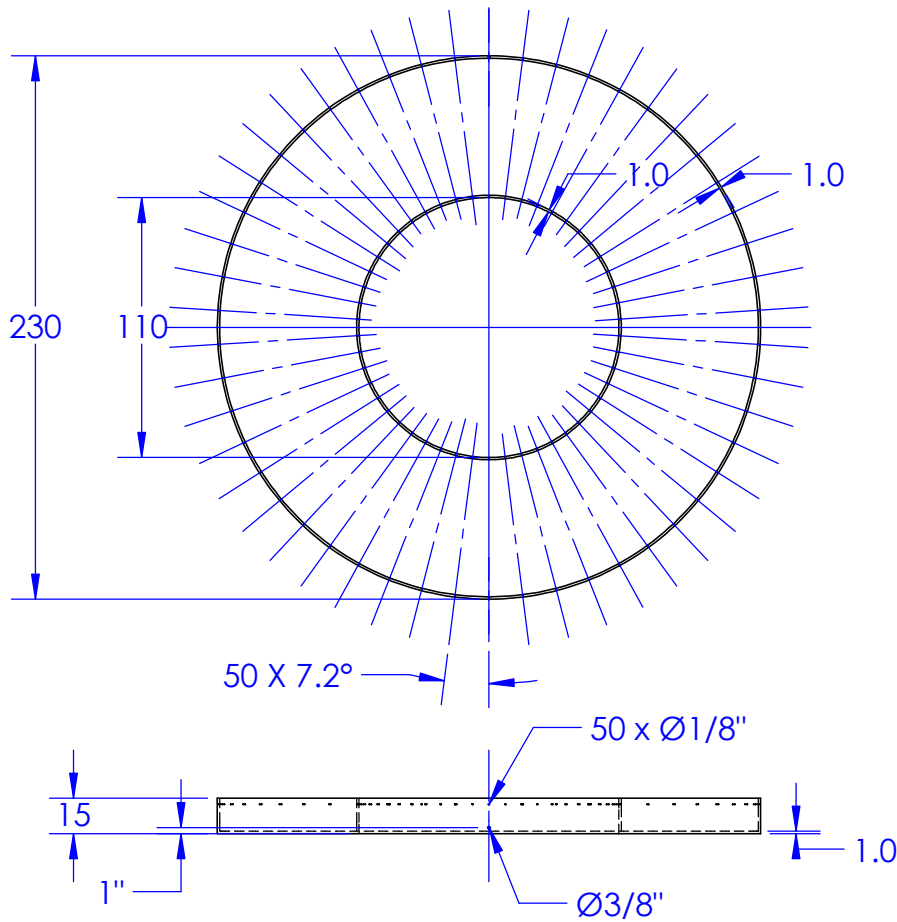
TITLE: Fluid Path Assembly		
SIZE A	DWG. NO. PATH	REV
SCALE: 1:15	WEIGHT:	SHEET 6 OF 19

2

1

B

B



A

A

PROPRIETARY AND CONFIDENTIAL
 THE INFORMATION CONTAINED IN THIS DRAWING IS THE SOLE PROPERTY OF TURBINE TECHNOLOGY PARTNERS. ANY REPRODUCTION IN PART OR AS A WHOLE WITHOUT THE WRITTEN PERMISSION OF TURBINE TECHNOLOGY PARTNERS IS PROHIBITED.

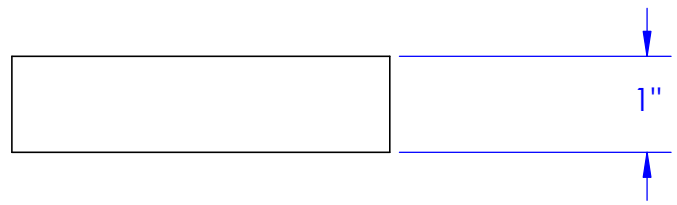
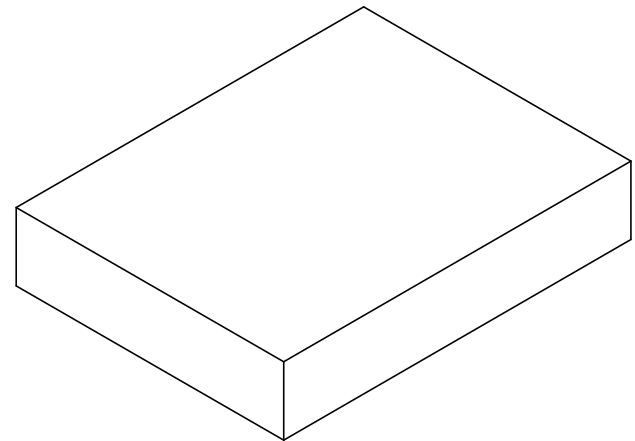
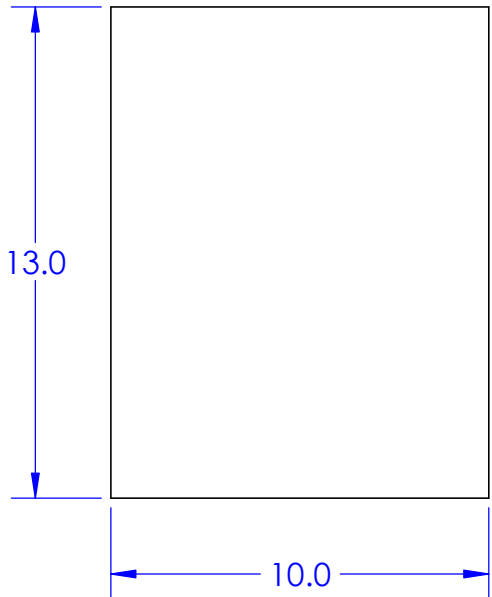
		UNLESS OTHERWISE SPECIFIED: DIMENSIONS ARE IN CM UNLESS OTHERWISE SPECIFIED TOLERANCES: ±1mm FRACTIONAL ANGULAR: MACH BEND TWO PLACE DECIMAL THREE PLACE DECIMAL		NAME	DATE
		INTERPRET GEOMETRIC TOLERANCING PER:	DRAWN	JOE B.	
		MATERIAL	CHECKED		
		FINISH	ENG APPR.		
NEXT ASSY	USED ON	PLASTIC	MFG APPR.		
APPLICATION		DO NOT SCALE DRAWING	Q.A.		
			COMMENTS: Stock part is unspecified at this time. Starting with a plastic pool or container with approximate dimensions would be convenient. Remaining geometry can be formed from plastic sheets and caulk		

TITLE: Reservoir		
SIZE A	DWG. NO. RES	REV
SCALE: 1:32	WEIGHT:	SHEET 7 OF 19

1

2

1



B

B

A

A

PROPRIETARY AND CONFIDENTIAL
 THE INFORMATION CONTAINED IN THIS DRAWING IS THE SOLE PROPERTY OF TURBINE TECHNOLOGY PARTNERS. ANY REPRODUCTION IN PART OR AS A WHOLE WITHOUT THE WRITTEN PERMISSION OF TURBINE TECHNOLOGY PARTNERS IS PROHIBITED.

		UNLESS OTHERWISE SPECIFIED:		NAME	DATE
		DIMENSIONS ARE IN CM UNLESS OTHERWISE SPECIFIED	DRAWN	JOE B.	
		TOLERANCES: ± 0.1CM	CHECKED		
		FRACTIONAL	ENG APPR.		
		ANGULAR: MACH BEND	MFG APPR.		
		TWO PLACE DECIMAL	Q.A.		
		THREE PLACE DECIMAL	COMMENTS:		
		INTERPRET GEOMETRIC TOLERANCING PER:			
		MATERIAL			
		WOOD			
		FINISH			
NEXT ASSY	USED ON				
APPLICATION		DO NOT SCALE DRAWING			

TITLE: Reservoir-to-leg Spacer		
SIZE A	DWG. NO. SPACER	REV
SCALE: 1:2	WEIGHT:	SHEET 8 OF 19

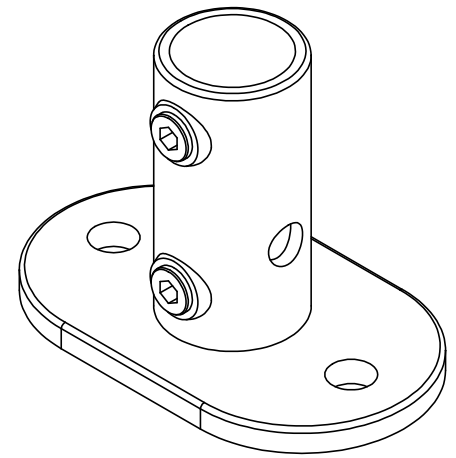
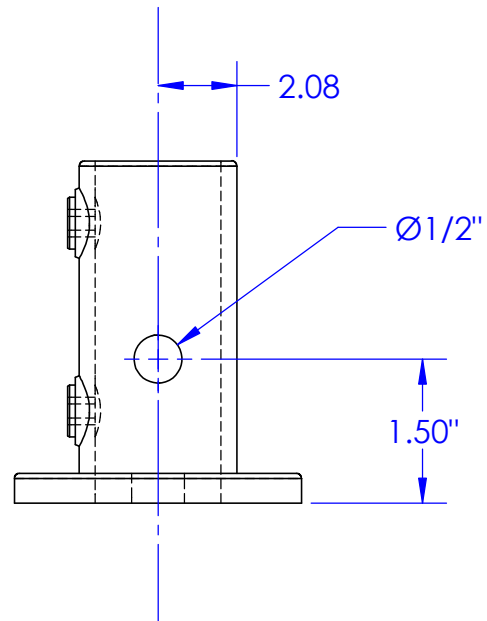
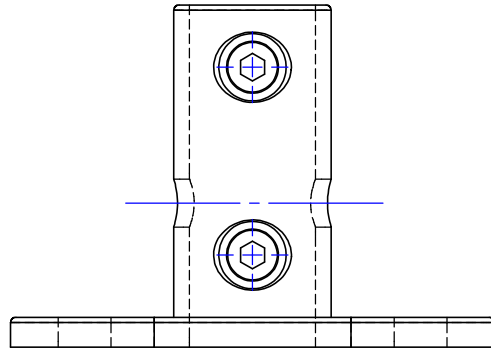
1

2

1

B

B



A

A

PROPRIETARY AND CONFIDENTIAL
 THE INFORMATION CONTAINED IN THIS DRAWING IS THE SOLE PROPERTY OF TURBINE TECHNOLOGY PARTNERS. ANY REPRODUCTION IN PART OR AS A WHOLE WITHOUT THE WRITTEN PERMISSION OF TURBINE TECHNOLOGY PARTNERS IS PROHIBITED.

		UNLESS OTHERWISE SPECIFIED: DIMENSIONS ARE IN CM UNLESS OTHERWISE SPECIFIED TOLERANCES: ±0.01cm FRACTIONAL ANGULAR: MACH BEND TWO PLACE DECIMAL THREE PLACE DECIMAL		NAME	DATE
		INTERPRET GEOMETRIC TOLERANCING PER:		DRAWN	JOE B.
		MATERIAL		CHECKED	
		FINISH		ENG APPR.	
NEXT ASSY	USED ON			MFG APPR.	
APPLICATION		DO NOT SCALE DRAWING		Q.A.	
			COMMENTS: Stock is part # 4698T133 from McMaster-Carr		

TITLE: Leg Foot		
SIZE A	DWG. NO. FOOT	REV
SCALE: 1:2	WEIGHT:	SHEET 9 OF 19

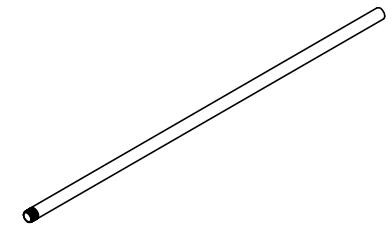
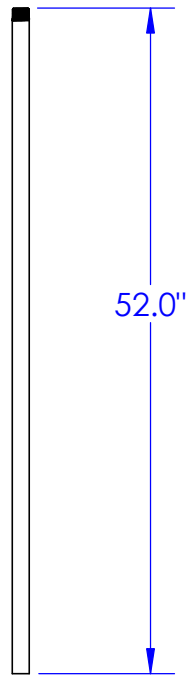
1

2

1

B

B



A

A

PROPRIETARY AND CONFIDENTIAL
 THE INFORMATION CONTAINED IN THIS DRAWING IS THE SOLE PROPERTY OF TURBINE TECHNOLOGY PARTNERS. ANY REPRODUCTION IN PART OR AS A WHOLE WITHOUT THE WRITTEN PERMISSION OF TURBINE TECHNOLOGY PARTNERS IS PROHIBITED.

		UNLESS OTHERWISE SPECIFIED: DIMENSIONS ARE IN INCHES UNLESS OTHERWISE SPECIFIED TOLERANCES: ±0.05" FRACTIONAL ANGULAR: MACH BEND TWO PLACE DECIMAL THREE PLACE DECIMAL		NAME	DATE
		INTERPRET GEOMETRIC TOLERANCING PER:	DRAWN	JOE B.	
		MATERIAL Galvanized Steel	CHECKED		
		FINISH	ENG APPR.		
NEXT ASSY	USED ON		MFG APPR.		
APPLICATION		DO NOT SCALE DRAWING	Q.A.		
			COMMENTS: Stock part is 4499K54 from McMaster-Carr		

TITLE:
Leg 1" pipe, 52" long

SIZE	DWG. NO.	REV
A	PIPE 52	

SCALE: 1:20 WEIGHT: SHEET 10 OF 19

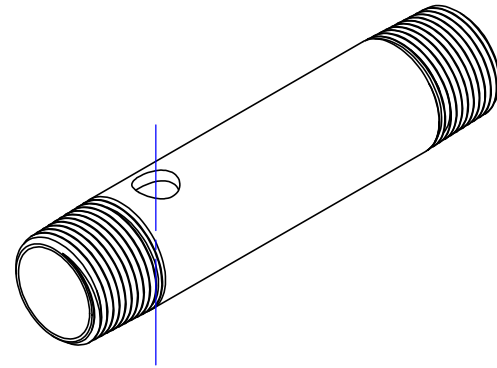
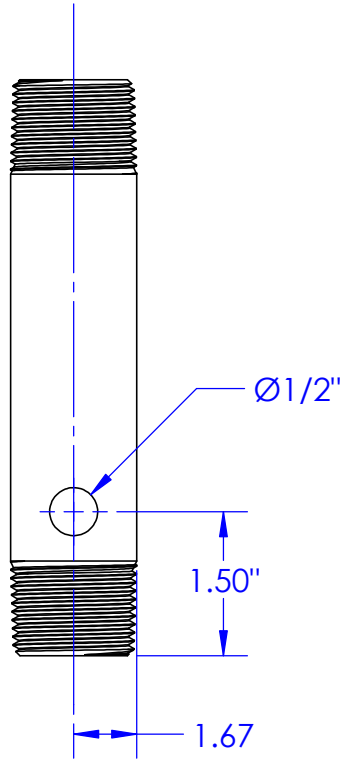
1

2

1

B

B



A

A

PROPRIETARY AND CONFIDENTIAL
 THE INFORMATION CONTAINED IN THIS DRAWING IS THE SOLE PROPERTY OF TURBINE TECHNOLOGY PARTNERS. ANY REPRODUCTION IN PART OR AS A WHOLE WITHOUT THE WRITTEN PERMISSION OF TURBINE TECHNOLOGY PARTNERS IS PROHIBITED.

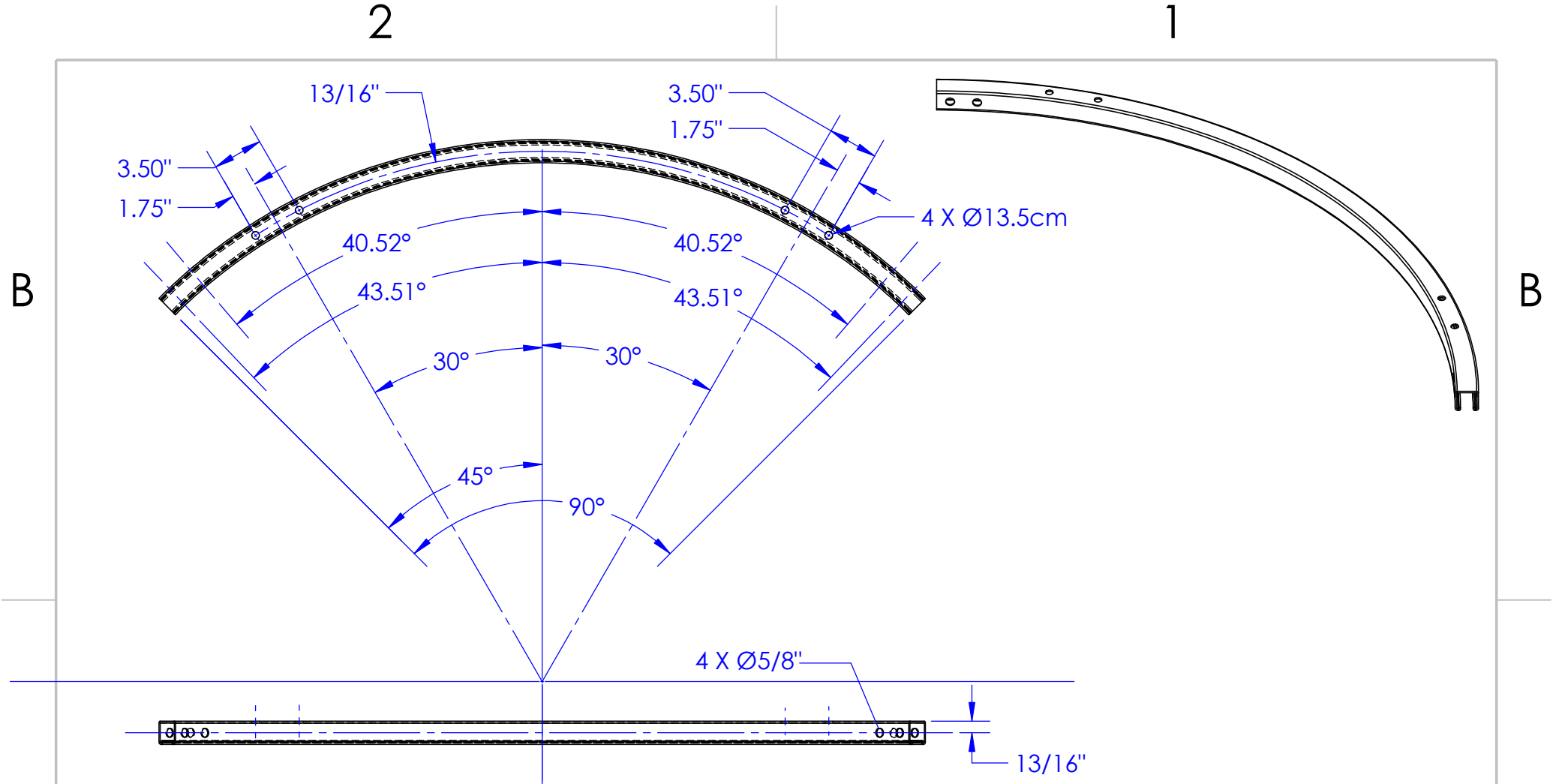
		UNLESS OTHERWISE SPECIFIED: DIMENSIONS ARE IN INCHES UNLESS OTHERWISE SPECIFIED TOLERANCES: ±0.05" FRACTIONAL ANGULAR: MACH BEND TWO PLACE DECIMAL THREE PLACE DECIMAL		NAME	DATE
		INTERPRET GEOMETRIC TOLERANCING PER:	DRAWN	JOE B.	
		MATERIAL Galvanized Steel	CHECKED		
		FINISH	ENG APPR.		
NEXT ASSY	USED ON		MFG APPR.		
APPLICATION		DO NOT SCALE DRAWING	Q.A.		
			COMMENTS: Stock part is 4549K621 from McMaster-Carr		

TITLE:
Leg 1" pipe, 6" long

SIZE A	DWG. NO. PIPE 6	REV
------------------	---------------------------	-----

SCALE: 1:2 WEIGHT: SHEET 11 OF 19

1



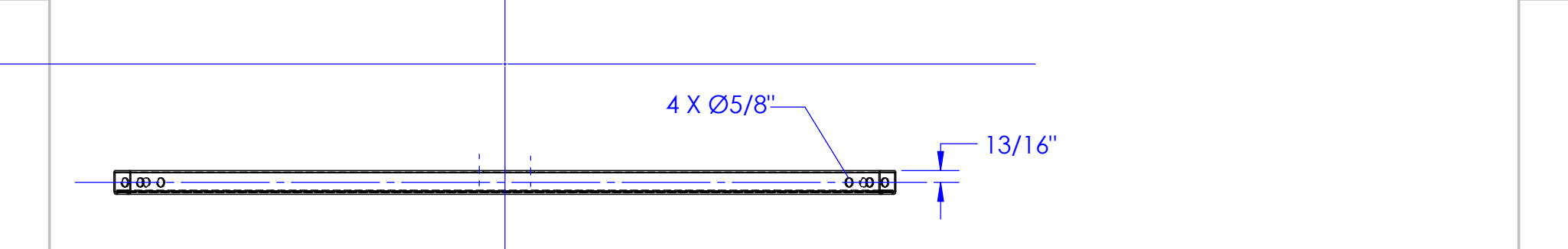
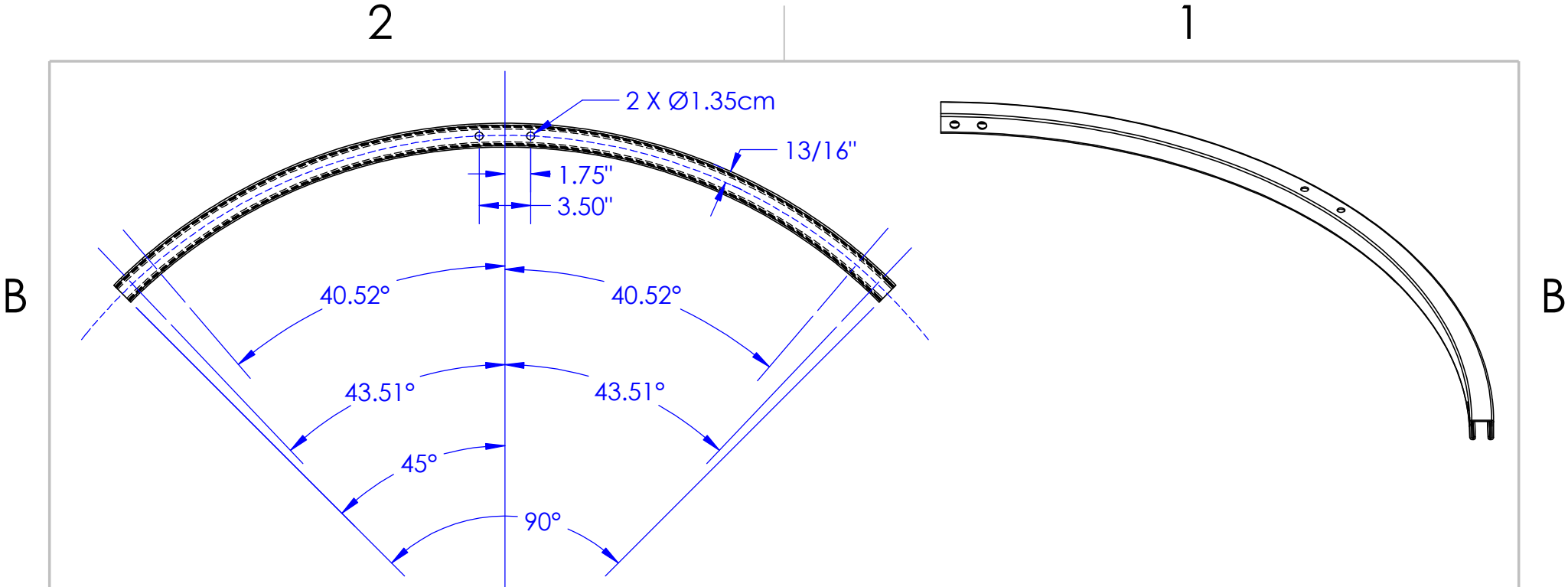
A

A

PROPRIETARY AND CONFIDENTIAL
 THE INFORMATION CONTAINED IN THIS DRAWING IS THE SOLE PROPERTY OF TURBINE TECHNOLOGY PARTNERS. ANY REPRODUCTION IN PART OR AS A WHOLE WITHOUT THE WRITTEN PERMISSION OF TURBINE TECHNOLOGY PARTNERS IS PROHIBITED.

		UNLESS OTHERWISE SPECIFIED: DIMENSIONS ARE IN CM UNLESS OTHERWISE SPECIFIED TOLERANCES: ±0.05cm, ±0.01in FRACTIONAL ANGULAR: MACH BEND TWO PLACE DECIMAL THREE PLACE DECIMAL		NAME	DATE
		INTERPRET GEOMETRIC TOLERANCING PER:	DRAWN	JOE B.	
		MATERIAL Zinc-plated Steel	CHECKED		
		FINISH	ENG APPR.		
NEXT ASSY	USED ON		MFG APPR.		
	APPLICATION	DO NOT SCALE DRAWING	Q.A.		
			COMMENTS: Stock part is 3147T1 from McMaster-Carr		

TITLE: Strut 1		
SIZE A	DWG. NO. STRUT 1	REV
SCALE: 1:25		WEIGHT:
SHEET 12 OF 19		



A

A

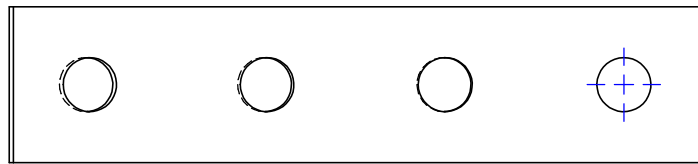
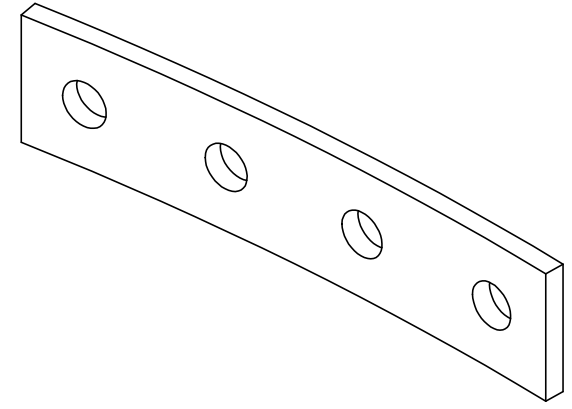
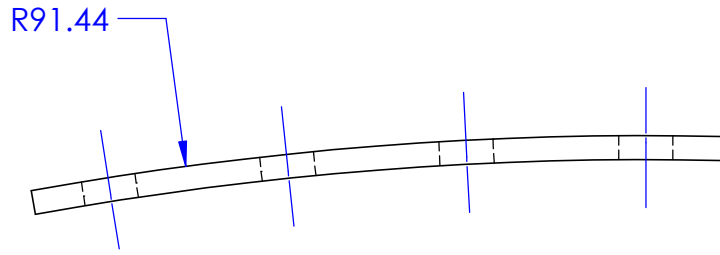
PROPRIETARY AND CONFIDENTIAL
 THE INFORMATION CONTAINED IN THIS DRAWING IS THE SOLE PROPERTY OF TURBINE TECHNOLOGY PARTNERS. ANY REPRODUCTION IN PART OR AS A WHOLE WITHOUT THE WRITTEN PERMISSION OF TURBINE TECHNOLOGY PARTNERS IS PROHIBITED.

		UNLESS OTHERWISE SPECIFIED: DIMENSIONS ARE IN CM UNLESS OTHERWISE SPECIFIED TOLERANCES: ±0.05cm, ±0.01in FRACTIONAL ANGULAR: MACH BEND TWO PLACE DECIMAL THREE PLACE DECIMAL		NAME	DATE
		INTERPRET GEOMETRIC TOLERANCING PER:		JOE B.	
		MATERIAL Zinc-plated Steel	DRAWN		
		FINISH	CHECKED		
NEXT ASSY	USED ON		ENG APPR.		
			MFG APPR.		
APPLICATION		DO NOT SCALE DRAWING	Q.A.		

TITLE: Strut 2		
SIZE A	DWG. NO. STRUT 2	REV
SCALE: 1:25	WEIGHT:	SHEET 13 OF 19

2

1



B

B

A

A

PROPRIETARY AND CONFIDENTIAL
 THE INFORMATION CONTAINED IN THIS DRAWING IS THE SOLE PROPERTY OF TURBINE TECHNOLOGY PARTNERS. ANY REPRODUCTION IN PART OR AS A WHOLE WITHOUT THE WRITTEN PERMISSION OF TURBINE TECHNOLOGY PARTNERS IS PROHIBITED.

		UNLESS OTHERWISE SPECIFIED: DIMENSIONS ARE IN CM UNLESS OTHERWISE SPECIFIED TOLERANCES: ±0.1cm FRACTIONAL ANGULAR: MACH BEND TWO PLACE DECIMAL THREE PLACE DECIMAL		NAME	DATE
		INTERPRET GEOMETRIC TOLERANCING PER:	DRAWN	JOE B.	
		MATERIAL Zinc-plated Steel	CHECKED		
		FINISH	ENG APPR.		
NEXT ASSY	USED ON		MFG APPR.		
APPLICATION		DO NOT SCALE DRAWING	Q.A.		
			COMMENTS: Stock part is 33125T126 from McMaster-Carr		

TITLE: Inner Strut Bracket		
SIZE A	DWG. NO. INNER	REV
SCALE: 1:2	WEIGHT:	SHEET 14 OF 19

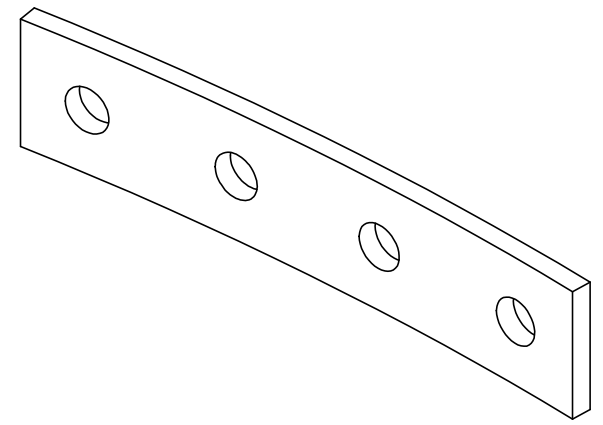
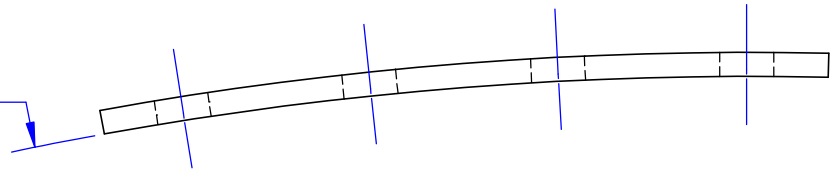
1

2

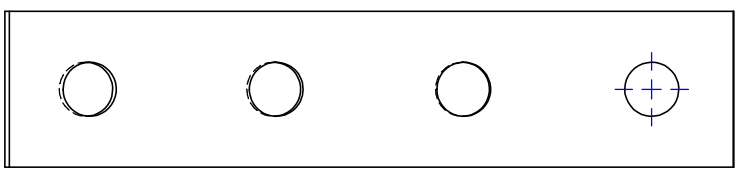
1

B

R95.57



B



A

A

PROPRIETARY AND CONFIDENTIAL
 THE INFORMATION CONTAINED IN THIS DRAWING IS THE SOLE PROPERTY OF TURBINE TECHNOLOGY PARTNERS. ANY REPRODUCTION IN PART OR AS A WHOLE WITHOUT THE WRITTEN PERMISSION OF TURBINE TECHNOLOGY PARTNERS IS PROHIBITED.

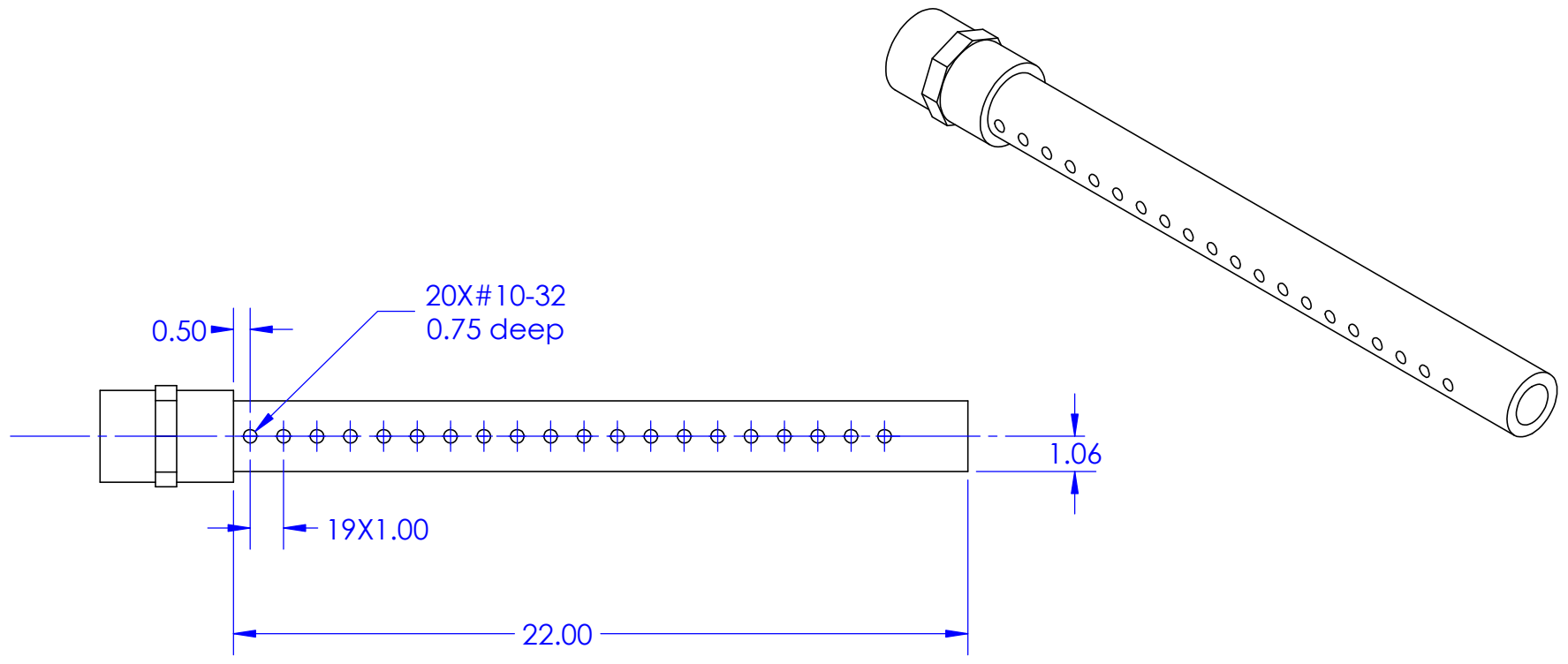
		UNLESS OTHERWISE SPECIFIED:		NAME	DATE
		DIMENSIONS ARE IN CM UNLESS OTHERWISE SPECIFIED TOLERANCES: ±0.1 FRACTIONAL ANGULAR: MACH BEND TWO PLACE DECIMAL THREE PLACE DECIMAL	DRAWN	JOE B.	
		INTERPRET GEOMETRIC TOLERANCING PER:	CHECKED		
		MATERIAL Zinc-plated Steel	ENG APPR.		
		FINISH	MFG APPR.		
NEXT ASSY	USED ON		Q.A.		
APPLICATION		DO NOT SCALE DRAWING	COMMENTS: Stock part is 33125T126 from McMaster-Carr		

TITLE:
Outer Strut Bracket

SIZE A	DWG. NO. OUTER	REV
------------------	--------------------------	-----

SCALE: 1:2 WEIGHT: SHEET 15 OF 19

1



PROPRIETARY AND CONFIDENTIAL
 THE INFORMATION CONTAINED IN THIS DRAWING IS THE SOLE PROPERTY OF TURBINE TECHNOLOGY PARTNERS. ANY REPRODUCTION IN PART OR AS A WHOLE WITHOUT THE WRITTEN PERMISSION OF TURBINE TECHNOLOGY PARTNERS IS PROHIBITED.

		UNLESS OTHERWISE SPECIFIED:		NAME	DATE
		DIMENSIONS ARE IN CM UNLESS OTHERWISE SPECIFIED TOLERANCES: ±0.05CM FRACTIONAL ANGULAR: MACH BEND TWO PLACE DECIMAL THREE PLACE DECIMAL	DRAWN	JOE B.	
		INTERPRET GEOMETRIC TOLERANCING PER:	CHECKED		
		MATERIAL	ENG APPR.		
		PVC	MFG APPR.		
		FINISH	Q.A.		
NEXT ASSY	USED ON		COMMENTS: Stock part is 49887 from ACE Hardware		
APPLICATION		DO NOT SCALE DRAWING			

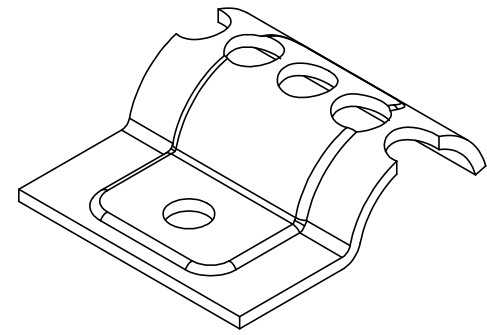
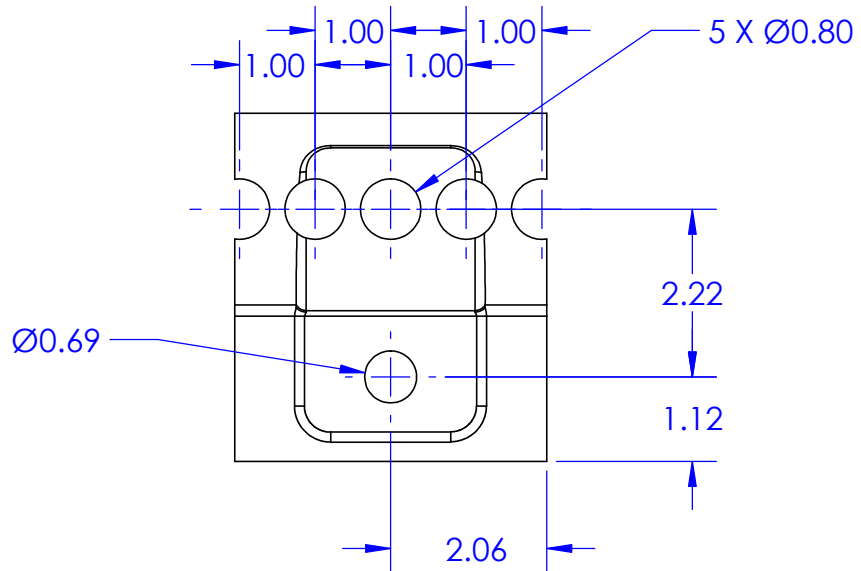
TITLE: Dropper PVC Pipe		
SIZE A	DWG. NO. D PVC	REV
SCALE: 1:5	WEIGHT:	SHEET 16 OF 19

2

1

B

B



A

A

PROPRIETARY AND CONFIDENTIAL
 THE INFORMATION CONTAINED IN THIS DRAWING IS THE SOLE PROPERTY OF TURBINE TECHNOLOGY PARTNERS. ANY REPRODUCTION IN PART OR AS A WHOLE WITHOUT THE WRITTEN PERMISSION OF TURBINE TECHNOLOGY PARTNERS IS PROHIBITED.

		UNLESS OTHERWISE SPECIFIED:		NAME	DATE
		DIMENSIONS ARE IN CM UNLESS OTHERWISE SPECIFIED TOLERANCES: ±0.05cm FRACTIONAL ANGULAR: MACH BEND TWO PLACE DECIMAL THREE PLACE DECIMAL	DRAWN	JOE B.	
		INTERPRET GEOMETRIC TOLERANCING PER:	CHECKED		
		MATERIAL Zinc-Plated Steel	ENG APPR.		
		FINISH	MFG APPR.		
NEXT ASSY	USED ON		Q.A.		
APPLICATION	DO NOT SCALE DRAWING		COMMENTS: Stock part is 3545T17 from McMaster-Carr		

TITLE: Strut Mount for Droppers		
SIZE A	DWG. NO. D MOUNT	REV
SCALE: 1:1	WEIGHT:	SHEET 17 OF 19

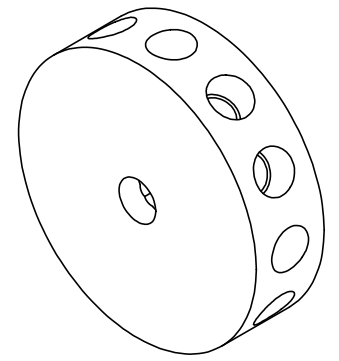
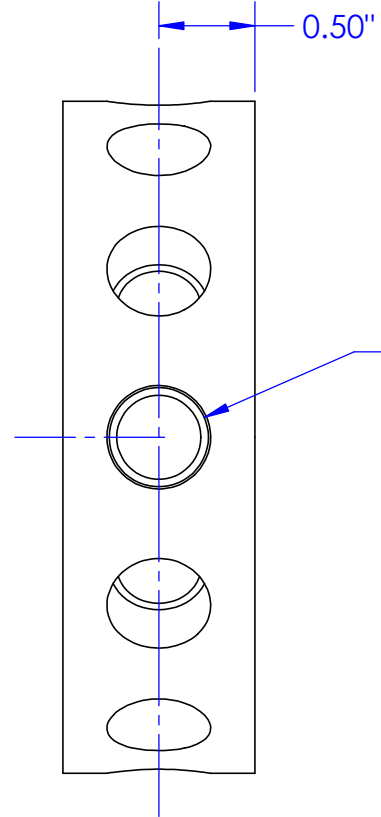
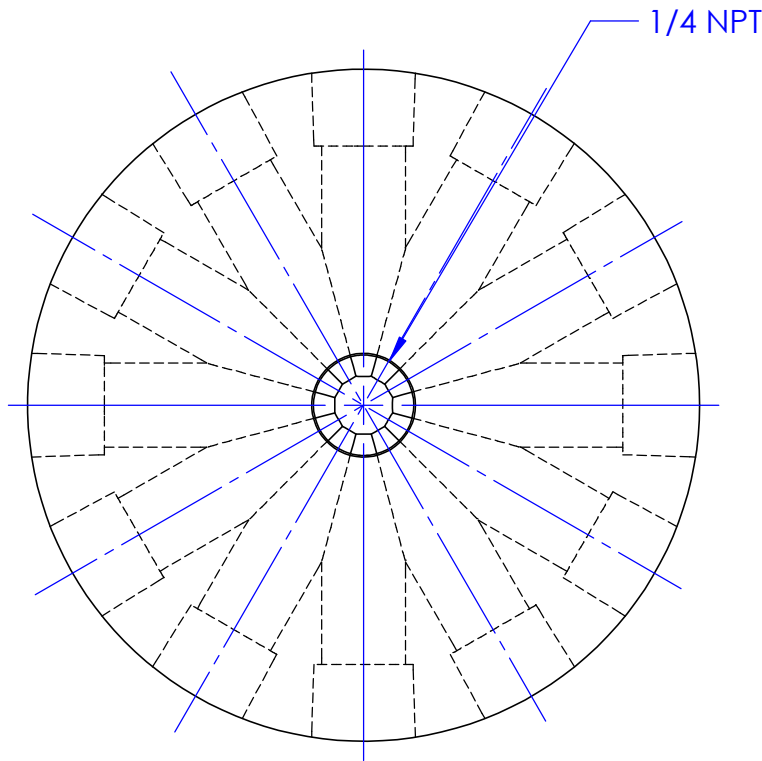
1

2

1

B

B



A

A

PROPRIETARY AND CONFIDENTIAL
 THE INFORMATION CONTAINED IN THIS DRAWING IS THE SOLE PROPERTY OF TURBINE TECHNOLOGY PARTNERS. ANY REPRODUCTION IN PART OR AS A WHOLE WITHOUT THE WRITTEN PERMISSION OF TURBINE TECHNOLOGY PARTNERS IS PROHIBITED.

		UNLESS OTHERWISE SPECIFIED:		NAME	DATE
		DIMENSIONS ARE IN CM UNLESS OTHERWISE SPECIFIED TOLERANCES: ±0.05cm FRACTIONAL ANGULAR: MACH BEND TWO PLACE DECIMAL THREE PLACE DECIMAL	DRAWN	JOE B.	
		INTERPRET GEOMETRIC TOLERANCING PER:	CHECKED		
		MATERIAL 6061 Aluminum	ENG APPR.		
NEXT ASSY	USED ON	FINISH	MFG APPR.		
APPLICATION		DO NOT SCALE DRAWING	Q.A.		
			COMMENTS: Stock part is 8974K88 from McMaster-Carr		

TITLE:
1:12 Flow Divider Body

SIZE	DWG. NO.	REV
A	SPLITTER	

SCALE: 1:1 WEIGHT: SHEET 18 OF 19

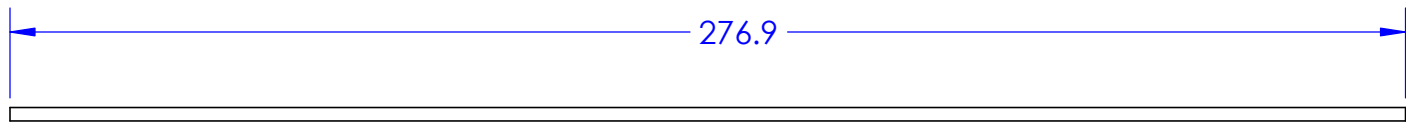
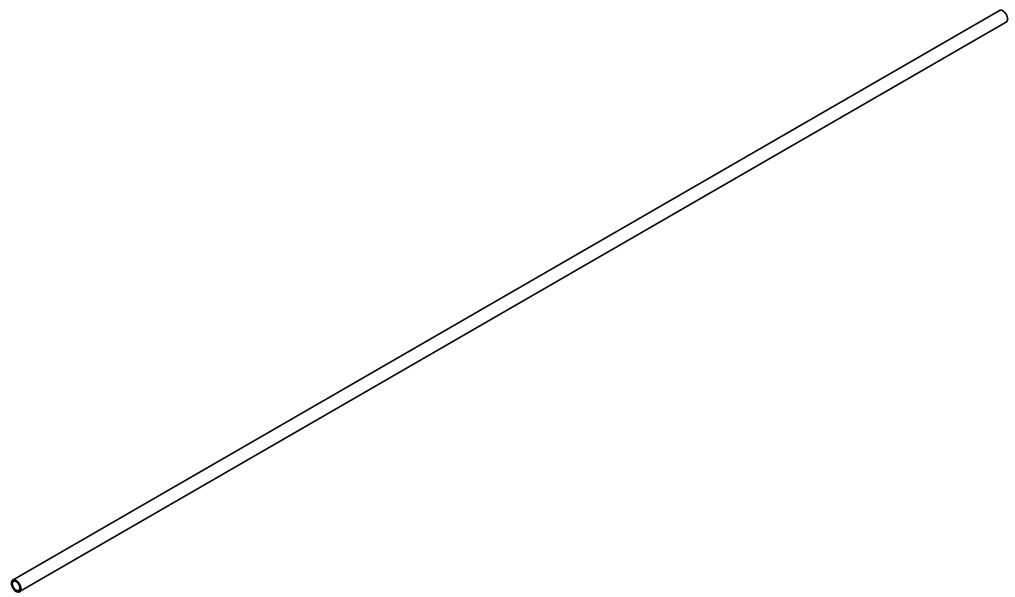
1

2

1

B

B



A

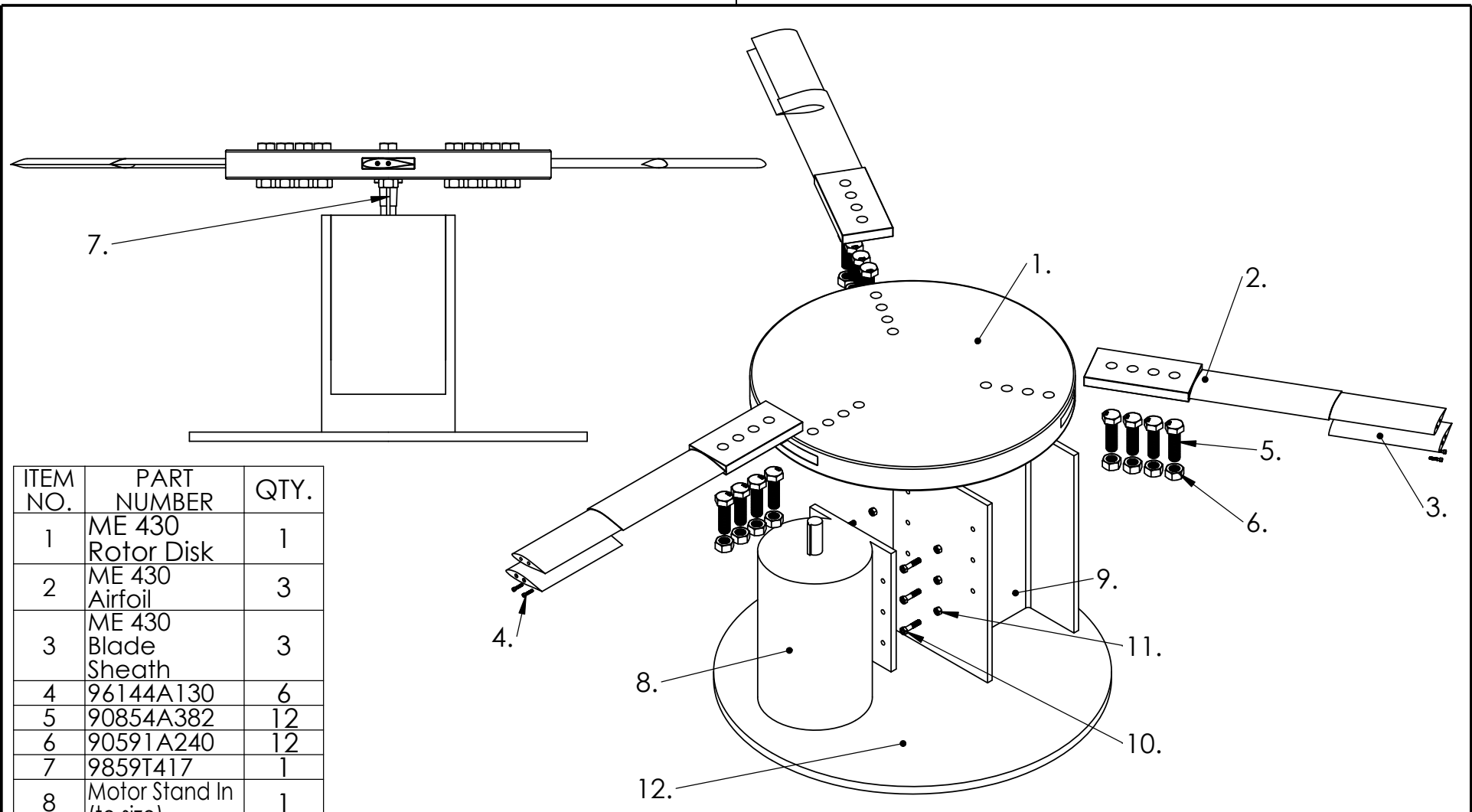
A

PROPRIETARY AND CONFIDENTIAL
 THE INFORMATION CONTAINED IN THIS DRAWING IS THE SOLE PROPERTY OF TURBINE TECHNOLOGY PARTNERS. ANY REPRODUCTION IN PART OR AS A WHOLE WITHOUT THE WRITTEN PERMISSION OF TURBINE TECHNOLOGY PARTNERS IS PROHIBITED.

		UNLESS OTHERWISE SPECIFIED: DIMENSIONS ARE IN CM UNLESS OTHERWISE SPECIFIED TOLERANCES: ±0.1cm FRACTIONAL ANGULAR: MACH BEND TWO PLACE DECIMAL THREE PLACE DECIMAL	DRAWN	NAME	DATE
			CHECKED	JOE B.	
			ENG APPR.		
			MFG APPR.		
		INTERPRET GEOMETRIC TOLERANCING PER:	Q.A.		
		MATERIAL PVC	COMMENTS: Stock part is 48925K12 from McMaster-Carr		
NEXT ASSY	USED ON	FINISH			
APPLICATION		DO NOT SCALE DRAWING			

TITLE: 3/4" PVC Rail		
SIZE A	DWG. NO. RAIL	REV
SCALE: 1:25	WEIGHT:	SHEET 19 OF 19

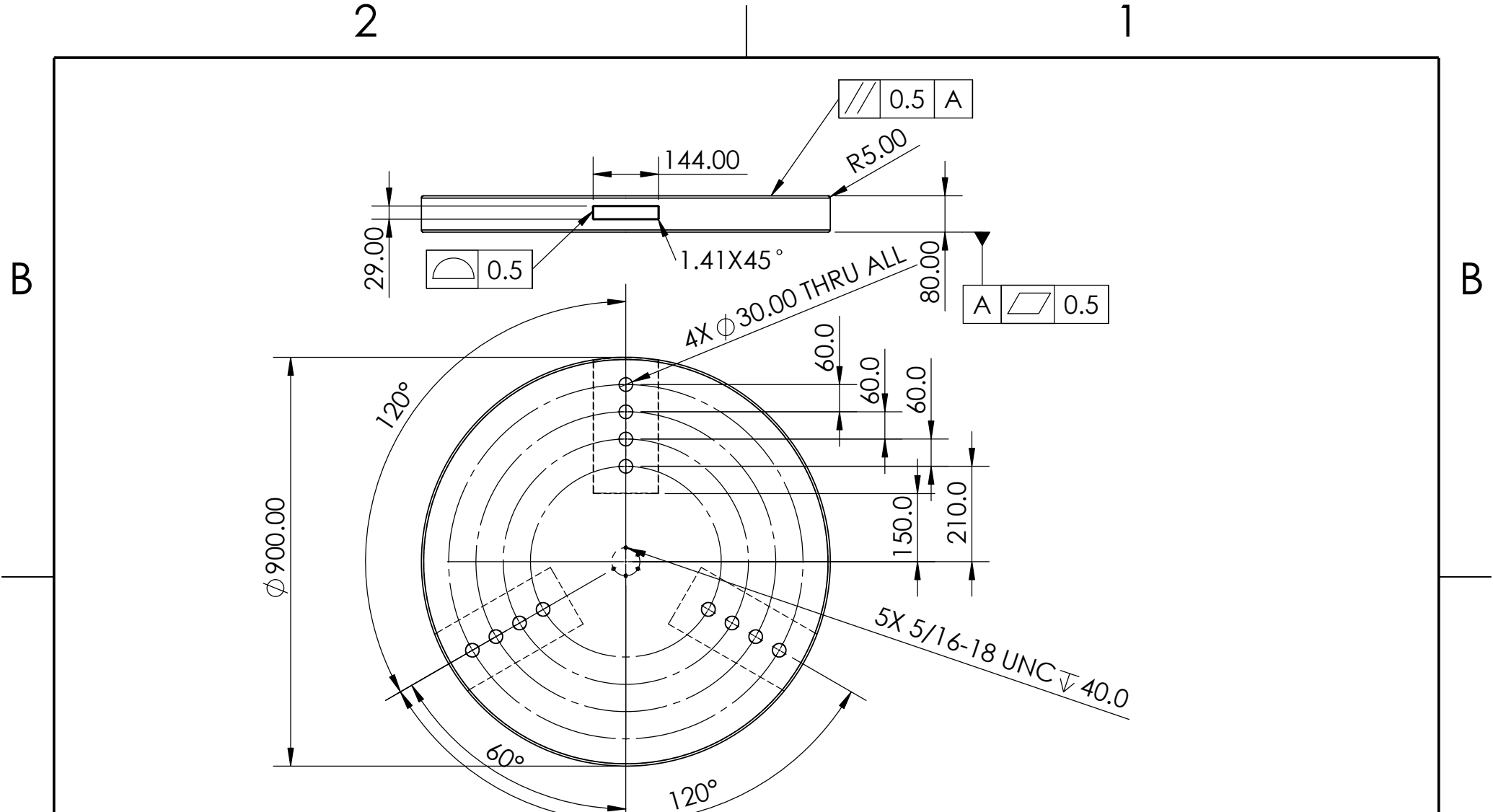
1



ITEM NO.	PART NUMBER	QTY.
1	ME 430 Rotor Disk	1
2	ME 430 Airfoil	3
3	ME 430 Blade Sheath	3
4	96144A130	6
5	90854A382	12
6	90591A240	12
7	9859T417	1
8	Motor Stand In (to size)	1
9	ME 430 I-Beam Support	1
10	91257A749	6
11	94895A825	6
12	ME 430 Base Plate	1

		UNLESS OTHERWISE SPECIFIED:		NAME	DATE
		DIMENSIONS ARE IN INCHES		DRAWN	TH 11/19/20
		TOLERANCES:		CHECKED	
		FRACTIONAL ±		ENG APPR.	
		ANGULAR: MACH ± BEND ±		MFG APPR.	
		TWO PLACE DECIMAL ±		Q.A.	
		THREE PLACE DECIMAL ±		COMMENTS:	
		INTERPRET GEOMETRIC TOLERANCING PER:		All part numbers refer to McMaster Carr parts. Indented BOM has further information	
		MATERIAL		Varies	
		FINISH		Varies	
NEXT ASSY	USED ON				
APPLICATION		DO NOT SCALE DRAWING			

TITLE:		
<h1>Exploded Assembly</h1>		
SIZE	DWG. NO.	REV
A	Rotating blade	
SCALE: 1:16	WEIGHT:	SHEET 1 OF 1



PROPRIETARY AND CONFIDENTIAL
 THE INFORMATION CONTAINED IN THIS DRAWING IS THE SOLE PROPERTY OF <INSERT COMPANY NAME HERE>. ANY REPRODUCTION IN PART OR AS A WHOLE WITHOUT THE WRITTEN PERMISSION OF <INSERT COMPANY NAME HERE> IS PROHIBITED.

		UNLESS OTHERWISE SPECIFIED:		NAME	DATE
		DIMENSIONS ARE IN mm	DRAWN	TH	11/19/20
		TOLERANCES:	CHECKED		
		FRACTIONAL ±	ENG APPR.		
		ANGULAR: MACH ±1° BEND ±	MFG APPR.		
		ONE PLACE DECIMAL ±1.0	Q.A.		
		TWO PLACE DECIMAL ±0.50	COMMENTS:		
		THREE PLACE DECIMAL ±0.05			
		INTERPRET GEOMETRIC TOLERANCING PER:			
		MATERIAL			
		AL6061			
		FINISH			
		Ra 0.8µm			
NEXT ASSY	USED ON				
APPLICATION		DO NOT SCALE DRAWING			

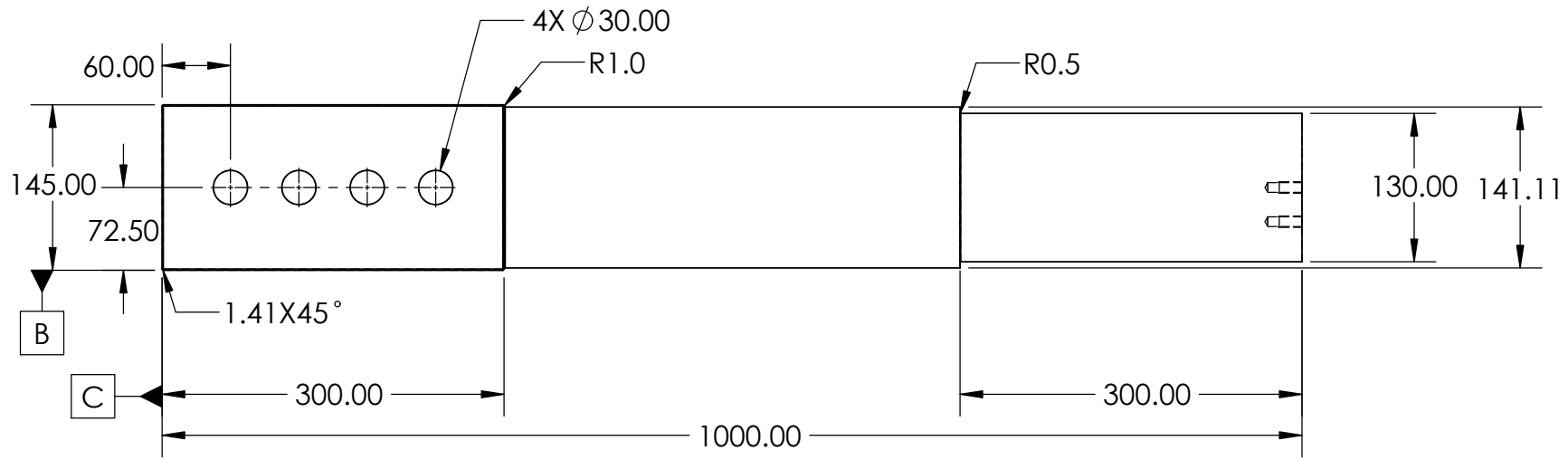
TITLE:		
Rotor Disk		
SIZE	DWG. NO.	REV
A	Rotor disk	
SCALE:1:12	WEIGHT:	SHEET 1 OF 1

2

1

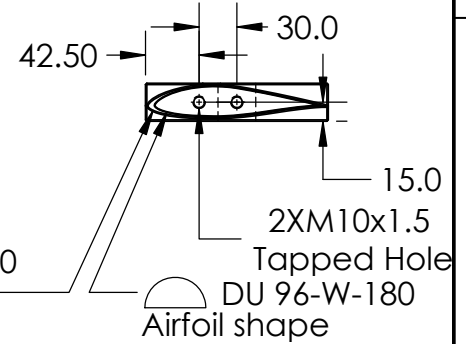
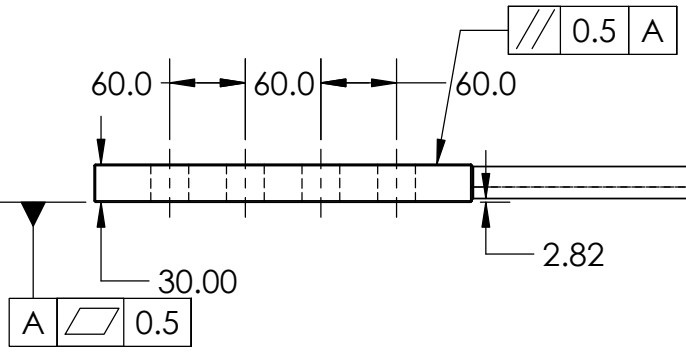
B

B



B

C



A

A

PROPRIETARY AND CONFIDENTIAL
 THE INFORMATION CONTAINED IN THIS DRAWING IS THE SOLE PROPERTY OF <INSERT COMPANY NAME HERE>. ANY REPRODUCTION IN PART OR AS A WHOLE WITHOUT THE WRITTEN PERMISSION OF <INSERT COMPANY NAME HERE> IS PROHIBITED.

		UNLESS OTHERWISE SPECIFIED:		NAME	DATE
		DIMENSIONS ARE IN mm	DRAWN	TH	11/19/20
		TOLERANCES:	CHECKED		
		ANGULAR: MACH ± BEND ±	ENG APPR.		
		ONE PLACE DECIMAL ±1.0	MFG APPR.		
		TWO PLACE DECIMAL ±0.50	Q.A.		
		THREE PLACE DECIMAL ±0.05	COMMENTS:		
		INTERPRET GEOMETRIC TOLERANCING PER:			
		MATERIAL			
		AL6061			
		FINISH			
		Ra 0.8µm			
NEXT ASSY	USED ON				
		APPLICATION			
		DO NOT SCALE DRAWING			

TITLE:		
Airfoil Blade		
SIZE	DWG. NO.	REV
A	Blade	
SCALE: 1:10	WEIGHT:	SHEET 1 OF 1

1

2

1

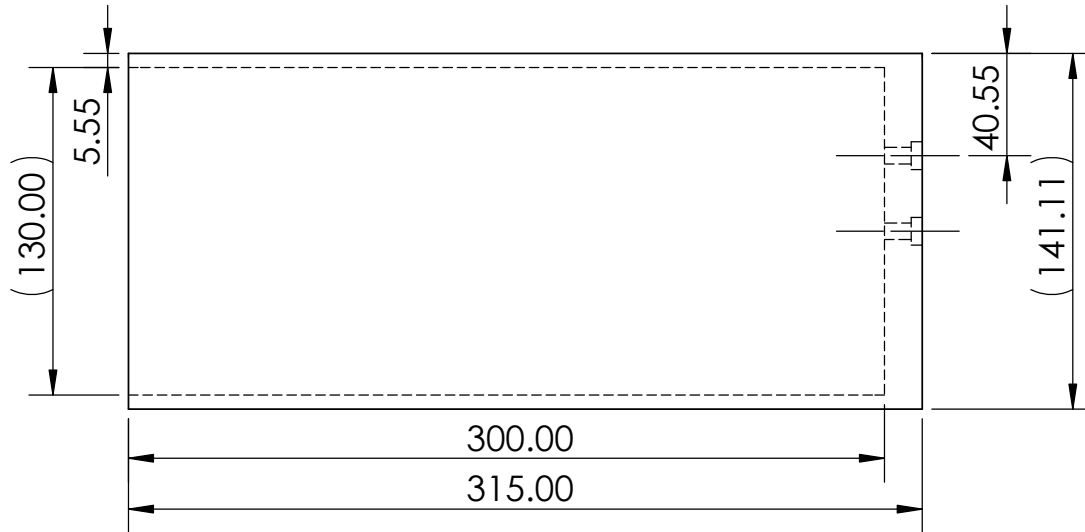
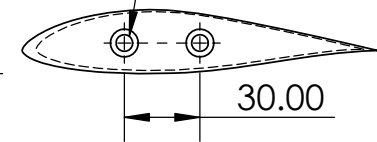
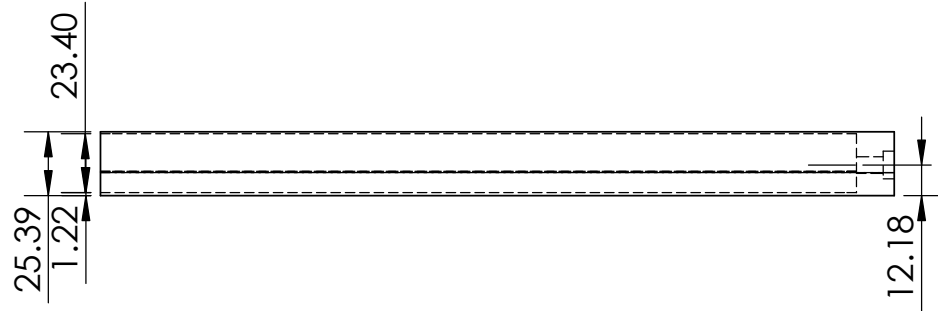
B

B

0.5 (DU 96-W-180 Airfoil Shape)

2X CBORE for M6 Hex Head Bolt

0.5 (DU 96-W-180 Airfoil Shape)



A

A

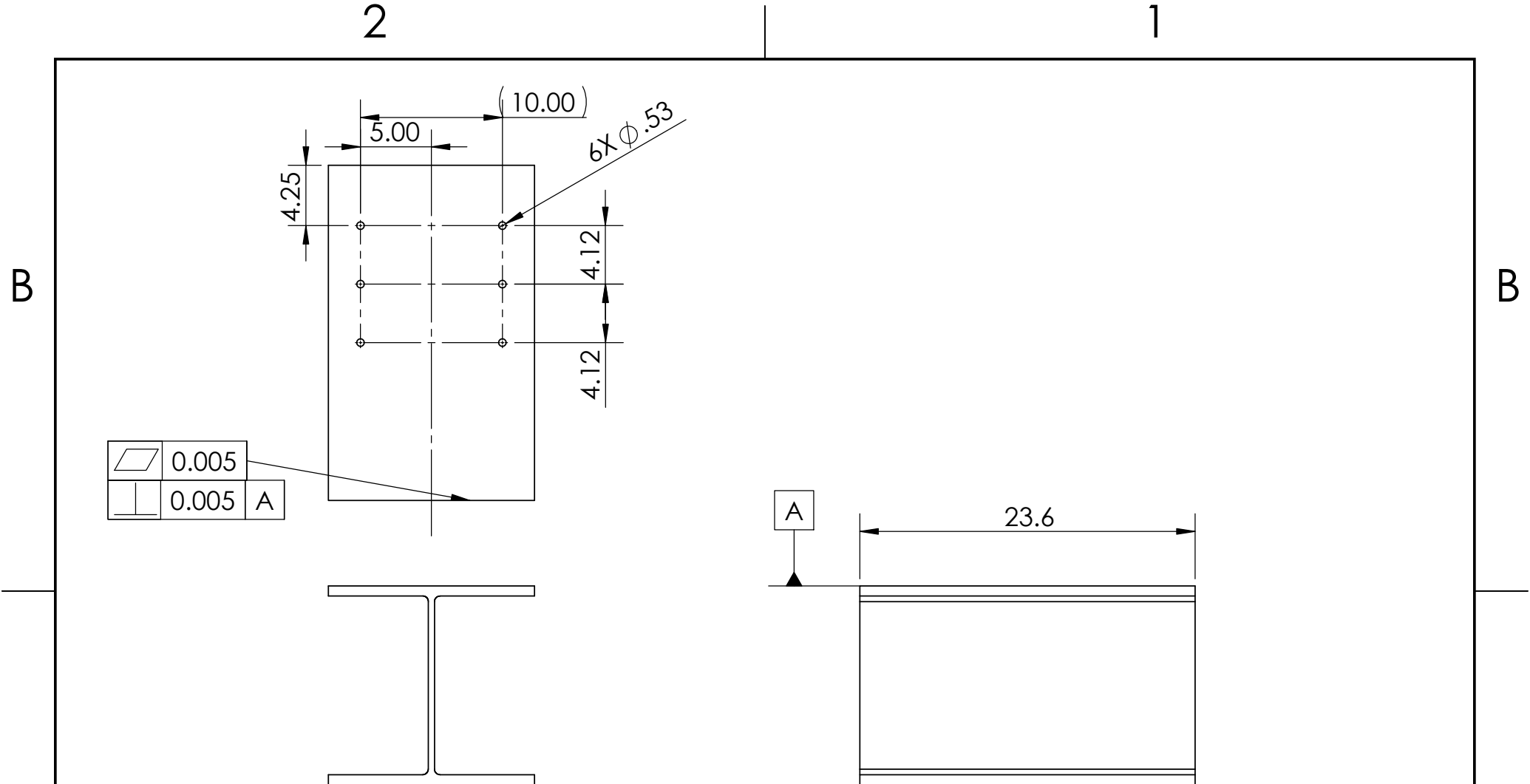
		UNLESS OTHERWISE SPECIFIED:		NAME	DATE
		DIMENSIONS ARE IN mm		DRAWN	TH
		TOLERANCES:		CHECKED	
		ANGULAR: MACH ± 1° BEND ±		ENG APPR.	
		ONE PLACE DECIMAL ±1.0		MFG APPR.	
		TWO PLACE DECIMAL ±0.50		Q.A.	
		THREE PLACE DECIMAL ±0.05		COMMENTS:	
		INTERPRET GEOMETRIC TOLERANCING PER:			
		MATERIAL			
		AL6061			
		FINISH			
		Ra 0.8µm			
NEXT ASSY	USED ON	DO NOT SCALE DRAWING			
APPLICATION					

TITLE: Blade Sheath

PROPRIETARY AND CONFIDENTIAL
 THE INFORMATION CONTAINED IN THIS DRAWING IS THE SOLE PROPERTY OF <INSERT COMPANY NAME HERE>. ANY REPRODUCTION IN PART OR AS A WHOLE WITHOUT THE WRITTEN PERMISSION OF <INSERT COMPANY NAME HERE> IS PROHIBITED.

SIZE	DWG. NO.	REV
A	Sheath	
SCALE: 1:3	WEIGHT:	SHEET 1 OF 1

1

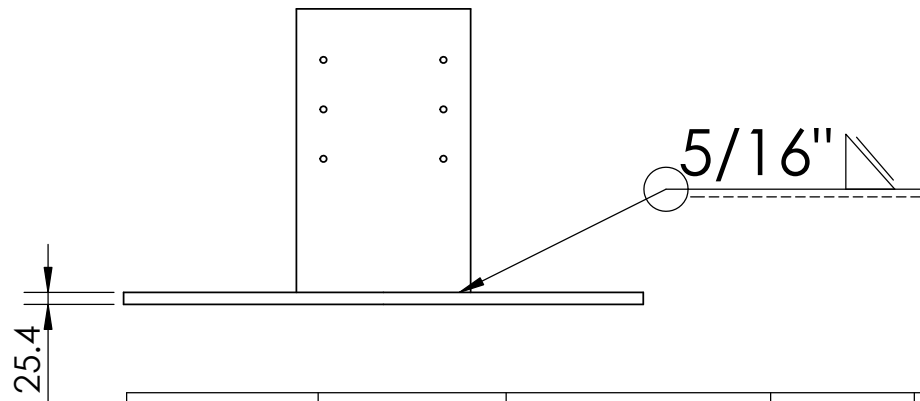
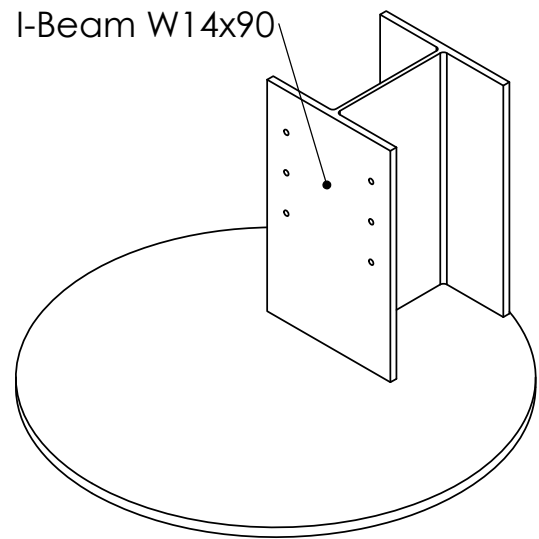
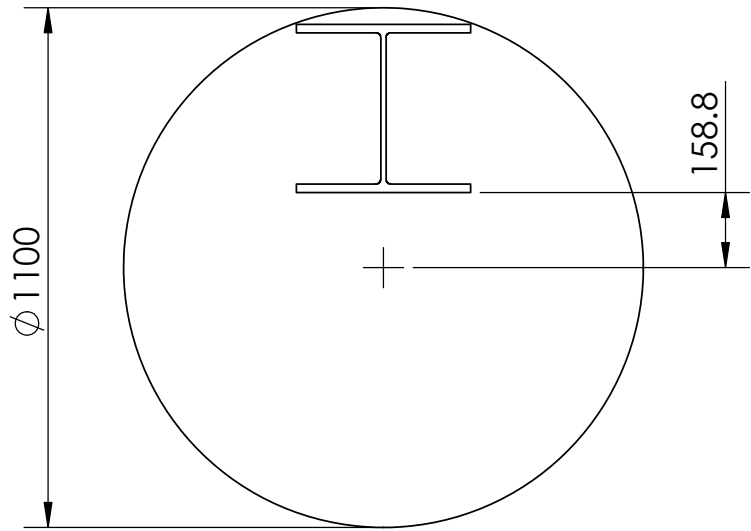


	0.005	
	0.005	A

<p>PROPRIETARY AND CONFIDENTIAL</p> <p>THE INFORMATION CONTAINED IN THIS DRAWING IS THE SOLE PROPERTY OF <INSERT COMPANY NAME HERE>. ANY REPRODUCTION IN PART OR AS A WHOLE WITHOUT THE WRITTEN PERMISSION OF <INSERT COMPANY NAME HERE> IS PROHIBITED.</p>			UNLESS OTHERWISE SPECIFIED:		NAME	DATE	<p>TITLE:</p> <h1>I-Beam W14x90</h1>		
			DIMENSIONS ARE IN INCHES	DRAWN	TH	11/19/20			
			TOLERANCES:	CHECKED					
			FRACTIONAL ±	ENG APPR.					
			ANGULAR: MACH ± BEND ±	MFG APPR.					
		ONE PLACE DECIMAL ±.050	Q.A.						
		TWO PLACE DECIMAL ±.010	COMMENTS:						
		THREE PLACE DECIMAL ±.005					SIZE	DWG. NO.	REV
		INTERPRET GEOMETRIC TOLERANCING PER:					A	Support	
		MATERIAL					SCALE: 1:10	WEIGHT:	SHEET 1 OF 1
		FINISH							
	NEXT ASSY	USED ON	DO NOT SCALE DRAWING						
	APPLICATION								

2

1



B

B

A

A

PROPRIETARY AND CONFIDENTIAL
 THE INFORMATION CONTAINED IN THIS DRAWING IS THE SOLE PROPERTY OF <INSERT COMPANY NAME HERE>. ANY REPRODUCTION IN PART OR AS A WHOLE WITHOUT THE WRITTEN PERMISSION OF <INSERT COMPANY NAME HERE> IS PROHIBITED.

		UNLESS OTHERWISE SPECIFIED:		NAME	DATE
		DIMENSIONS ARE IN mm	DRAWN	TH	11/19/20
		TOLERANCES:	CHECKED		
		ANGULAR: MACH ± BEND ±	ENG APPR.		
		ONE PLACE DECIMAL ±1.0	MFG APPR.		
		TWO PLACE DECIMAL ±0.50	Q.A.		
		THREE PLACE DECIMAL ±0.05	COMMENTS:		
		INTERPRET GEOMETRIC TOLERANCING PER:			
		MATERIAL			
NEXT ASSY	USED ON	FINISH			
APPLICATION		DO NOT SCALE DRAWING			

TITLE: Motor Mount		
SIZE A	DWG. NO. Motor mount	REV
SCALE: 1:20	WEIGHT:	SHEET 1 OF 1

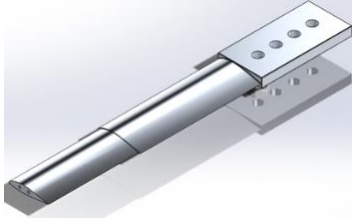
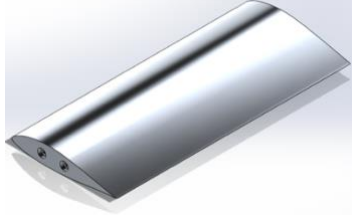
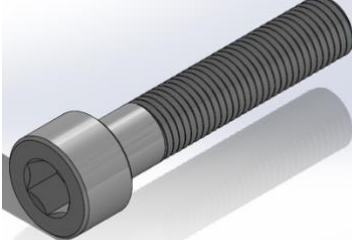
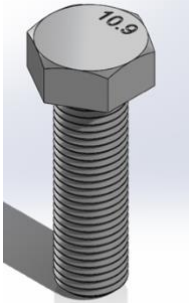
1

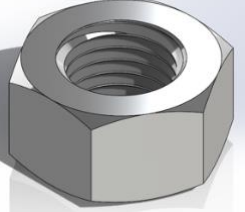
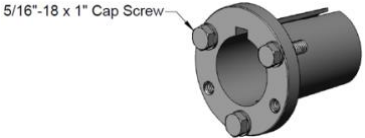
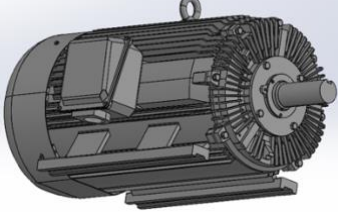
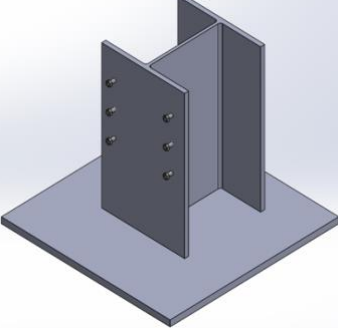
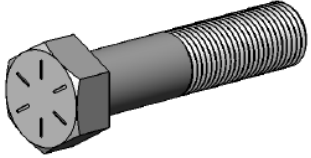
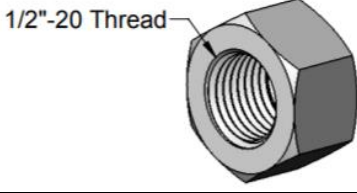
Wind Turbine Erosion Testing Unit Group

Joe Blakewell, Tim Holt, Kevin Vartan

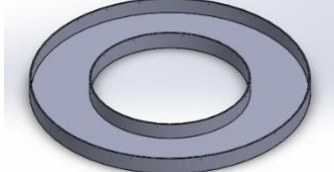

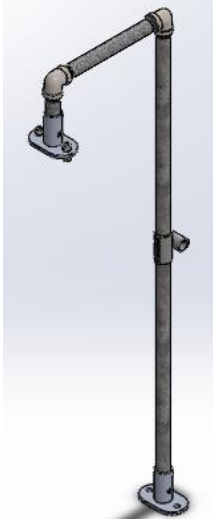


Operator's Manual



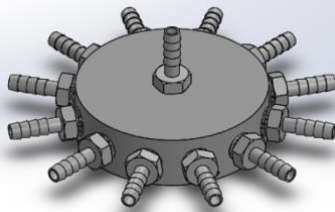





Parts List for Rotating Blade System


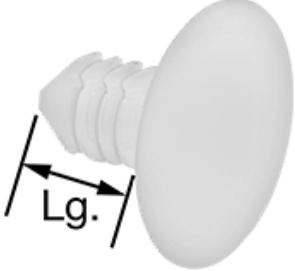

#	Part	Part Description	Count	Image
1	Disk	Central rotating hub that blades and motor connect to	1	
2	Blade	DU 96-W-180 aluminum airfoil	3	
3	Sheath	Sheath that fits on end of airfoil	3	
4	Sheath Bolts	M6, 30mm long, fully threaded steel bolts	6	
5	Blade Bolts	M30, 100mm long, fully threaded steel bolts	12	

6	Blade Nuts	M30 nuts, steel class 8	12	
7	Motor to disk mount	Keyed flanged bushing to mount disk to motor shaft	1	
8	Motor	5 HP, General Purpose Motor, 3-Phase, 900 RPM	1	
9	Motor Mount	W14x90 I-beam welded to thick plate of steel to ensure system does not tip	1	
10	Motor Bolts	$\frac{1}{2}$ " High strength steel bolts	6	
11	Motor Nuts	$\frac{1}{2}$ " High strength steel nuts	6	

Parts List for Regular Fluid Delivery System Assembly

#	Part	Part Description	Count	Image
1	Reservoir Body	Hollow ring-shaped plastic pool	1	
2	Curved Strut and Connecting Hardware	Zinc-plated steel curved strut, ID = 3ft, 90 degree bend	4	
3	Leg Assembly and Hardware	1" steel pipe, 90 degree elbows, J-shaped with feet on ends 30mm m12 bolts with m12 washers and locknuts	6	
4	Alignment piece	Connects reservoir to legs	6	
5	Peristaltic Pump	Peristaltic pump, positive displacement	1	

6	In-line Filter and tubing	Filters particles out of system before they reach the peristaltic pump. Tubing goes from reservoir to filter, and filter to peristaltic pump inlet.	1	
7	Dropper Bracket Assembly and Hardware	Mounts around support ring and holds dropper nozzles connected by tubing	48	
8	1:12 flow divider	6061 Aluminum disc-shaped, divides flow from 1 line into 12 equally. Tubing stretch 2 lines are pre-attached	4	
9	Tubing stretch 1	¼" flexible PVC plastic tubing from peristaltic pump outlet, through first two y-connectors, to inlet of 1:12 divider	1	
10	Tubing stretch 2	¼" flexible PVC plastic tubing from outlet of 1:12 divider to inlet of Dropper Bracket Assembly		
11	Leg-to-rail crossover bracket	Attaches the rail that supports the curtain to the legs of the support structure.	6	
12	¾" PVC Pipe	¾" PVC pipe, 2.73m long	3	
13	¾" PVC Fittings		3	

14	Plastic curtains with hooks	108" wide Plastic curtains that surround ring and legs and funnel spray back into reservoir. Each curtain has 19 hooks	4	
15	Plastic Rivets	Push-In Rivets with Ribbed Shank for 0.062"-0.25" Material Thickness, 0.321" Long	50	
16	Cable Ties	Nylon Cables Ties		

Assembly

Assembly Area Selection

Select a flat area with concrete or steel flooring. The area must have an open floorspace that can fit a circular footprint with a diameter of at least 3.5 meters.

Reservoir

Place reservoir body (part #1) in the center of the area where you want to set up the testing unit.

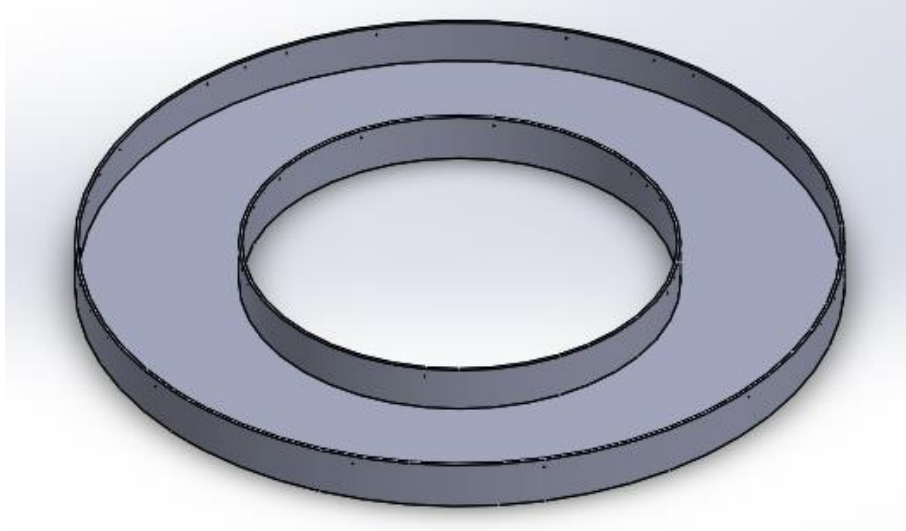


Figure 1. Reservoir body

Rotating Blade System

Motor Mount

Following the steps to set up the base of the fluid delivery system, the user must first mount the motor (8) to the floor of the testing room. They shall do this by bolting the steel plate with motor mount welded to the plate into the floor in the center of the testing room. Once the motor mount (9) is in place, mount the motor to it using 6 ½" high strength steel bolts (10) and their corresponding nuts.

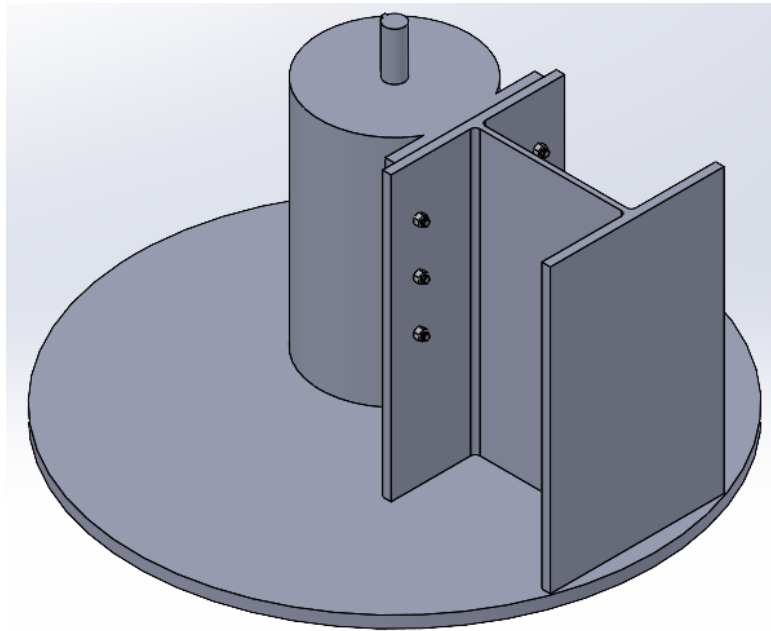


Figure 2. Motor mounted to floor

Disk Mounting

Once the motor is mounted to its mounting bracket, then bring in the disk (1). Using a minimum of three people, place the disk on the shaft of the motor. Bolt the motor to the shaft using 5 5/16"-18 screws (7). Ensure that the disk is level using a spirit level.

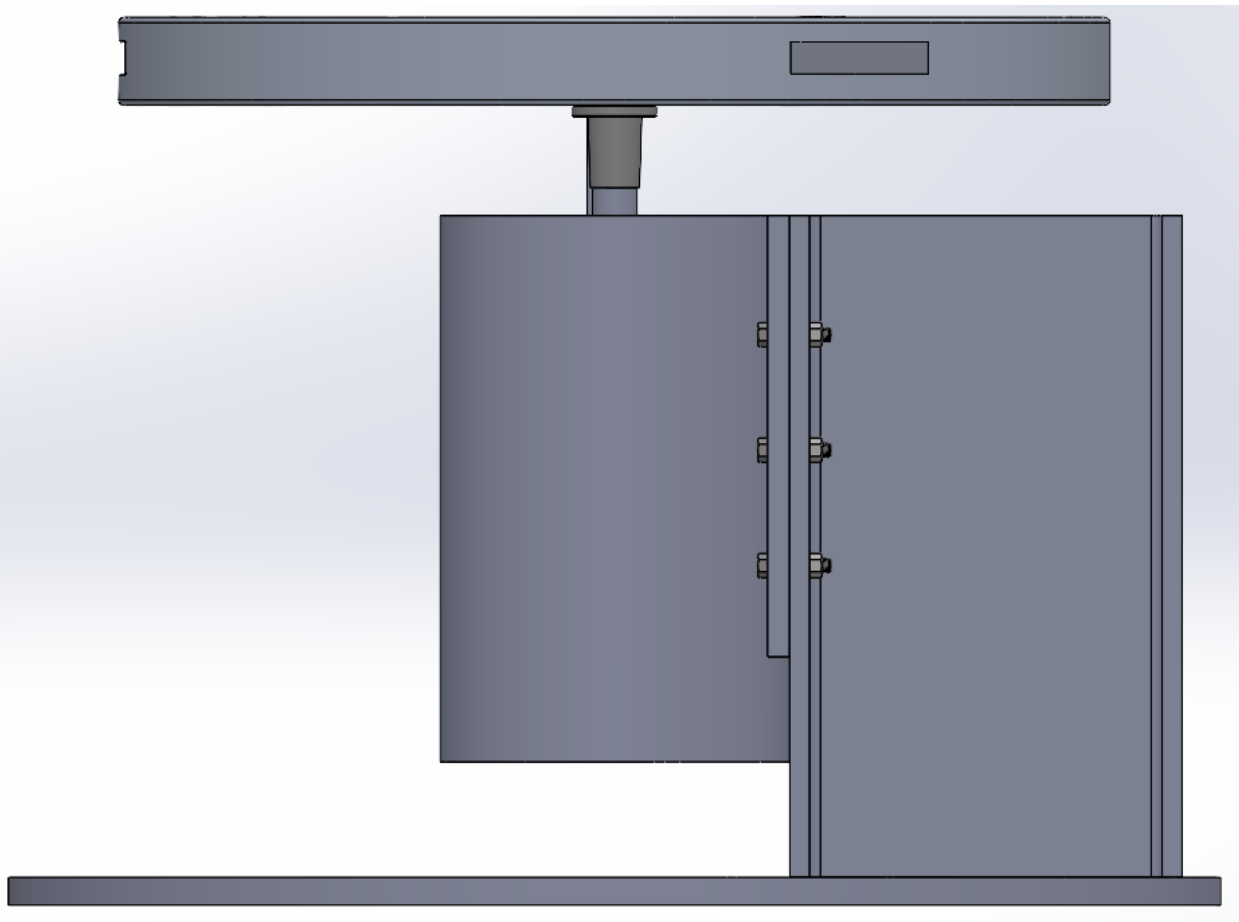


Figure 3. Disk mounted to motor shaft

Blade Attachment

Once the disk is mounted and level, insert all three blades (2) simultaneously to ensure that the disk does not become weighted off axis. After all three blades are inserted into their slots, insert the largest bolts (5) through the disk and the blade and use the largest nuts (6) to tighten them down to 1750 N•m.

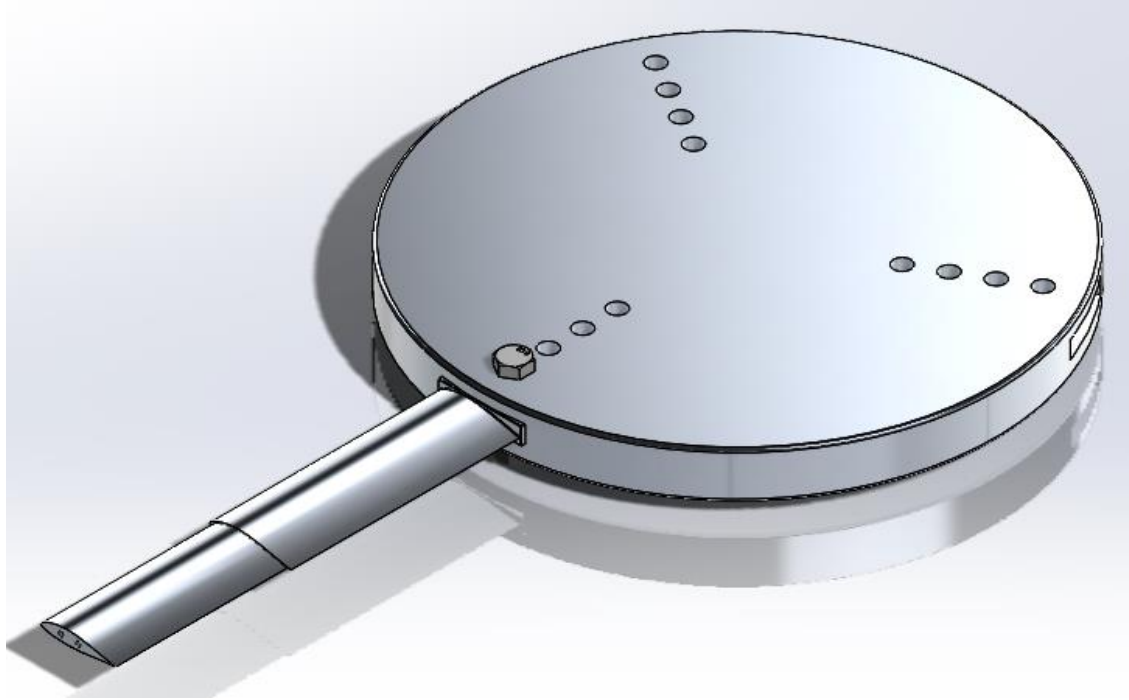


Figure 4. Blade inserted into disk with first bolt and matching nut

Sheath Attachment

When the blades are inserted and bolted to the disk, the user may slide a sheath (3) over each blade end and screw in the sheath bolts (4). Tighten these bolts down to 15 N•m. Each sheath MUST have some form of LE protection on it so the aluminum sheath is not worn down.

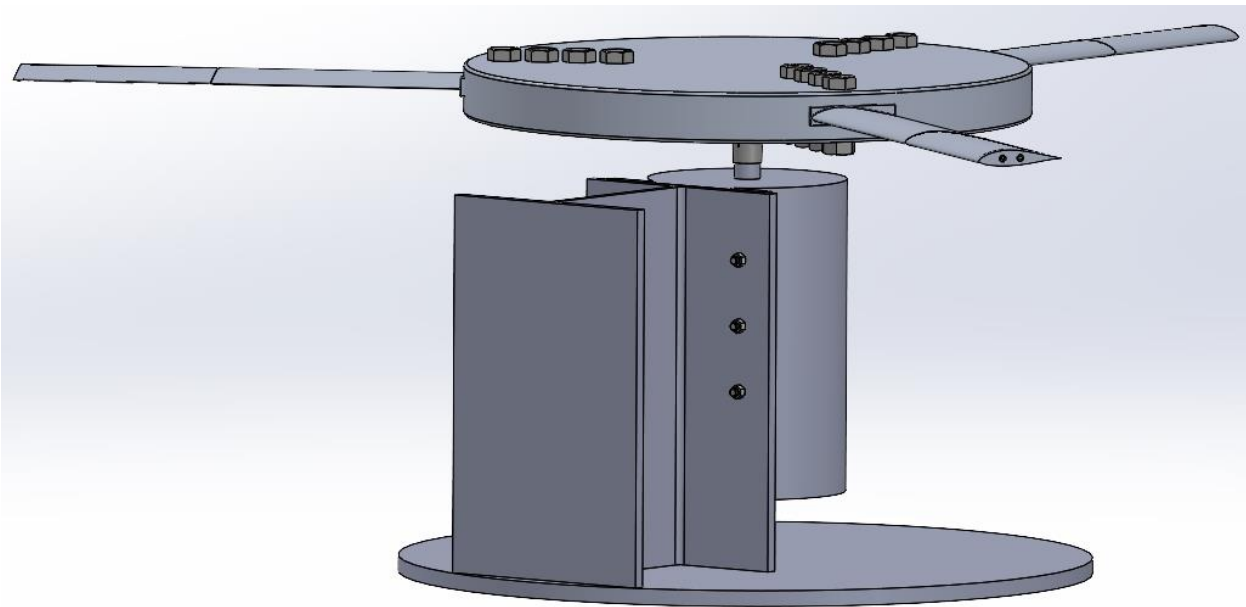


Figure 5. Total assembly of rotating blade system

Fluid Delivery System Structure

Lay out the four curved strut pieces on the ground so that pairs of holes on the top of the struts are all 60 degrees apart around the ring. Attach the curved struts together using the connecting plates and hardware already on each strut to create the support ring.

Attach the short ends of the J-shaped legs (part #3) to the top of the assembled support ring using the m12 hardware on the foot fitting. The channel of the struts face down and the legs should be oriented outside of the ring. The final structure should look like the image below.



Figure 6. Support structure made up of ring and legs

Place alignment pieces (part #4) between the reservoir and each leg to ensure the structure is centered with the reservoir.

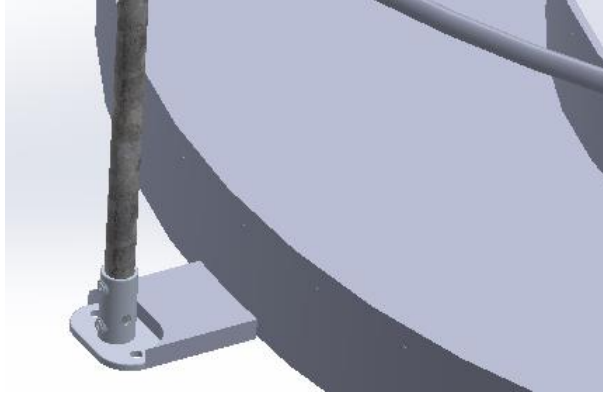


Figure 7. Alignment piece placed

Dropper Mounting Brackets

Identify the dropper bracket assemblies and hardware (part #7). They will look like the following image:

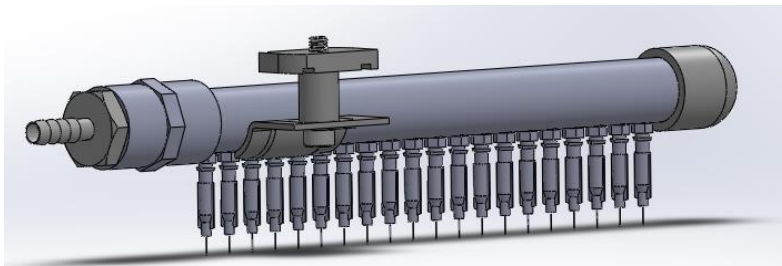


Figure 8. One dropper bracket assembly

Attach all 48 of the dropper mounting brackets on the support ring equal distance apart. This can be done by loosening the m6 mounting bolt and turning the strut track nut so that it fits into the strut track of the support ring. Then align the strut nut with the support ring strut track with the tubing adapter of the dropper configuration pointing towards the center of the support ring. Tighten the m6 mounting bolt to secure the dropper mounting brackets to the strut track of the support ring. They should each be separated by about 7.5 degrees around the support ring, or ... cm linearly between each bracket bolt. The mounted dropper brackets should look like the following figures.

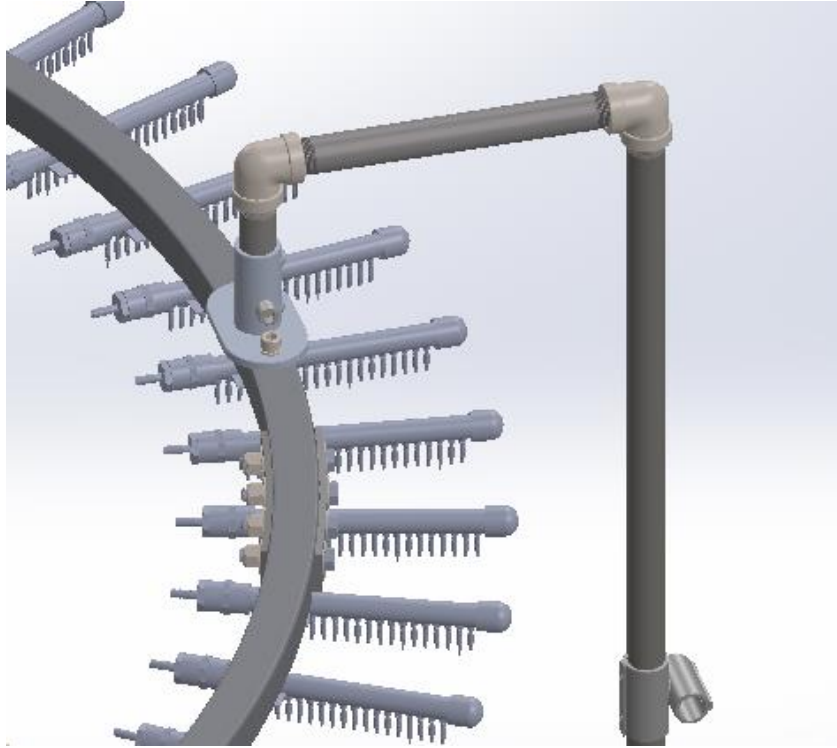


Figure 9. Close up of dropper mounting brackets on support ring

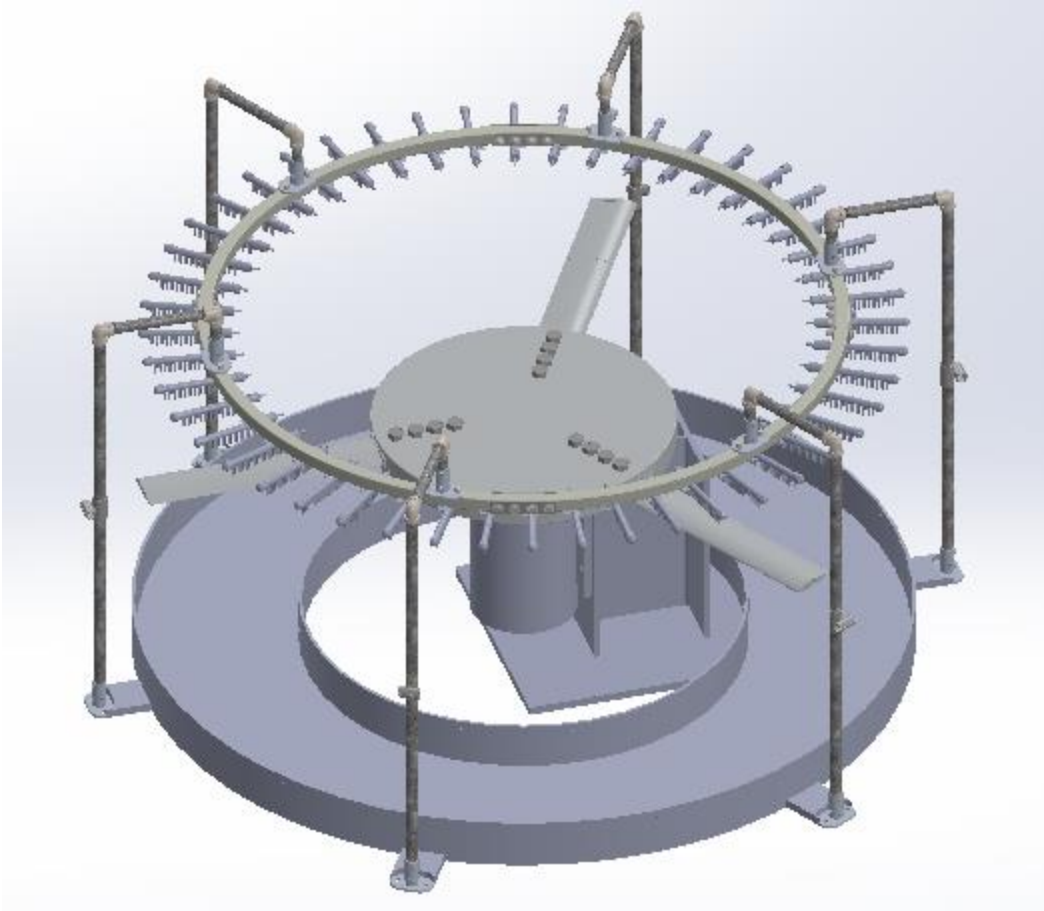


Figure 10. Assembly up to this point

Pump and Tubing

Setup peristaltic pump (part #5) according to manufacturer's operator's manual on the floor next to the outlet hole on the side of the reservoir body. Attach the tubing with the in-line filter (part #6) between the outlet hole of the reservoir and the inlet tubing of the peristaltic pump as shown in the following figure. Attach tubing stretch 1 (part #9) to the outlet tubing from the peristaltic pump as shown in the following figure. Route the first length of tubing stretch 1 up the leg that the peristaltic pump is sitting next to. Use the nylon cable ties (part #16) to secure the tubing to the leg.

Route the final 4 lengths of tubing stretch 1 to the inlet of the four 1:12 flow dividers (part #8). Place these dividers evenly on top of the support ring. Use more cable ties to secure the flow dividers and tubing to the support ring.

Attach the tubing stretch 2 lines (part #10) from the outlets of the 1:12 flow dividers to the inlets of the dropper bracket assemblies.

Fill the reservoir with tap water making sure that the water level does not go higher than the holes in the reservoir wall. Use about 300 liters of water total.

Slide the $\frac{3}{4}$ " PVC pipe (part #12) through one of the crossover brackets mounted on the longest part of the leg assembly. Bend the PVC pipe to fit it through the crossover bracket on the next leg as well. Repeat this with the other two lengths of PVC pipe so that each crossover bracket has PVC pipe going through it. Connect the loose ends of the PVC pipes with the $\frac{3}{4}$ " PVC fittings (part #13). This creates a rail for the curtain to be hung from.

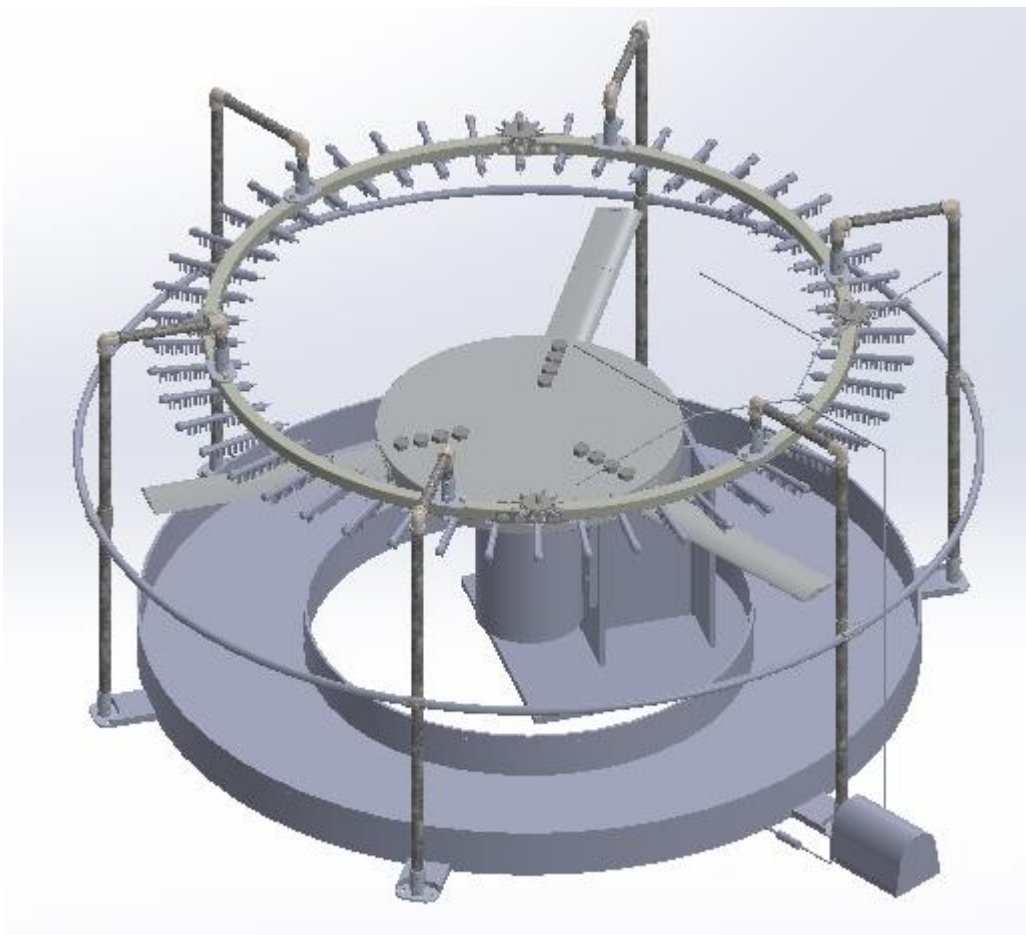


Figure 11. Assembly up to this point not including tubing stretch 2

Hang the four curtains (part #14) from the PVC curtain rail so they completely surround the assembly. Place the bottom of the curtains so they fall into the reservoir. Use the plastic rivets (part #15) to secure the curtains to the inside wall of the reservoir. The curtains should be fairly tight when they are attached to the reservoir wall.

Fluid Delivery System Operation

Once assembly is complete, follow peristaltic pump manufacturer's operator's manual to set pump flowrate to 603 ml/min.

Watch for droppers to start producing drops. This could take up to 30 minutes. Ensure that all droppers are producing drops at approximately the same rate. If any droppers are not

producing drops after 30 minutes, check dropper nozzles and tubing connections for pinches or blockage. If pinches or blockage are found, turn off the pump and replace the faulty section of tubing. Repeat this step after the replacement is made to ensure proper system function.

Rotating Blade System Operation

For operation of the Rotating Blade System, carefully check that all bolts are properly tightened. Ensure that there are no pieces that are dangling from the Water Delivery System that might interfere with the blade's path. Clear all people but the operator from the room. Operator follow the instructions from Worldwide Electric Corp. to turn on the PEWWE5-9-254T motor. Operator must also then leave the room and allow the motor to spin up to speed.

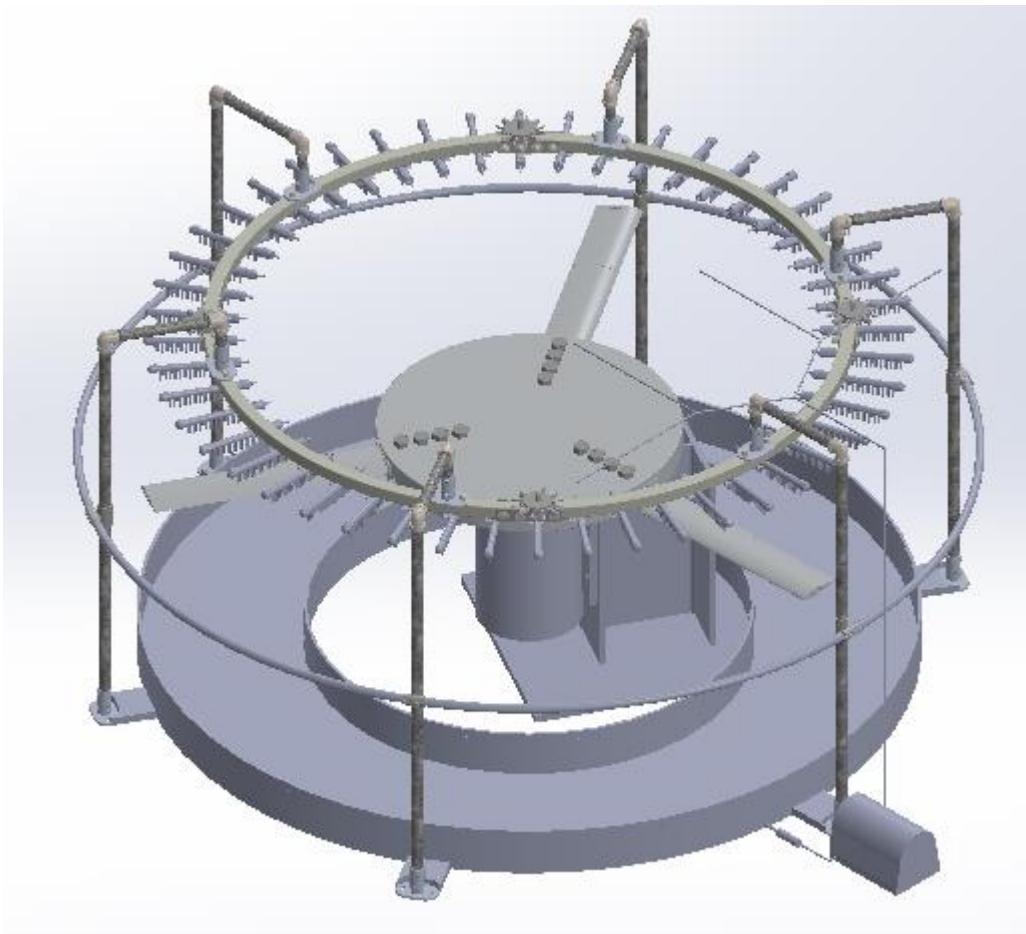


Figure 12. Turbine Blade Erosion Testing Unit fully assembled not including tubing stretch 2 or curtains